The Development of a MWCNT-DAO Biosensor for the Detection of Cadaverine in the Assessment of Periodontal Disease

Mohsin Amin

A Thesis Submitted For The Partial Fulfilment Of The Requirements Of Liverpool John Moores University For The Degree Of Doctor Of Philosophy

This Research Programme Was Carried Out In Collaboration With Manchester Metropolitan University

June 2023

Acknowledgements

This thesis is dedicated to Sky and Nala

I would like to begin by acknowledging my supervision team starting with my director of studies Dr Badr M. Abdullah. You have been amazing during this PhD, providing support whenever it was required and being understanding in times which I needed. I would like to extend my thanks towards Dr Stephen Wylie, who helped and supported me throughout the entire project, taking time out of his schedule to review and critique my work. To Prof Kathryn Whitehead I give my thanks for supporting me throughout the years and mentoring me through my research career. I would like to extend my gratitude to my supervisory team, Dr Liliana Shalamanova and Dr Rebecca Taylor for making time for me and being there to support and guide me in the early stages of this work. A thank you to my family for supporting me not only during this PhD but also throughout my entire life. I would also like to thank Steven Ryder for all the lab banter and lunches, and a special thanks to Ying Tang, for supporting me throughout these last 3 years and being there for me whenever I needed and thank the microbiology techs, Dr Paul Benson-White and Csilla Czeto for their help and guidance. A final thanks to Hayley Andrews, for even on short notices, providing assistance and images with the SEM and Raman.

Table of Contents

Abstract

Periodontal disease is one the most common afflictions of human populations and is a major challenge in both the developed and developing world. Cadaverine is a biomolecule which has implications in a myriad of human diseases, in particular periodontal disease. *Porphyromonas gingivalis* has been suggested as one of the key microorganisms in periodontal disease, and its pathogenesis has been extensively researched. It has a number of metabolites which contribute towards its pathogenicity, and among them, cadaverine has seen particularly detrimental effects in both oral and systemic health. Traditional testing methods for periodontal disease do not provide clinicians with active disease state measurements, but instead provide information on the history of the disease. Thus, the development of a real-time biosensor, providing point-of-care information regarding the metabolite status of the oral cavity would be of significant impact for oral disease diagnostics.

This thesis reports the development and testing of a newly designed working electrode fitted to a flexible screen-printed sensor platform for the detection of the biogenic amine, cadaverine. The results in chapter 3 showed that DAO enhanced MWCNT dispersion and increased overall electrode surface topographies, resulting in a more wettable electrode for faster, more efficient electron transfer kinetics. Scanning electron microscopy, UV-Vis, Fourier transform intra-red spectroscopy, raman spectroscopy, and energy diffraction x-ray spectroscopy confirmed the functional group changes the MWCNT's underwent during modification. Investigations into the modified biosensors heterogenous electron transfer rates were carried out and determined an increase to the peak to peak separation, possible due to the additional modification layers on the electrode surface, and the presence of a binder.

Chapter 4 investigated electrochemical efficacy of the MWCNT-DAO biosensor against cadaverine in stock solutions, and artificially simulated saliva. The biosensor demonstrated positive concentration dependant correlations towards cadaverine from a range of 3 μg/ml to 150 μg/ml. Similarly in artificial saliva, the biosensors efficacy remained consistent, and presented a potential for the biosensor to function outside of stock sample solutions.

The cytotoxic effects of *P. gingivalis* and cadaverine were investigated in Chapter 5. Initial monocyte differentiation into macrophages was confirmed using flow cytometry. Scanning electron microscopy was used to demonstrate the phagocytic effects of macrophages towards *P. gingivalis* and resulted in phagocytosis being visualised by the pseudopodia-like appendages engulfing the bacterium. Cell viability, and cell migration assays, and showed significant reductions in the viability and migratory effects of human epithelial keratinocyte and M0 macrophage cells in response to a *P. gingivalis* infection, and as a response to increasing cadaverine levels, above the physiological normal thresholds.

The findings from this study present a MWCNT-DAO biosensor which was able to detect cadaverine at concentrations which are respective to those in periodontal disease, in stock solutions and in simulated human saliva. Furthermore, the cytotoxic effects of cadaverine and its precursor bacteria, *P. gingivalis* were elucidated, and showed significant detrimental effects towards human macrophage and human epithelial keratinocyte cells. thus, the biosensor developed in this study may be used as a tool for determining the extent of a patient's periodontal disease, using a rapid, cost effective and point-of-care biosensor.

Declaration

No portion of the work referred to in the thesis has been submitted in support of an application for another degree or qualification of this or any other university or other institute of learning.

List of Figures

List of Tables

CHAPTER 1

Literature Review

1.1 Introduction

The importance of oral health and its influence on systemic disease has been emphasised throughout history. Periodontal disease, one of the major diseases in human adult populations, has affliction rates per capita of up to 50% (Nazir et al., 2017). It has been suggested that this prevalent disease may be associated with other systemic illnesses (Holmstrup et al., 2017). It is thought that if such a major disease in humans is a key factor in the onset of systemic disease, then understanding this relationship is of paramount importance to reduce human disease morbidity. However, there has been a severe lack of understanding in the relationship between periodontal disease and other systemic ailments. Some of the major challenges with reducing the rates of periodontal disease is its early asymptomatic presentation and its inability to be monitored or quantified in real time. Current techniques of periodontal disease assessment involve measurement of patient disease history and probing of the gum line without gaining insight into the active state of the disease or any qualitative measurements. With this in mind, the aim of this PhD thesis was the development of a biosensing device which utilised electrochemical assessment to identify bacterial metabolites within human saliva and use these to quantify the current state of periodontal disease. The metabolites selected for detection the are polyamines, in particular cadaverine. This metabolite has been implicated in a number of previous diseases (Kovacs et al., 2019; del Rio et al., 2019); however, this study focuses on their involvement in the active state periodontal disease. Such compounds are able to be detected electrochemically with the addition of enzymatic conjugation reactions, of which cadaverine and similar polyamines demonstrate redox properties. Thus, it was hypothesised that the development of a medical device which enabled the production of quantifiable real time data could enhance the monitoring of active periodontal

disease, resulting in earlier treatment options and more effective patient care and outcomes.

1.1.2 Aim and Objectives

1.1.2.1 Academic aim

Contribute to the fundamental understanding of periodontal disease diagnostics through the detection of cadaverine via the development of a novel sensitive and selective electrochemical biosensing platform, utilising enzyme technology.

1.1.2.2 Objectives

- Development of screen-printed multi-walled carbon nanotube based biosensing device for the detection of the polyamine cadaverine.

- Characterisation of functionalised working electrodes through topographical, physicochemical and wettability measurements.

- Electrochemical assessment of the biosensing device.

- Optimisation of biosensor sensitivity and selectivity through surface specific modifications.

- Determination of cadaverine and *P. gingivalis* cell cytotoxicity towards immortalised human cell lines.

1.1.3 Statement of Novelty

This thesis describes the development and modification of a screen-printed electrochemical biosensor with a carboxylated multi-walled carbon nanotube and diamine oxidase functionalised working electrode for the real time measurement of cadaverine. The work in this thesis demonstrates a novel functionalisation for the detection of cadaverine, using diamine oxidase in conjunction with MWCNTs. Furthermore, the work elucidates the potential applicability of this device for use in the dental industry as an early real-time monitoring device for periodontal disease. At the point of writing this thesis, and to the authors knowledge, no such device exists in the dental profession which provides real-time data into the active metabolic activity of an individual's active disease state. Furthermore, the cytotoxicity profiles of *P. gingivalis* and cadaverine against HK-2 and M0 monocyte cells presents a novelty in this work, in particular the concentrations used, which are indicative of the concentrations found in periodontal disease.

1.1.4 Thesis Overview

In order to achieve the aim and meet the objectives of this research, the thesis is structured into chapters.

Chapter 1 discusses the aetiology of periodontal diseases and their significance in human populations. Further, the identified polyamine toxins which are responsible for periodontal disease progression are also identified and discussed, along with biosensor design to detect these molecules.

Chapter 2 provides a detailed overview of the research methods, including the functionalisation of the MWCNT's and development of the working biosensor, using electrochemistry to analyse the electroactive properties of the electrode and cadaverine. Furthermore, the experimental protocols for the cytotoxicity and migration studies were elucidated in this chapter.

Chapter 3 focuses on the production of the enzymatic biosensor platforms modelled using screen-printing technologies due to the discussed advantages over conventional methods and includes the sensor design, printing process, validation, characterisation, and initial experimental approaches. This characterisation of the electrodes with both the, physical surface characterisation and electrochemical characterisation of the electrodes is demonstrated.

Chapter 4 investigates the electrochemical properties of the DAO/MWCNT biosensor and establishes its effective towards the target analyte, cadaverine. The current state of electrochemical biosensing towards polyamines is discussed and evaluated. The

electroactive performance of the biosensor was tested in both stock solutions and artificial saliva, to increase the devices technological readiness level. Comparative analysis between the unmodified and modified biosensors was carried out and standard curves for the detection of cadaverine were established.

In Chapter 5, the cytotoxic effects of *P. gingivalis* and cadaverine were investigated. The biological analysis of the periodontal disease precursor bacterium was initially disseminated and the implications the bacterial lysates on the phagocytic abilities of macrophages are investigated. Cell viability and migration assessments were carried out in response to incubation with *P. gingivalis* and cadaverine to determine the cytotoxic, and anti-migratory effects which they would elicit during a periodontal infection.

Chapter 6 provides an overall summary and conclusion to the findings in this thesis, and further explains the limitations and future work considerations.

1.2 Literature Review

1.2.1 The Oral Cavity

The oral cavity is of unique design, whereby hard and soft tissues are located next to each other, and these are continually exposed and challenged by numerous external material pressures (Taylor and Preshaw, 2016). Being one of the most complex regions of the human body, the oral cavity plays a vital role for providing entry, transit and exit for the digestive and respiratory systems, and contributes towards mastication and chemical pre-processing of foods (Yven et al., 2006). The primary structures of the oral cavity are the teeth, which enable the grinding and chewing of food to allow for ingestion, the tongue which compresses food against the palate to form bolus, and the palate, which forms a mechanical barrier to separate the oral cavity and nasal respiratory tract and allows for simultaneous respiration and food intake. The oral cavity contains hard tissues which include the dentine and enamel, components which make up the teeth. These are juxtaposed against the soft tissues of the buccal mucosa, soft and hard palate, the tongue, and the periodontium. The periodontium is a collective term which describes the tooth supporting and investing tissues such as the gingiva, root cementum, periodontal ligament, and alveolar bone (Cho and Garant, 2000).

1.3 Oral Biofluids

1.3.1 Saliva

In the oral cavity, there are two key biofluids present, these being saliva and gingival crevicular fluid (GCF). Saliva is a complex fluid which is secreted from three major

glands in the mouth (90% total saliva production), along with a large quantity of minor glands (10% of total saliva production) (deAlmeida et al., 2008). Secretion of the saliva from the salivary glands is a response mediated by the autonomic nervous system and its role comprises of, protecting the teeth, oral and peri-oral tissues, and to facilitate eating and speech (Dodds et al., 2015). The production of saliva is increased significantly upon the acknowledgment of food in the mouth through both mechanical and chemical stimuli (Neyraud et al., 2003). Both visual and olfactory stimuli have also been shown to increase saliva production (Keesman et al., 2016). The continual bathing of saliva in the mouth, this has shown to have a profound influence on the oral ecology and resulting microenvironment (Dodds et al., 2015).

1.3.2 Gingival Crevicular Fluid

The GCF is an oral inflammatory exudate of the oral cavity, and is derived from the periodontal tissues, which is located in the sulcus between the tooth and the gingiva (Lamster, 1997; Subbarao et al., 2019). Its role is to facilitate the antimicrobial defence of the periodontium and to maintain the structure of the junctional epithelium in response to a microbially mediated inflammatory event (Subbarao et al., 2019). Under normal conditions, GCF is sourced in small volumes of 0.43 – 1.56 μL/h (Khurshid et al., 2017). However, the amount of GCF produced significantly increases, up to 44 μL/h in response to stimuli from the immune system and during periodontal disease. The constituents of GCF originate from the blood, surrounding cells and the various tissues of the periodontium (Lamster and Ahlo, 2007). Although the role of GCF is to prevent microbial mediated damage to the oral cavity, an increase in GCF has been shown to increase localised nutrients and provide a suitable physical environment for

periodontal microorganisms, thus developing a positive feedback loop (Hickey et al., 2020).

1.4 Oral Microbiome

Comprised of over 700 diverse species of microorganisms, the oral cavity is a host for bacteria, fungi, mycoplasma and protozoa (Kuramitsu et al., 2007). This oral microbiome is defined as the entire genome of microorganisms that reside within the oral cavity and it provides host to the second largest microbial community in humans (Deo and Deshmukh, 2019; Gao et al., 2018). It consists of a core microbiome and a variable microbiome. The core microbiome is common amongst all individuals, whereas the variable microbiome changes are dependent on the lifestyle of the individual and physiological pressures (Kilian et al., 2016). The oral microbiota is imperative in the normal development of the host, effectively contributing to host defences, and it is involved in the synthesis of important vitamins such as vitamin B and K which aids in digestion. The oral microbiota is also involved in the prevention of exogenous pathogenic microorganisms, thus the relationship between host and oral microbiota is not one which is singularly passive (Patil et al., 2013; Marsh, 2009). In terms of mutual and functional integration, the relationship and multifaceted balance between host and oral microenvironment determines the health status of the oral cavity (Cornejo-Ulloa et al., 2019). There are two types of surfaces which bacteria in the mouth are able to effectively colonise, the hard tissues such as the teeth, and soft tissues of the oral mucosa (Deo and Deshmukh, 2019).

1.5 Diseases of the Oral Cavity

1.5.1 Gingivitis

There are two diseases which have been frequently associated with the infection of the periodontium, gingivitis, and periodontitis. Gingivitis and periodontitis are a form of gingival inflammation. Gingivitis represents reversible inflammation of only the gingiva, with rates as high as 90% amongst children aged 7-14 years. The initial inflammation of the gingiva can be considered a physiological defence against the onset of a microbial attack (Rathee and Jain 2022). In gingivitis, the clinical findings at the early stage of the disease are primarily the development of supra- and sub- gingival plaque, which is consequentially accompanied by the formation of calculus and significant gingival inflammation (Fons-Badal et al., 2020).

1.5.2 Periodontal Disease/ Periodontitis

Periodontitis is the most common microbially derived chronic inflammatory disease of the periodontium and is incurable, resulting in eventual mandibular bone destruction and tooth loss (Hajishengallis, 2015). Periodontitis manifests as reoccurring inflammation of the gingiva, gingiva bleeding and the formation of the hallmarked periodontal pockets and It is estimated that between 20% – 50% of the global adult population are afflicted with periodontitis, making it the sixth most prevalent disease worldwide (Nazir, 2017; Shatzle et al., 2004). The categorisation of periodontal disease can be broken down into four stages, gingivitis, mild periodontal disease, moderate periodontal disease, and advanced periodontal disease. Periodontitis results in eventual loss of the periodontal ligament and subsequent destruction of alveolar bone by compromising the integrity of supporting tooth structures (Fig. 1.1)

(de Pablo et al., 2009; Al Moharib et al., 2014). From initiation, the disease progresses with the detachment of collagen fibres from the root cementum, apical migration of the junctional epithelium, deepened pocket formation and finally, resorption of the alveolar bone (Tsuchida et al., 2017). Periodontitis will ultimately progress to bone destruction if untreated, leading to increased tooth mobility with subsequent tooth loss (Hienz et al., 2015).
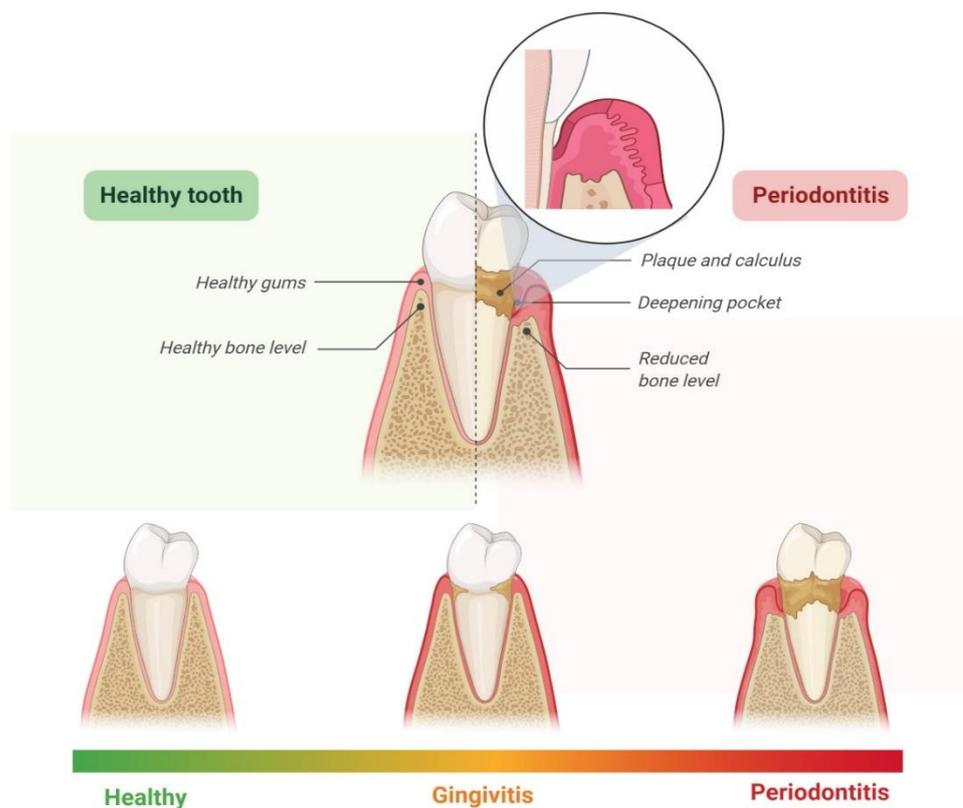
Figure 1. 1. The decline of the healthy tooth and periodontium with the onset of gingivitis, leading to periodontitis.

1.5.2.1 Periodontal Disease Grading and Assessment

The American Academy of Periodontology categorised, and classified periodontitis based on a grading system with respect to the severity of the disease. This grading

was utilised for the purpose of identifying the extent of a patients disease based on a measurable amount of destroyed tissue as a result of periodontitis. Clinical attachment Loss (CAL) should be used as the initial stage of grading and is determined at stage 1 of periodontitis as having 1-2 mm of loss confirmed. This is continued to stage 2 with 2-3 mm of attachment loss, and stage 3 with ≤5 mm of loss. Stage 4 is similarly represented with ≤5 mm of loss but is shown to be accompanied by the loss of ≤5 teeth (Tonetti et al., 2018). Further analysis include bleeding on probing (BOP) and analysis of radiographs of current alveolar bone levels which should be considered should previous assessment s with CAL provide insufficient evidence of disease (Fig. 1.2) (Preshaw, 2015).
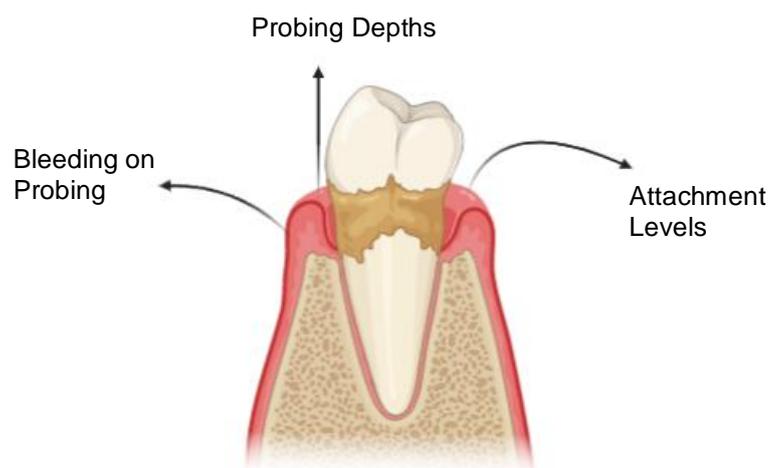
Figure 1. 2**.** Clinical means of periodontal disease assessment utilising traditional methods of bleeding on probing, probing depths and clinical attachment levels. Figure adapted from (Taba et al., 2005).

1.6 Microbial Attachment Mechanisms

Fimbria, long protein filament structures present on the surface of cells, enable bacteria to adhere to surfaces in the initial attachment and are found on bacteria such

as *Aggregatibacter actinomycetemcomitans* and *Porphyromonas gingivalis*. Proteins such as lipopolysaccharides, M proteins, capsules, glycocalyx and lipoteichoic acids are all examples of direct and indirect adhesins (Amano, 2007; How et al., 2016). Previous studies have shown that the membrane of host cells and bacteria are both negatively charged, resulting in them to repel each other. Through the use of adhesins, however, bacteria are able to modify their hydrophobicity, enabling them to adhere to cells more readily. After attachment, bacteria release a range of biomolecules, such as endotoxins and enzymes, which are able to cause host cell and tissue damage. Endotoxins in particular are produced by Gram-negative bacteria including, *P. gingivalis* are normally expressed on their cell wall and are released en masse as a response to bacterial lysis (Marcano et al., 2021). The over reactive response to these endotoxins such as LPS can cause serve inflammatory disease as seen in periodontitis.

1.6.1 Oral Dental Biofilm

The significant number and variety of structures within the oral cavity allow for the potential colonisation of a substantial number of microorganisms on the oral surfaces. Oral microbial biofilms are able to develop on dental tooth surfaces due to the adherence of Gram-positive 'early coloniser' bacteria. The biofilm is comprised primarily of microorganisms but also has varying types of organic and inorganic components, which exist within an extracellular matrix, derived from the constituents of saliva, gingival crevicular fluid and bacterial products, such as proteins and polysaccharides (Saini et al., 2011). The bacterial constituents are present in saliva and are able to adhere to dental surfaces through initial nonspecific physicochemical means, and then *via* specific interactions with surface adsorbed salivary proteins

(Lassere et al., 2018). Once initial bacterial colonisation of a dental surface occurs, bacterial proliferation develops into a bacterial biofilm. The key characteristic of a dental biofilm is that the micro-colonies which exist in the film are able to attach to a solid surface and biofilm attachment is the initial stage in the development of the dental biofilm. Dental biofilm formation occurs in multiple stages, initialising with the formation of an acquired film through the adsorption of host and bacterial molecules onto the surface of the teeth. The development of this film allows for the microorganisms which arrive at this site through active transport to interact with the film via Van der Waals and electrostatic forces, creating a weak bond. Later in the biofilms development the weak bonds formed are reinforced through bacterial adhesins with the complementary receptors in the dental biofilm itself. Over time, this process of aggregation will allow for the recruitment of new colonisers and cement the formation of a biofilm (Martinez and Figuero, 2006).

1.6.2 Periodontal Lesion Formation and Progression

Upon removal of the dental biofilm through cleaning the normal homeostasis of the oral environment resumes. However, if allowed to progress unhindered, the development of the initial lesion is able to manifest and progress. The initial lesion occurs in response to the activation of resident leukocytes and endothelial cells in response to the bacterial biofilm (Cekici et al., 2013). At this clinical stage, inflammation is still non apparent, but histological changes to the gingival tissues can be observed through microscopy, which include epithelium changes like the acanthosis type, the presence of polymorphonuclear leukocytes in the stratified squamous epithelium, and epitheliocyte keratinisation (Popescu et al., 2013). Through a bacterial trigger, the gingival junctional epithelium stimulates the production of

cytokines and encourages the production of neuropeptides to induce vasodilation of local vessels (Cekici et al., 2013).

In the early lesions, the increased number of neutrophils enable the activation of various complement pathways. The epithelium eventually proliferates and extends and forms rete pegs, a clinical histological observation of gingival inflammation, alongside gingival bleeding and increased GCF flow (Kayal, 2013). The established lesion subsequently develops within a period of 2-3 weeks after early lesion development. Through the activation of B cells, the established lesion contributes to the loss of the marginal gingival connective tissue matrix, but the alveolar bone remains unaffected (Figueredo et al., 2019). The endpoint of the established lesion progressing towards the advanced lesion is the formation of the gingival pocket, due to the migration of polymorphonuclear leukocytes through the junctional epithelium. The advanced lesion, also known as the destructive phase, is the stage at which the transition from gingivitis to periodontitis occurs and destruction to the periodontium beings to show irreversible damage.

1.7 Microorganisms of Periodontal Disease

Dental bacterial biofilms (also known as plaques) are the main aetiological agents which causes gingival inflammation to progress to periodontitis (Hajishengallis, 2015). These dental plaques, associated with changes in the bacterial species, dysregulate the normal oral microbiota and as a result cause the inflammatory response of which periodontitis is indicative (Wahid et al., 2013). The increase in microbial colonisation

causes a resultant increase in GCF flow, which has been shown to favour more anaerobic bacteria (Kilian et al., 2016).

Anaerobic microorganisms, which include *P. gingivalis*, *Tanneralla forsythia* and *Treponema denticola* have been shown to be the most prevalent anaerobic bacteria associated with human periodontitis and they are frequently isolated in the majority of cases (Mohanty et al., 2019). These periodontopathogens alongside other "key accessory" microorganisms have been categorised into complexes subject to their chronological colonisation of the gingival crevice and virulence in the subgingival plaques (Table 1.1).

Table 1. 1. Subgingival bacterial classification in Socransky complexes (Socransky et al., 1998).

Bacterial Species	Complex
Streptococcus gordonii	
Streptococcus intermedius	Yellow
Streptococcus mitis	
Streptococcus sanguinis	
Campylobacter rectus	
Fusobacterium nucleatum	Orange
Peptostreptococcus micros	
Prevotella intermedia	
Actinobacillus actinomycetemcomitans	
Tannerella forsythia	Red
Porphyromonas gingivalis	
Treponema denticola	

The red complex bacteria encompass what is known to be the most pathogenic bacteria in human periodontal disease (Suzuki et al., 2013). These Gram-negative bacteria become more prevalent during the later stages of dental biofilm development (Kesavalu et al., 2007). Studies have shown that there is an upwards of 96% infection rates of *P. gingivalis*, of which, 75% are in active periodontal sites, and 59.7% of *P. gingivalis* colonisation is found in inactive regions (Hernández et al., 2011; López, 2000). The colonisation of these areas by such microorganisms enables the initiation of inflammation to develop in the surrounding tissues, which can result in the loss of

connective tissues and alveolar bone. This facilitates the conversion of the junctional epithelium to pocket epithelium (Bosshardt, 2018).

1.8 Dysbiosis in Periodontitis

Historically, it has been thought that the red complex microorganisms were entirely responsible for the dysbiosis observed in the normal oral microflora through dysregulation of cell signalling pathways (Darveau et al., 2002). However, this understanding has since evolved, and it has now been suggested that periodontitis is a much more complex disease and is not solely regulated by one group of microorganisms. As a result, the descriptor of periodontitis infection is now based on the polymicrobial synergy and dysbiosis model (PSD) (Wang, 2015; Hajishengallis and Lamont, 2012). This model specifically refers to the communication between metabolically compatible microorganisms within an environment, which acquire functional specialisation through synergistic activities (Shaikh et al., 2018). The gingival crevice is colonised by an assembly of compatible microorganisms, grouped into heterotypic communities, to which the red complex bacteria and key accessory microorganisms interact. Such interactions increase community virulence and result in dysbiosis and tissue homeostasis disruption, causing the destruction of periodontal tissues (Hajishengallis and Lamont, 2012). However, the bacteria at a specific region of the oral cavity change in relation to the tissues and structures to which they are bound and also to local differences in environmental pressures. An example of this occurs in fissures, on proximal tooth surfaces and in the gingival crevice, where two distinct variations of bacterial accumulations can be observed (Lamont and Hajishengallis, 2015).

Table 1. 2. Changes in the microbiota of the oral cavity at different anatomical sites, the proximal tooth surface, and the gingival crevice (Asikainen et al., 2010).

Isolated microorganisms	Proximal tooth surface	Gingival crevice
Streptococcus spp.	*mutans, cricetus, oralis, parasanguinis, sanguinis, gordonii, salivarius, vestibularis, constellatus, intermedius, anginosus*	Not detected
Enterococcus spp.	*faecalis*	Not detected
Peptostreptococcus spp.	*prevotii, anaerobius, magnus, micros*	Not detected
Candidia spp.	*albicans*	Not detected
Staphylococcus spp.	*epidermidis, haemolyticus*	Not detected
Prevotella	*intermedia, oralis, melaninogenica*	*denticola, oris, pallens*
Leptotrichia spp.	*buccalis*	Not detected

***Campylobacter* spp.**	Not detected	*gracilis, rectus*
***Aggregatibacter* spp.**	Not detected	*actinomycetemcomitans*
***Capnocytophaga* spp.**	Not detected	*ochracer, sputigena*
***Porhyromonas* spp.**	Not detected	*gingivalis, endodontalis*
***Tannerella* spp.**	Not detected	*forsythia*
***Neisseria* spp.**	*flavens*	Not detected
***Treponema* spp.**	Not detected	*denticola*

The infection of the periodontal tissues presents a potential portal to enable periodontal microorganisms, bacterial metabolites and further biomarkers such as antigens into the body. Such bacteria and molecules may promote disease elsewhere in the body *via* dissemination of the circulatory system (Hickey et al., 2020). Such is evident in cases of Alzheimer's disease, and chronic kidney infections (Laugisch et al., 2018; Wahid et al., 2013).

1.9 *Porphyromonas gingivalis*

Of the oral microorganisms suggested to be responsible for the pathogenesis of periodontal disease, the red complex microorganism, *P. gingivalis*, has been considered as the most influential due to its innate ability to avoid the host immune response. *P. gingivalis* is a 1 – 2 µM in size, Gram-negative, black pigmented non –

motile asacchrolytic, obligatory anaerobic coccobacilli with a myriad of virulence factors which have shown to contribute to the destruction of host periodontal tissues. *P. gingivalis* rapidly adheres to the host cell surfaces followed by the internalisation through lipid rafts and incorporation of the bacterium into early phagosomes. *P. gingivalis* is able to activate cellular autophagy in order to developed and replicative niche while maintains suppression of apoptosis. The vacuole component of *the P. gingivalis* cell contains host proteins which have been delivered via autophagy and are utilised by the bacterium to replicate within the host cell.

1.10 The Host Immune Response in Periodontitis

Upon invasion of host cells, namely epithelial and fibroblast cells, bacteria initiate colonization almost immediately (Tribble and Lamont, 2000). There are complex bacterial strategies in place to aid in the successful colonization of bacteria in the host (Bartold and Dyke, 2000). The key mechanisms in which microorganisms invade include host cell adhesion, release of toxins causing host cell damage, and development of resistance profiles towards anti-microbial defences of the host, to ensure survival of the invading species (Hajishengallis, 2015). Such mechanisms are of particular importance in establishing persistent, chronic infections as seen during periodontitis.

1.10.1 Macrophages

Macrophages are myeloid cells of the innate immune system and reside on the surface of the highly permeable epithelium to rapidly respond to an infection. They play a role in host defence against bacterial infections by acting as antigen presenting cells,

functioning as phagocytosis cells, and secreting cytokines to further progress the immune response and stimulate an inflammatory status. Macrophages are able to recognise PAMPs and generate chemotactic molecules for the recruitment of non localised leukocytes such as neutrophils. Neutrophils are the most abundant leukocytes within the gingival crevice and migrate to the site of infection to clear invading microorganisms. They realise pro-inflammatory cytokines to aid in the phagocytosis of bacterial pathogens and are responsible for the maintenance of periodontal tissue homeostasis.

The recruitment of phagocytes to the site of cell death is a normal process of the immune response and aims to promote the end of inflammation at the site (Rock and Kono, 2008). Previous works have shown that macrophages which have been treated with *P. gingivalis* proteases have significantly reduced migratory effects towards apoptotic cells (Castro et al., 2017). These effects result in the ability of oral microorganisms such as *P. gingivalis* to promote and prolong chronic inflammatory states within hosts.

1.10.2 *P. gingivalis* in Periodontal Inflammation

P. gingivalis has been shown to manipulate immune system signalling pathways leading up to polymorphonuclear leukocyte migration (Sochalska and Potempa, 2017). During the inflammatory processes of periodontal disease, the numbers of polymorphonuclear leukocytes are vastly increased beyond the physiological levels (50% - 70%) of circulating leukocytes, in the peripheral blood (Miller et al., 1984). This increase in concentration is exacerbated due to chemokines and adhesion molecules

from the innate immune response, and as a result, the site of infection is flooded with an influx of leukocytes.

P. gingivalis is able to produce proteases that interfere with the immune regulatory mechanisms. In a typical instance, the C5a anaphylatoxin receptor (C5aR) is activated as part of the complement cascade, activating the regulatory, inflammatory and antimicrobial functions for bacterial elimination in oral tissues. However, the introduction of proteases into this system results in crosstalk interference between the C5a receptor and toll-like receptor signalling, effectively preventing the intracellular killing mechanisms towards *P. gingivalis* (Shaikh et al., 2018; Cortés-Vieyra et al., 2016). Such work has demonstrated the ability of bacteria which are indicative of periodontitis to effectively contribute to their own survival and the exacerbation of the disease. Through the regulation of the hosts inflammatory mediatory processes, the oral microorganisms are able to exacerbate or prolong inflammation.

1.11 The Importance of Biomarkers in Human Disease

A biomarker is defined as a biochemical, cellular, or molecular alteration which is measurable in any biological media such as the human tissues, cells or fluids (Mayeux, 2004). Biomarkers are able to represent an objective indication of the medical state on an individual, and can be observed outside of the body, and measured with precision whilst maintaining a high degree of replicability (Strimbu and Tavel, 2010; Choong and Tsafnat, 2012). In the late 1990's, the National Institute of Biomarker Definitions working group described a biomarker as 'a characteristic that is objectively measured and evaluated as an indicator of normal biological processes, pathogenic

processes or pharmacological responses to a therapeutic intervention' (Strimbu and Tavel, 2010). These biomarkers were divided into two distinct categories: exposure biomarkers, which enable the assessment of potential health risks, and disease biomarkers, which are currently in use for screening, diagnostics and monitoring existing diseases (Hwang et al., 2018; Strimbu and Tavel, 2010; Lowry, 1995). In order for a biomarker to demonstrate a clear predictive value in which a disease or biochemical process can be effectively measured, definitive values for the biomarker need to be established.

1.11.1 Existing uses of Clinical Biomarkers

In modern medicine, biomarkers are frequently utilised for screening of diseases such as Alzheimer's disease, cancer, and periodontal diseases (Table 1.3) (Goossens et al., 2015; Sharma and Singh, 2016). Within such diseases, the uses of biomarkers may allow for confirmation of a diagnosis, initial detection of the suspected disease, or for monitoring the outcomes of theraputic interventions (Selleck et al., 2017). Biomarker research is now at the point where there is significant research input in the field of new biomarker discovery, and susequently, biomarkers are being constantly developed and refined. This has resulted in significant breakthroughs in the fields of drug discovery, clincal trials, epidemiology and personlised medicine (Collinson, 2013; White and Xie, 2013).

Table 1. 3. Exisiting biomarkers used for the detection of current human diseases (Stathopoulou et al., 2015; Lopez-Giacoman and Madero, 2015; Sauter, 2017; Sharma and Singh, 2016).

Alzhiemers disease	Cancer	Kidney disease	Periodntal disease
Tau protein	ctDNA (oral cancer)	Serum creatinine	Lypopolysaccarides
Phosporylated tau protein	Cytokeratin (in 90% of breast cancers)	Urinary albumin	Matrix metalloproteases
Amyloid B plaques	Ki-67 (cellular proliferation)	Cystatin C	Serum IgG

For biomarkers in human disease to be effectively measured, they must be detected within their respective biofluids. Current biofluids such as blood plasma, serum, urine and cerebrospinal fluid are routinely used as a source of detecting biomarkers indicative of disease (Xu and Veenstra, 2008; Kulic and Unschuld, 2016). The ability to effectively replicate measurements of biomarkers to a high degree of accuracy and sensitivity has been at the forefront of medical and epidemiological research (Thyagarajan et al., 2016; Tarnanas et al., 2015). Within humans, the degree of biomarker variability between people results in a range of acceptable 'normal' values. In such fluids, biomarkers are used as indicators of a clinical manifiestation, disease stage, or to determine an alternate manifestation of the disease in question (Mayeux, 2004). It is extremely important that the surrounding biofluid does not interfere with the signal produced by the selected biomarker. Previous studies have shown that although biomarkers may potentially have the capability to demonstrate levels which may be indicative of disease assocation, they may demonstrate low levels of repeatability (Thyagarajan et al., 2016). Thus, the reproducibility of biomarker measurements when used for for disease detection is still of concern (Yeh et al., 2017). However, it is evident that biomarkers potentially have signficant advantages to be used in disease detection over traditional diagnostic methods, although consideration needs to be given to the natural variability between human participants.

1.11.2 Infection Biomarkers of Bacterial Driven Disease

The use of biomarkers where typical diagnosis methods are insuffcant, expensive and/or time consuming, may result in the most successful application for the use of

biomarkers (Lubell and Althaus, 2017). Since biomarkers are able to provide a clinican with valuable diagnositc and prognostic information regarding the current health staus of an individual, their applicability in various bacterially driven diseases is of major importance (Tang et al., 2017; Gomez et al., 2019). For example, tuberculosis (TB), is a communicable infectious disease that is known for having a long incubation time (2-8 weeks), resulting in severely delayed confirmation diagnosis. This is due to the detection methods relying on the bacteria being cultured to provide a positive confirmation. However, new biomarkers in the form of lipoarabinomannan, a virulence factor and glycolipid of the cell wall of the causative agent of TB (*Mycobacterium tuberculosis*) has shown good specificity to determine the presence of TB in the blood and urine, without the use of bacterial cultures (Goletti et al., 2016; Correia-Neves et al., 2019; Wallis et al., 2010). This example demonstrates the effectiveness of the potential of new biomarkers as rapid detection alternatives. The use of such systems have the possiblity to reduce diagnosis times whilst maintaining comparable levels of diagnostic accuracy to that of traditional techniques.

1.11.3 Periodontal Disease and its Associated Biomarkers

Traditional techniques for the assessment of periodontal disease involve a routine visit to the dental clinic. In the periodontium of healthy individuals there should be no distinguishable loss of epithelial attachment or the formation of the hallmarked pockets, which must be less than 2 mm deep. Whilst such measures are useful in the assessment of patient disease history, these traditional methods provide little to no information about the patient's current health, the active state of the disease, or risk of

potential future periodontal breakdown (Srivastava et al., 2017). CAL readings for example, which are measured using periodontal probes for pocket depth and loss of gingival attachment or radiographic evaluations of the alveolar bone loss measure damage which has incurred from past episodes of destruction and require 2 mm to 3 mm threshold changes before an active disease site can be identified as having experienced major anatomic event (Taba et al., 2008). Furthermore, as periodontitis presents with minimal bleeding and attachment loss in its early stages, many individuals neglect to treat the disease, and if left untreated, it can rapidly progress to periodontitis. As mentioned previously, there is no cure for periodontal disease, however, once most periodontal disease has been successfully diagnosed, treatment options exist to reduce the burden it has on the afflicted individual. Therapeutic interventions for periodontal disease aim to initially change or eliminate the origin of the microorganisms and potential contributing risk factors. In doing so, these interventions may halt the progression of the disease and aim to re-establish the healthy state of the periodontium (Kim and Amar, 2006).

The current aim for biomarkers in the field of periodontal research is to develop rapid, high impact diagnostics, which enhance clinical decision making. This should result in affordable, economically viable healthcare and an increase in favourable patient outcomes (Urdea et al., 2011). For such biomarker-based tests/measurements to become widely utilised, they must be at least of equal calibre to existing clinical diagnostics but show improvements in saving time, cost and also be easy to use for both the user and recipient.

1.11.4 Salivary Biomarkers in Periodontal Disease

It has been suggested that the saliva and GCF can be used to determine the periodontal health status of an individual since the oral fluids contain specific disease biomarkers indicative of periodontitis (Patil and Patil, 2011). Saliva, which is readily available and collected without invasive interventions provides an ideal source of periodontal biomarkers. A significant proportion of compounds which are located in the body are also isolated from whole saliva. Molecules are able to be transported either into or out of the saliva through cells *via* passive diffusion, active transport, or by extracellular ultra-filtration (Srivastava et al., 2017). When individuals present with chronic inflammation, which accompanies periodontitis, the saliva becomes host to a myriad of biomarkers (Table 1.4).

Table 1. 4**.** Periodontal disease associated biomarkers which are currently measurable in whole saliva. Each biomarker is indicative of a respective hallmark of periodontal disease.

Alveolar Bone Loss	Collagen Breakdown	Soft Tissue Inflammation
Alkaline phosphatase	Aspartate aminotransferase	Prostaglandin E2
Osteocalcinin	Alanine aminotransferase	β-glucuronidase
Collagen telopeptides	Tissue inhibitors of metalloproteinases (TIMPs)	Interleukin-1β
Pyidinoline cross links of type 1 collagen	Matrix metalloproteinases	Interleukin-6
Receptor activator of nuclear factor – kappa β (RANKL)	Macroglobulin – α	Tumour necrosis factor – α
Osteoclastin	Collagenase	Matrix metalloproteinase (MMP 8, 9, 13)

1.11.5 Gingival Crevicular Fluid Biomarkers

In recent years, the use of GCF has gained wide interest as a source of biomarkers for periodontal disease since it shows clear changes during different stages of periodontal disease progression (Majeed et al., 2016; Ghallab, 2018; Barros et al., 2016) (Table 1.5). Collection of GCF is a non-invasive procedure and it is simple to collect from people with underlying comorbidities, since it is an inflammatory exudate which increases in volume in response to a periodontal infection. Thus, GCF appears to be an attractive option for use as a diagnostic fluid.

Table 1. 5. Cellular and molecular biomarkers which present in the GCF during periodontal disease.

Gingival crevicular fluid biomarker	Region of origin	Function
Cathepsin β	Macrophages	Enzyme active during proteolysis
Interleukin- 4, 6, 8	Basophils, T-cells, macrophages, osteoblasts	Regulator of T and B cell growth, Recruitment and activation of macrophages
Immunoglobulin A, G, M	Plasma cells	Antigen neutralisation
TNF-α	Neutrophils, macrophages, lymphocytes	Delays neutrophil apoptosis
Erythrocytes	Gingival blood vessels	Small blood vessel damage
Leukocytes	Gingival blood vessels	Polymorphonuclear leukocytes are utilised in the innate immune response to periodontitis

1.11.6 Biomolecules for Periodontal Disease Detection

Periodontal disease can be attributed to the presence of certain bacterial species and as such, there has been numerous studies suggesting that the presence of antibodies directed towards the detection of these bacteria may implement new strategies for targeted biomarkers. In both the GCF and saliva of periodontitis patients, the presence of IgA and IgG antibodies have been sourced towards four periodontal disease specific bacteria, *P. gingivalis*, *A. actinomycetemcomitans*, *P. intermedia* and *F. neucleatum*. In periodontal disease patients, similar results between each bacterium were found, whereby significantly elevated levels of bacteria specific IgG and IgA antibodies have been detected when compared to healthy controls (Plombas et al., 2002). Moreover, studies comparing 50 healthy individuals and 50 periodontitis afflicted patients have been carried out, with significantly elevated levels of IgA and IgG antibodies respective to four keystone periodontal pathogens (*P. gingivalis*, *T. denticola*, *T. forsythia* and *A. actinomycetemcomitans*) being identified and demonstrating a periodontitis stage dependant increase in antibody concentration (Gadekar et al., 2018; Dye et al., 2009). Thus, IgA and IgG antibodies specific to keystone periodontitis pathogens in the GCF and to a lesser extent the saliva, are potentially able to indicate the potential 'at risk' sites for periodontitis due to their increased concentration (Takahashi et al., 1997).

The majority of damaging interactions which occur in periodontal disease take place at the crevicular and junctional epithelium (Fujita et al., 2018). Biomolecules, such as enzymes, endotoxins, nucleic acids, proteins, carbohydrates, degradation products and immunoglobulins, which result from periodontal bacteria residing in the GCF, have been shown to induce significant host tissue damage (Cekici et al., 2014; Barnes et

al., 2014). Recent evidence would suggest that the host inflammatory response to periodontal bacteria may also aggravate periodontal disease and demonstrate commonly identified disease specific pathologies (Nędzi-Góra et al., 2017). It has been demonstrated that under activation due to numerous chemical signalling molecules, polymorphonuclear leukocytes produce increasing levels of reactive oxygen species and proteolytic enzymes (Mariggiò et al., 2004). The hyperactivity of this response significantly contributes to the host tissue destruction during periods of active periodontal disease (Nair et al., 2014). During this host pathogen interaction, many free amino acids and metabolites are significantly elevated (Barnes et al., 2009). Such elevation of potential biomarkers due to the mechanisms of infection can result in whole saliva and GCF providing a large, easily accessible pool of biomolecules for which periodontal disease detection and staging can potentially be evaluated. Further study is warranted, to optimise the repeatability of measurements taken using such biomarkers and to determine how such markers are directly correlated with disease extent and progression.

1.12 Polyamines and Periodontal Disease

The colonisation of bacteria into gingival tissues is limited through salivary flow and muscular movements (Pedersen and Belstrøm, 2019). The Gram-negative "keystone" red complex bacteria are able to exacerbate the inflammatory events occurring in the periodontium though the release of specific biomolecules. One potential class of molecules, the polyamines, may be utilised as potential biomarkers to determine the incidence and severity of a periodontal infection.

1.12.1 Polyamine Biosynthesis

The polyamines, cadaverine, putrescine, spermine and spermidine, are a group of organic polycationic molecules which are required for growth and differentiation of almost every eukaryotic and prokaryotic cell (Fig. 1.3) (Shah and Swiatlo, 2008; Takahashi and Kakehi, 2010).
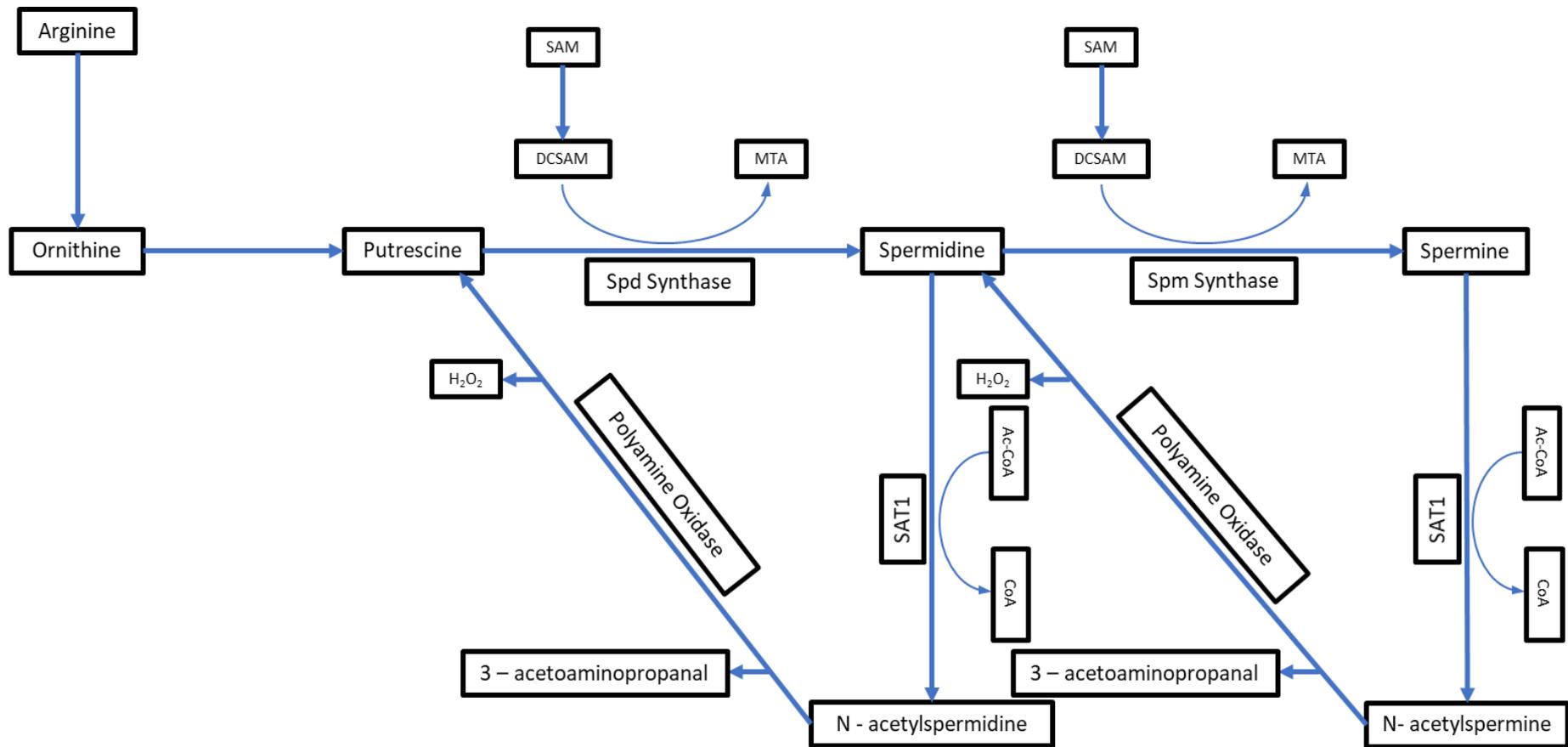
Figure 1. 3. Biosynthetic pathways demonstrating the degradation of the biogenic amine, putrescine into its respective secondary and tertiary polyamines, spermidine and spermine (Amin et al., 2021),

These aliphatic polycationic molecules are ubiquitous in all tissues and cells in both plants and animals. Their roles within humans, span a broad range of functions, and this includes the influencing of cell apoptosis, cellular division, differentiation, proliferation, DNA and protein synthesis, gene expression signal transduction and homeostasis (Fig. 1.4) (Kusano et al., 2008; Pegg, 2016; Handa et al., 2018). Based on cellular distribution alone, putrescine and spermine are the most prominent within human biosystems, aiding in cellular growth and division in both eukaryotic and prokaryotic cells (Handa et al., 2018).
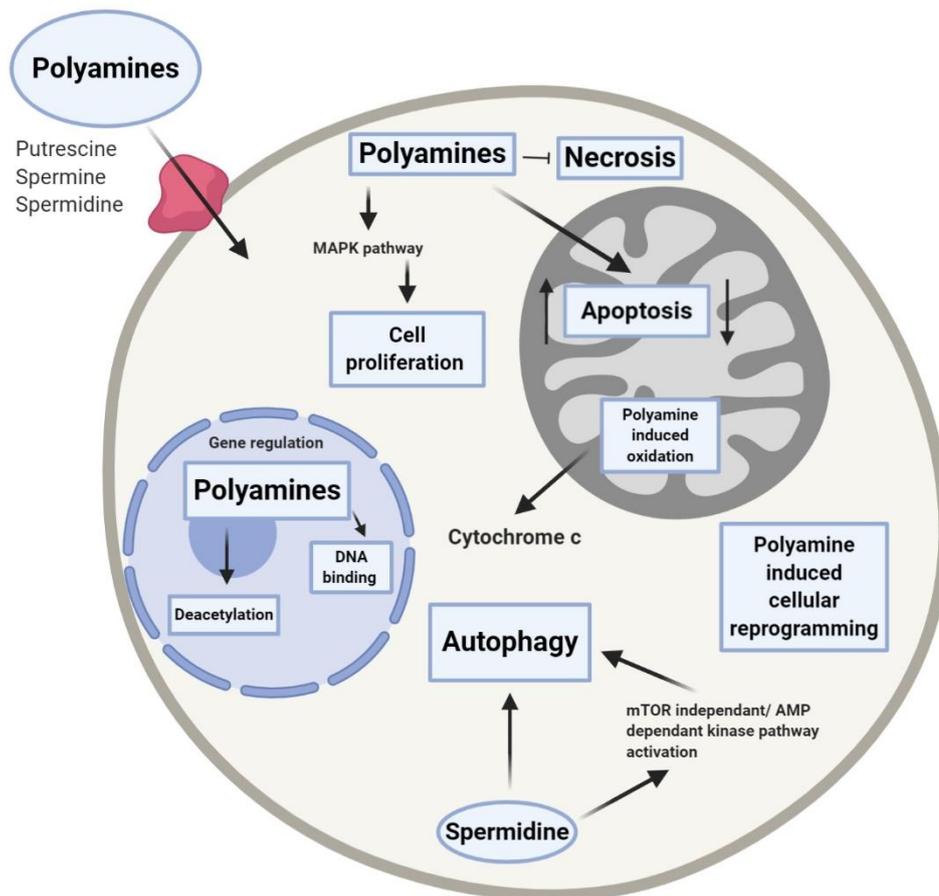
Figure 1. 4. Polyamines express various functions upon entering the cell. The nucleus, mitochondria and cytoplasm are influenced differently, although, polyamines are a necessity for each cell component. Polyamines are involved in the regulation cell proliferation and termination, and also gene expression and translation. There is now increasing evidence to suggest that polyamines play a role in cellular reprogramming and autophagy (Amin et al., 2021).

1.12.2 Polyamines in Bacteria

Putrescine, cadaverine, spermidine and spermine are the predominant polyamines which reside in bacteria and show some availability in cellular tissue (Guerra et al.,

2018). The role of bacterially derived polyamines has been shown to be associated with cell metabolism, cell-to-cell communication and bacterial cell differentiation, and also it contributes significantly towards bacterial signalling, motility, and cell division (Igarashi and Kashiwagi, 2000; Kurihara et al., 2005; Miller-Fleming et al., 2015). Individually these polyamines provide different mechanisms for enhancing bacterial cells for example, putrescine has been determined to constitute to the outer membrane walls of some Gram-negative bacteria such as *Salmonella enterica* and *Proteus mirabilis*, and cadaverine has been associated with the peptidoglycan of *Villonella* spp. suggesting the importance of polyamines of maintaining the outer surface structures of bacteria (Kamio, 1987; Vinogradov and Perry, 2000; Shah and Swiatlo, 2008;). Their synthesis relies on the presence of functional precursor molecules, similar to humans and these are detected at millimolar concentrations in bacteria (Tofalo et al., 2019). The intracellular concentrations of spermidine are determined to be the highest in bacteria at 1 – 3 mM/mL, whilst putrescine demonstrate the lowest levels at 0.01 – 0.02 mM/mL (Shah and Swiatlo, 2008).

Recent studies have investigated the impact of polyamines in bacteria (Goforth et al., 2013; Nakamya et al., 2018). Polyamines are suggested to play a vital role in aiding the pathogenesis of bacterial species. There have been several studies in which distinct pathways for specific virulence mechanisms of bacterial species, (*Francisella*, *Legionella*, *Salmonella* spp. and *Shigella* spp.), have shown that polyamines were an essential requirement to establish an infection (Jelsbak et al., 2012; Nasrallah et al., 2011). Jelsbak et al (2012), demonstrated that by inhibiting polyamine synthesis pathways in *Shigella* spp, the virulence was severely limited by reducing bacterial

ability to invade cells. This suggests that polyamines play a vital role in the modulation of the virulence of bacterial pathogens.

1.12.3 Polyamine in Periodontal Disease

Two polyamines, cadaverine and putrescine have been previously identified as up-regulated biomolecules in periodontal disease and their role in the pathogenesis of periodontal disease has been suggested in a number of previous studies (Lamster et al., 1987; Mariggiò et al., 2004; Lohinai et al., 2012). Despite their abundance in cells, polyamine levels are tightly regulated, and it has been shown that the over production of polyamines such as putrescine and cadaverine (39.76 mM and 40.72 mM respectively) can result in significant cell cytotoxicity (Del Rio et al., 2019). Further work by Lamster et al (1987), determined polyamine analysis of the GCF conducted before and after two weeks of mucoperiosteal flap surgery on patients who exhibited periodontitis (Lamster et al., 1987). These areas demonstrated high values of putrescine pre-operatively (1020 pmol/mL). Similarly, putrescine values were measured at one week and two weeks post operatively (124 pmol/mL and 880 pmol/mL respectively). The polyamine content in the supragingival plaque of periodontitis afflicted individuals presented with putrescine (1.49 nmol/mg) in the highest abundance, followed by spermine (0.03 nmol/mg) and finally spermidine (0.90 nmol/mg). The reduction in the concentration of spermine and spermidine was to be expected, this being due to the direct degradation of putrescine, resulting in the formation of spermidine and spermine respectively (Pegg, 2016). The measure of putrescine in GCF provided better differentiation between relative periodontal health and staging criteria since it was observed to be present at significantly higher levels in

deep periodontal pocket sites in comparison to milder presentations of the disease and in healthy controls (Ozeki et al., 2016; Lamster et al., 1987). Overall, it was suggested that the ability to quantify putrescine, spermine and spermidine within active periodontal sites was possible and such concentrations were potentially correlated with the severity of an individual's periodontal disease stage.

1.12.3.1 Polyamine Upregulation in Periodontal disease

The use of polyamines as potential biomarkers has been suggested in a number of previous studies, in particular putrescine and cadaverine isolated in the GCF of periodontitis afflicted individuals have been shown to be increased over normal physiological levels in patients with periodontitis (Nakajima et al., 2018; Park and Igarashi, 2013; Sakanaka et al., 2017). Since they are resident in bacterial cells, and show significant increases upon measures of the GCF, one may speculate that their release from the internal bacterial environment may occur as a result of bacterial breakdown, as is evident during periodontal disease. As the severity of peritonitis progresses, the immune host mechanisms which are attempting to combat the site of infection would also increase, thus enabling the killing of more bacteria in order to clear the infection. The release of these polyamines into surrounding host biofluids and tissues due to the actions of the host immune system may suggest a new method of assessment for periodontitis.

1.12.4 Cadaverine as a Periodontitis Biomarker

The use of cadaverine specifically as a salivary biomarker for periodontal inflammatory status may be a possibility, since results have been shown to coincide with findings from previous metabolomics analyses of saliva from patients with predetermined periodontal disease (Barnes et al., 2014). The presence of cadaverine in human biofluid at greater than physiological concentrations is something typically introduced *via* an external source. Sakanaka et al (2017), postulated that cadaverine was actively metabolised by periodontal microorganisms due to significantly increased concentrations during periodontitis, thus its presence in saliva can be correlated to the number of bacteria colonising a specific region of the oral cavity (Sakanaka et al., 2017). Moreover, cadaverine, has been specifically identified to positivity correlate with periodontal inflamed surface area (PISA) levels and these levels have been used to investigate disease associated metabolic signatures of periopathogens through a salivary metabolomics based approach (Kuboniwa et al., 2016).

Work by others has demonstrated the efficacy of cadaverine at reducing the secretion of bactericidal superoxide enzymes, resulting in the disruption of host immune response signalling pathways which in turn reduces leukocyte migration to the site of inflammation (Köhler et al., 2002; Kang et al., 2007; Lohinai et al., 2012). Cadaverine has been shown to modulate bacterial viability, through the inhibition of phagocytic leukocytes (McCormick et al., 1999; Walters et al., 1995). Cadaverine has also been implicated in enhancing oral bacterial proliferation through the inhibition of leukocytes thus, decreasing the likelihood of bacterial phagocytosis (Lohinai et al., 2012).

1.12.4.1 Systemic Influences of Periodontal Disease Infection

A growing body of evidence has shown the possible connection between periodontal disease and disease at distal organs. Periodontitis is an immune mediated inflammatory disease that is prevalent as a result of a microbial infection. The innate and adaptive immune responses are both stimulated by periodontal pathogens and the releaseates of bacterial products and the additional release of inflammatory mediators from periodontal pockets has shown to result in low grade systemic inflammatory events (Delbove et al., 2021). Moreover, the relationship between periodontitis and systemic diseases such as cardiovascular disease and diabetes is relatively well documented. Recently there has been increasing amounts of evidence to suggest a strong supporting argument for the association of periodontitis and chronic kidney disease (CKD), owing to the theory of more severe periodontal breakdown coinciding with the progression of kidney disease.

1.13 Biosensors and Biosensing

The monitoring and quantification of biochemical or biological processes are of the utmost importance for biological, biotechnological, and medicinal applications. However, it is difficult to convey a biological event into an electronic signal due to the complexity of relaying an electrical device into a biological environment. Electrochemical biosensors provide a promising means of analysing biological events due to direct biological signal conversion into an electrical readout.

1.13.1 Biosensors

A biosensor is a device which measures electrochemical reactions via the generation of electrical signals which are proportionate to the concentration of the analyte being determined (Bhalla et al., 2016). Biosensors are employed in a number of applications including disease detection, drug discovery, pollutant detection, microorganisms, and bodily markers in bio-fluids (Bhalla et al., 2016; Singh et al., 2020). The development of the first biosensor dates back to the early 1900s whereby the concentration of an acid in a solution was proportional to the electrical potential which arose between the glass membrane used in the study.

1.14 Biosensor Advancements

The most significant advancement of biosensors was by Clark and Lyons (1962) which was the development of the glucose biosensor for the measurements of glucose in biological samples (Yoo and Lee, 2010). This sensor utilised the electrochemical detection of oxygen or hydrogen peroxide species though the enzyme, glucose oxidase. The processed converted the simple platinum electrode into a powerful analytical device for the monitoring of glucose. Since this time, innovative approaches made by researchers have progressed the field of biosensing significantly, with the development of optical transducers utilising antibodies in the development of point of care bio-affinity sensors. Such sensors paved the way for a second generation of biosensors to be developed. The enzyme electrode and the affinity electrode initially found utility in the laboratory setting, however, due to the advances in manufacturing coupled with the transduction techniques of electrochemistry, the enzyme based biosensors found major clinical use in both clinics and at home over optical devices

(Wang et al., 2008). Since this time, the use of electrochemistry has become a pioneering technique in diagnostic biosensing, whilst optical biosensing has found its niche within the laboratory setting (Turner, 2013).

1.15 Biosensor Characteristics

There are specific attributes which every biosensor possesses, and the optimisation of these properties is what enables the various performance changes of the individual biosensor. Selectivity is perhaps the most influential feature of the biosensor, and this refers to the ability of the bioreceptor to detect a specific analyte in a sample which may contain contaminants and other admixtures (Bhalla et al., 2016; Naresh and Lee, 2021). This is demonstrated by the antibody – antigen interaction whereby a selected antigen is exposed to an antibody conjugated transducer in which the antibody selectively reacts with the antigen (Lim and Ahmed, 2019). The reproducibility of a biosensor refers to the ability of the device to generate identical signals in response to duplicate experimental setups. It is measured by the precision and accuracy of the transducer and the electronics used in the device itself. Precision is the ability of the device to provide replicate results continually over a number of repeat sample measurements, and the accuracy indicates the sensors capacity to provide a mean value close to the true value when a sample is measured more than once. The reproducibility signals provide high reliability and robustness, so the interference made in the response to the biosensor in minimised. The degree of susceptibility to disturbances in and around the bio-sensing system is referred to as stability. The drift caused by the disturbances in the output of the signals of the biosensor under measurement can cause an error in the measured concentration and can affect the

accuracy and precision of the biosensor. The measure of the sensor's stability is one of the most important aspects of sensor design especially in the application of long term monitoring and is particularly important in areas where long incubation times will test the sensors stability over the long term such as the medical and food industries.

1.16 Nanomaterials

Nanomaterials for biosensing applications gained significant attraction over recent years as the necessity to develop new sensors with more specific characteristics has been increased. With the ever-increasing requirement for more accurate and sensitive bio devices, carbon nanomaterials provide a potential alternate to current strategies.

1.16.1 Carbon Nanotubes

Carbon nanotubes (CNTs) have emerged as one of the most extensively studied nanomaterials. CNTs are hollow cylindrical carbon nanostructures with one or more walls, existing in the nanoscale diameter. They are oriented and linked by Sp_2 bonds making them the most ridged carbon material to date. They offer unique magnetic, electromagnetic, mechanical and chemical applications of which lend themselves to be particularly effective in the field of sensor development and biomolecule immobilisation. Furthermore, the hollow structure of the nanotube enables effective enzyme loading via one of the methods of immobilisation. Depending on the arrangement of the graphene cylinders, three individual types of nanotubes can be obtained. The orientation of these nanotubes can affect the geometrical structures which are specified dependent on their chirality and directly influence their electronic properties. The dependency on this orientation of the graphene lattice with respect to

the tube axis, three types can be obtained, including, Armchair (n,n), zigzag (n,0), and chiral (n,m).

There are currently many methods of biosensor development which enable the utilisation of nanotube biosensors for medical detection applications. Screen-printing has been one the most effective methods utilised to date, enabling cost efficiency, customisability, and the use of a larger array of substrates to be printed upon.

1.16.1.1 Single-Walled Carbon Nanotubes

Depending on the number of walls of the CNTs, they can be designed as either single or multi walled. The sidewalls of the CNTs are made up of a hexagonal lattice of carbon atoms, similar to those of the other carbon nanomaterial, graphene, and are capped off at both ends by one half of a fullerene like molecule. Single-walled carbon nanotubes possess the simplest morphology and can be identified as a single graphene cylinder, and usually form as close packed hexagonal bundles. Upon further investigation of the tube axis, the structure of the nanotube can be defined through its chiral vector.

1.16.1.2 Multi-Walled Carbon Nanotubes

Multi-walled carbon nanotubes (MWCNTs) are composed of two to several coaxial cylinders, each made of a single graphene sheet which surrounds a hollow core of up to 100 nM in length and the distance between sheets can be as close as 3.5 Å. Since CNTs have such a high surface area to volume ratio, they act as ideal platforms for the immobilisation of biomolecules, such as acting as receptor moieties for

applications in biosensing. Although CNTs in their various forms present very attractive properties and advantages for biosensing applications, their dispersion remains one of their major limiting factors and hinders further progress. CNTs possess high surface energy thus are intrinsically hydrophobic making them non-suspensible in water and numerous common solvents. Therefore, the application specific process for CNTs need further functionalisation to increase their suspensibility and functional properties.

1.17 Screen-Printed Biosensors

Screen-printing is a technology which has been previously well established in the field of electro-analytical devices and has been made evident through the commercialisation of glucose screen printed biosensors (Garcia-Miranda Ferrari et al., 2021; Hayat and Marty, 2014; Ridhuan et al., 2018). These inexpensive, disposable, rapid and accurate sensors are significantly researched (Costa-Rama et la., 2021; Whittingham et al., 2021). Furthermore, the portability of such biodevices is of major fundamental importance in terms of applicability and commercialisation.

Screen-printed electrodes address the issues of cost effectiveness, but they also satisfy the need of highly reproducible and sensitive methods of detection towards biological analytes. The adaptability of screen printed electrodes is of major benefit in areas of research, due to their ease of modification towards the printed electrodes in the system, and ease of alteration of the ink in the formulations for the working electrode. Using these methods, the counter, reference and working electrodes can be adapted and produced for specific target analytes within the medical field (Hayat and Marty, 2014).

The process of screen-printing involves the printing of thixotropic fluids through a screen mesh used to determine the size and shape of the electrode. The thixotropic fluid contains substances such as graphite, carbon black, various solvents, and binders. The inks utilised in this work have a high viscosity, however, when forced through the mesh screen the fluid undergoes sheer thinning which allows for penetration through the screen and deposition of the final sensor shape and size. Upon contact with the substrate, the ink returns to its previous viscous state and forms the intended printed design. If the final sensor designs have a thickness in the range of 20 mm to 100 mm they are thicker than other printing technology and are thus termed "thick film technology".

The screen printing of electrochemical biosensors provides an ideal platform for the functionalisation of a number of different nanoparticles and require no prior electrode treatment such as electro-deposition, or electrode polishing which are common practices with other electrode materials.

1.18 Electrode Material Selection

1.18.1 Working Electrode

When considering electrodes for electrochemical assessment, attention needs to be given not only to the electrode material, but also to the nature of the experiment. The working electrode is the key region of interaction for the bio-device, thus selecting the optimum electrode material is of utmost importance. Carbon and various metals have been commonly used to prepare electrode systems. Metals such as platinum, silver, gold and steel have been long utilised for electrode surface materials due to their

excellent chemical, electrical, and mechanical properties. Carbon-based materials such as carbon black, graphite and carbon fibre have been frequently used for the construction of working electrodes. These carbon based materials have a high chemical inertness and are able to provide a stable baseline for electrochemical detection (Zhao et al., 2018).

1.18.2 Reference Electrode

The reference electrode is a major component in electrochemical systems and is a specific type of electrode which has a known stable potential to which all other electrode potentials in the system are referenced to. The Ag/AgCl reference electrode is the most common used in electrochemical analysis. The structure of Ag/AgCl reference electrode consists of a silver wire, immersed in an Ag/AgCl coating which is submerged in a salt electrolyte of potassium chloride (KCl). The Ag/AgCl reference electrode operates due to a slight leakage of the internal electrode solution, which comes into contact with the sample and provides an electrical contact point with a stable unchanging potential. The leak path contact point via the electrode junction, can be made through a range of materials according to the requirements of the experiment. This reaction is demonstrated in the following equation:

$$AgCl + e^- \leftrightarrow Ag + Cl^- \qquad [1]$$
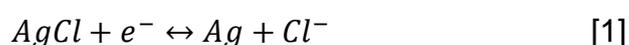
Other types of more frequently utilised reference electrode materials are listed (Table 1.6). The decision when determining which reference electrode is optimum for the experiment is dependent on the experimental parameters itself.

Table 1. 6**.** Currently utilised reference electrodes and their usage (Nickell et al., 2006; Szabo and Bakos, 2010; Dawkins et al., 2021).

Reference electrode	Usage
Hg/HgCl (Saturated Calomel)	pH measurements, general aqueous chemistry. Very stable however contains mercury so unsuitable for food applications or environment studies
Ag/AgCl (wire or paste)	Printed sensors, ion-selective electrodes
Cu/CuSO$_4$	Corrosion control systems
Hg/HgSO$_4$	Mercury sulphate is used as a substitute for chloride ions when they cannot be tolerated in the electrolyte
Hg/HgO	Alkaline solutions

1.18.3 Counter Electrode

Counter electrodes are the final electrode used in the typical 3-electrode setup. This type of setup is most common when aiming to study the reactions which occur at the working electrode site when a known potential is applied between the working and reference electrodes; to protect the reference electrode from potential shifts, the current flows between the counter and working electrodes.

1.19 Enzymatic Biosensors

Enzymes are of major interest as biosensor transducer molecules due to their high catalytic activity, specificity, ease of production and the ability to function under mild conditions. Thus, enzymes are of significant benefit for a range of applications, however, despite the number of advantages of enzymes, their industrial applications are limited by a number of factors including short shelf life, instability and low reusability which may result in increased costs associated with large scale commercialisation. Even with these shortcomings. They are the most common bioreceptor in current electrochemical devices, since their configuration results in minimal flat positive responses, which has shown to achieve efficient electron transfer between the enzyme active site and the electrodes.

One of the key challenges in today's bio-enzymatic electrode design and development is the complexity of the organic component of the electrode, which can result in issues such as enzyme leakage (Kudo et al., 2008). To prevent enzyme leakage, it is required to form chemical bonds between the enzyme and amino groups on to the surface of the nanotubes. Amide bond formation is a slow and nonspontaneous processes at room temperature and direct condensation can only be achieved at temperatures of

over 200 °C. However, this destroys the enzyme structures resulting in denatured and ineffective biomolecules. Therefore, conjugating compounds can be used as coupling reagents to instigate a reaction. Amongst these reagents, carbodiimides are the most frequently considered for this mode of work (Han et al., 2013; Cammarata et al., 2015). One consideration which must be noted is that carbon nanotubes possess a high level of reactivity towards proteins, and it has been suggested that some protein is adsorbed onto carbon nanotubes even after their initial oxidation and carboxylic acid group additions. These electrode modifications have led to the enhanced performance of surfaces due to the enabling of increased bio-molecule loading, enhanced sensitivity and this has resulted in reductions of several orders of magnitude in the detection limits of molecules.

However, there are challenges which affect enzyme based electrochemical devices and these include overcoming the inefficient electron transfer between enzyme and the electrode surface. One of the main reasons for this is that the enzyme active site is located deep within the enzyme and for the enzyme to work efficiently, the enzymes have to orientate favourably in accordance with the electrode surface. Also, there remains other challenges which are associated with electrochemical biosensors which include, nonspecific binding and limited functional adequacy with real world samples due to issues such as poor sensitivity or electrode fouling.

1.19.1 Immobilisation of Biological Elements

Traditional materials which are used as cross linking reagents such as glutaraldehyde (GA) and hexamethyl diisocyanato are able to form cross reactions between the bio-catalytic species on the electrode surface. This process, which is referred to as coarticulation, creates complex matrices between enzymes and substrates. The most

common method of chemical enzyme immobilisation is using GA crosslinking. GA has been a key component in the design of biosensors since its first use in enzymatic devices, due to its ability to maintain enzyme conformation after immobilisation (House et al., 2007).

1.19.2 Enzyme Electron Transport

Enzymes exhibit high specificity and sensitivity towards target substrates due to their tri-dimensional structure (Rago et al., 2015). The active site of an enzyme can limit the rate of electron transfer between the enzyme and the electrode, and the electron transfer process can dramatically decrease as the distance between the active site and the electrode increases. To better facilitate electron transport, the electron transfer pathway should be situated as close to the electrode surface as possible, with two current methods used in practice: direct electron transfer (DT), and mediator electron transfer (MT).

1.19.2.1 Direct Electron Transport

During the process of DT, electrons from the active redox site of the enzyme are shuttled to the electrode surface without the aid of further mediators. In this instance, the enzyme is fixated to the electrode surface directly and functions as a molecular transducer. To further enhance the DT process, it is essential that the orientation of the enzyme be carefully considered as to shorten electron tunnelling distances. To overcome this issue, redox mediators may be utilised to aid in long distance electron tunnelling. Redox mediators directly 'shuttle' electrons from the redox site of the enzyme to the electrode surface.

Enzymes are able to be directly adsorbed onto the electrode surface, which conveniently situate their active redox site close to the electrode surface which increases the efficiently of DT. In situations whereby the distance between the redox site and the electrode surface are too distant, fast and efficient electron transfer becomes unlikely. The possibility to add readily diffusing redox mediators to electrolytic solutions after an enzyme has already been immobilised for DT has previously been elucidated (Bollella and Katz, 2020). This approach while seemingly effective in some applications, is not practical in some instances due to the contamination the electrolyte solution incurs via the mediator.

1.19.2.2 Mediator Electron Transport

MET sensors use redox active mediators known as, relays, which are electroactive molecules that aid in the shuttling of electrons between the enzyme active site and the electrode surface (Bollella and Katz, 2020; Scheller et al., 1991). Such mediators can be freely diffusing in the surrounding solution or be tethered to side chains of redox polymers on the electrode. One of the major advantages of MET is the utilisation of the entire surface of the enzyme for active transport, and not relying on a singular DT pathway, which only covers a small proportion of the electron pathways and resulting in unsatisfactory efficiency (Gemunde et al., 2022).

1.20 Enzyme Immobilisation

The immobilisation of enzymes refers to the confining or localisation of enzyme within a matrix in the insoluble phase, whilst retaining all or most of the enzyme's catalytic activity. (Pinyou et al., 2019). In order to overcome these drawbacks, enzyme

immobilisation demonstrates an advantageous method with promising results. A suitable support for enzyme immobilisation is required to possess attributes such as inertness, high stability, and the ability to reduce product inhibition. Several methods have been proposed for enzyme immobilisation which are highlighted in (Table 1.7).

Table 1. 7. Different methods of enzyme immobilisation onto a solid carrier.

Immobilisation Method	Advantage	Disadvantage	Application	Reference
Adsorption	Chemically and mechanically stable support	Enzyme denaturation	Scaffold for carbon materials	(Jaros and Rohm, 2011)
Covalent	Stable to hydrolysis at neutral pH	Esters unstable in aqueous conditions	Antibody, protease and oxidase enzyme immobilisation	(Bai et al., 2012)
Physical entrapment	Reduces negative interference on enzyme surface. Is thermally and mechanically stable	Enzyme-substrate complex formation is limited	Biosensor development using antibodies or enzymes	(Hakala et al., 2013)
Encapsulation (lipid vesicles)	Strong reproducibility	Sheer force enzyme inactivation	Enzyme replacement therapy	(Soldatkin et al., 2012)
Biodegradable polymers	Longer circulation lifetime in biofluids	Entrapment efficacy is low with low enzyme stability	Control enzyme release in enzyme replacement therapy	(Apetrei et al., 2013)

1.20.1 Enzyme Immobilisation on CNTs

Recently, the uses of nanomaterials have become an increasing viable option for enzyme immobilisation, in particular in the field of biosensing. Nanomaterials such as nanotubes, nanoparticles, nanofibers and nanopores have all shown to be effective materials as enzyme immobilisation supports. Amongst these nanomaterials, carbon nanotubes have gained significant attention due to their biocompatibility along with exceptional mechanical, electrical, and thermal properties (Naghshbandi et al., 2018). Biomolecule immobilisation is a critical step in ensuring efficient electron transfer between the enzyme active site and electrode. Enzyme loading and entrapment onto electrode surfaces has been extensively studied (Nguyen et al., 2019; Putzbach and Ronkainen, 2013). Physical adsorption is the simplest and most cost effective method of manufacturing enzymatic biosensors. Positively charged amino acid residues of enzymes are able to be electrostatically adsorbed onto negatively charged colloidal surfaces on electrodes, through simple incubation steps (Zhu, 2017). Although this method is fast and simple, it results in unfavoured enzyme orientation thus, negatively impacting heterogenous electron transfer rates (Fig. 1.5).
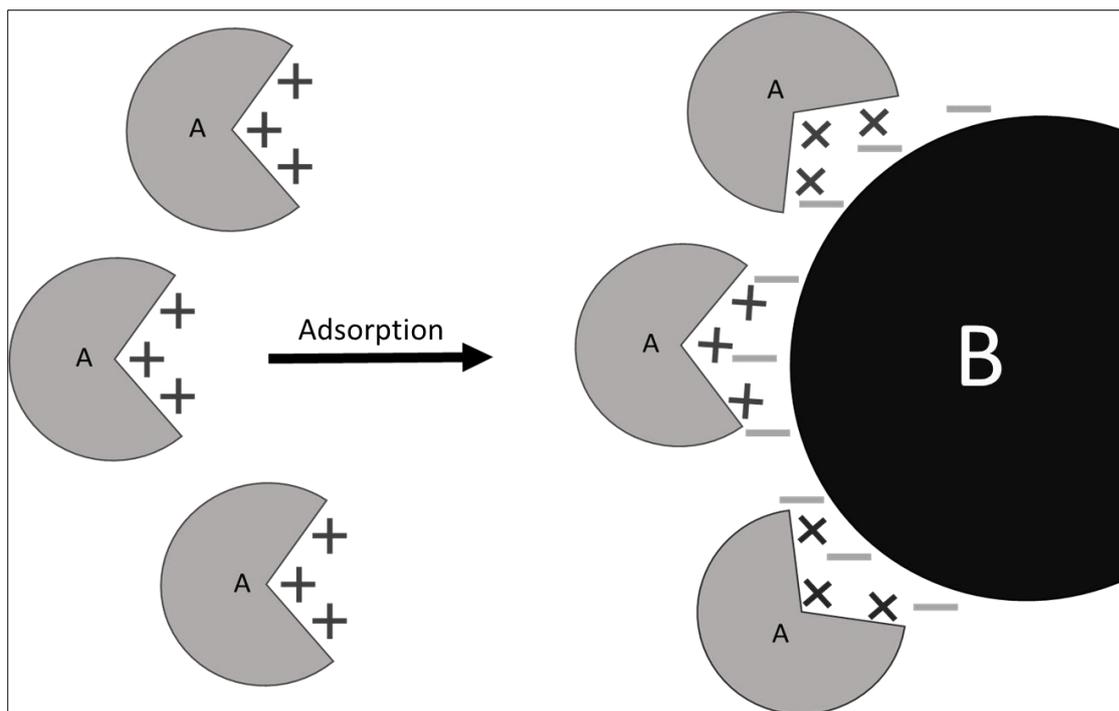
Figure 1. 5. Positively charged amide groups on enzymes (A), electrostatically binding to the negatively charged functionalised working electrode surface (B).

In order to effectively facilitate enzyme immobilisation onto an electrode surface a number of pre-functionalisation steps can be implemented onto electrodes to aid in increased enzyme loading. Covalent attachment of proteins onto an carbon structures such as CNTs, is one such method that demonstrates highly favourable sensitivity and selectivity increases as a pre-functionalisation in the development of biological sensing platforms (Yates et al., 2018). 1-ethyl-3(3-Dimethylaminopropyl)Carbodiimide (EDC) is a water soluble zero length crosslinker which is utilised in the development of sensing platforms (Vashist, 2012). It is utilised in the coupling of carboxyl groups, etched onto the CNT surface (Fig. 1.6), by binding them to primary amines. EDC undergoes nucleophilic substitution in the presence of strong nucleotides, such as primary amine molecules, and forms an unstable O-acylisourea intermediate (Wickramathilaka and Tao, 2019). This intermediate is readily hydrolysable, thus able

to rapidly revert back to its original carboxylate molecule. To overcome this, N-Hydroxysuccinimide (NHS) has been frequently utilised to develop a more stable intermediate prior to amine introduction (Fig. 1.6) (Staros et al., 1986; Fischer, 2010).
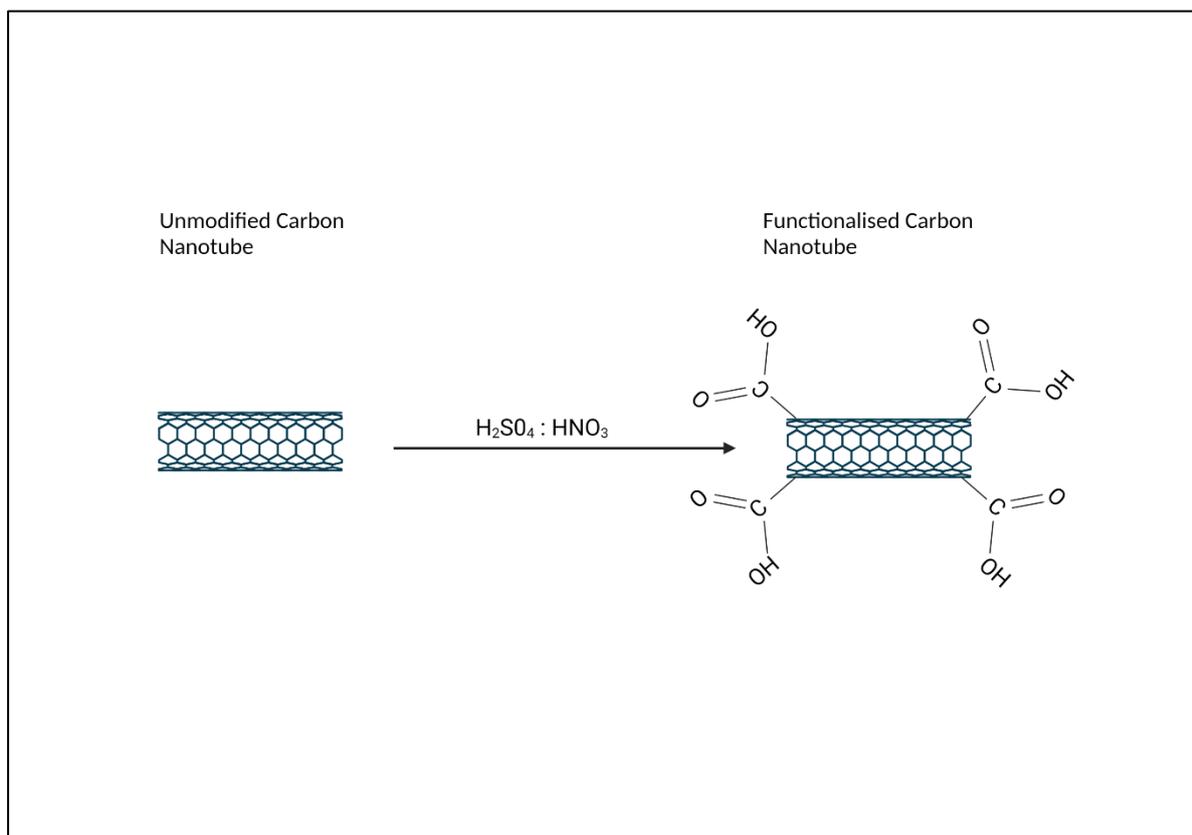
Figure 1. 6. Acidic carboxylation of carbon nanotubes utilising 98% sulfuric and 70% nitric acid at a ratio of 3:1, resulting in carboxylic acid functionalised carbon nanotubes.
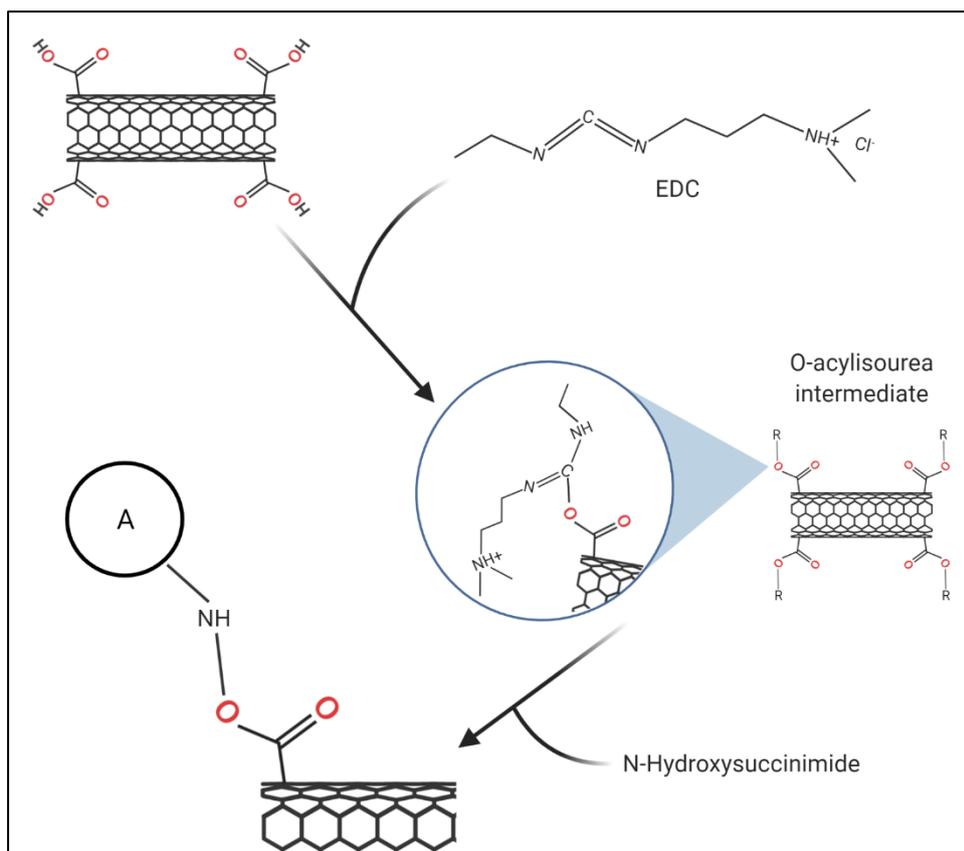
Figure 1. 7. Carboxylic acid functionalised carbon nanotube coupling demonstrated utilising 1-ethyl-3(3-Dimethylaminopropyl)Carbodiimide (EDC) and N-Hydroxysuccinimide for the formation of an initial O-acylisourea intermediate, followed by protein (A) conjugation via amide groups. Figure adapted from Amin et al., (2022)

1.21 Surface Topography of Carbon Screen-Printed Electrodes

Screen-printed electrode surfaces are topographically variable with peaks and valleys at the micrometre and nanometre scales. The roughness profiles of surfaces are frequently characterised by the arithmetical average roughness (S_a), maximum peak height (S_p) and root mean square height (S_{pv}). These values are determined via spatial parameters in order to calculate the two dimensional roughness as opposed to the traditional line method (R values). The S values are parameters which enable a robust characterisation of the topography of the surface in contrast to one dimensional line methods. Capacitance dispersion has been shown to decrease as a direct result of decreasing electrode roughness, due to the dispersion of capacitance being a result of electrode geometrical origin (Champigneux et al., 2018). Furthermore, electrical conductance has been shown to be reduced by the addition of films to electrode surfaces, since this decreases the surface nano-roughness (Song et al., 2022). In addition, the nano-roughness of electrodes has been shown to influence molecular adsorption on electrode surfaces and the concentration of the adsorbed species has demonstrated reduced quantities of enzyme being immobilised on a rougher surface than that of a smoother one (Champigneux et al., 2018).

1.22 Fundamentals of Electrochemistry and Electrochemical Analysis

The discipline of electrochemistry encompasses a plethora of device related fields such as electroanalytical sensors, batteries, fuel cells and electrochromic displays. In

typical instances, the majority of chemical assessments involve the interaction of bulk solutions, however, electrochemical interactions take places on the electrode surface. The differentiation of electrochemical techniques can be divided broadly into potentiometry and voltammetric, owing to the electrical signal utilised for quantification. These electrochemical techniques rely on the presence of an electrochemical cell, which consists of at least two electrodes (working and reference), the conductors, and a contacting electrolytic solution. The two electrodes for the cell allow for a surface junction between the ionic and electronic conductors. The study of charge transfer processes at the electrode-solution interface which is based on non-zero currents refer to potentiostatic techniques. In potentiostatic conditions, the electrode potential is used to facilitate the electron transfer reaction whereby, a resulting current is determined as a reflection of the rate at which electrons are transferred across the electrode - electrolyte interface.

1.22.1 Electroanalysis

Techniques which involve electroanalytical analysis occur due to their electrical and chemical interactions, in particular the measurements of electrical quantities, such as current, potential or charge. Many chemical analysis techniques involve bulk solutions; however, electrochemical processes take place at the electrode solution interface, lowering the quantity of analyte required for a reaction to take place. Such techniques can be characterised into two principal types; potentiostatic and potentiometric, which are distinguished via the electrical signal used in their quantification (Colburn et al., 2021). Similarly, both methods require at least a two electrode setup, and a corresponding electrolyte solution to fulfil the requirements for an electrochemical cell.

The electrode surfaces in this cell represent the intersection between the ionic and electronic conductor. The working electrode is the electrode which responds to the target substrate, the reference electrode is of a constant potential which is independent of the interactions in the working solution.

1.22.2 Potentiometry

Potential sweep based experimentation takes into consideration the effects of the measured current arising from the potential of the WE which is swept from potential value V_1 to V_2. The rate at which this potential sweep occurs is referred to as the scan rate (V s^{-1}). In cyclic voltametric analysis, the original potential sweep can be extended so that when the value of V_2 is reached, the direction of the sweep is reversed, and the electrode potential is scanned in reverse to the original value of V_1. The current to time relationship of such measurements can be determined through the resulting concentration to time profiles. The region within the electrode which becomes depleted to reactants is known as the diffusion layer.

1.22.3 Cyclic Voltammetry

Cyclic voltammetry is the most common technique used for formulating qualitative data to elucidate electrochemical interactions. It involves the identification of the redox potential of a target electro-active species and provides information about the thermodynamics of a redox process, heterogeneous electron transfers kinetic reactions, coupled electrochemical reactions and adsorption processes. In cyclic voltametric analysis the potential is linearly scanned of the working electrode through

a triangular potential waveform and depending on the measurements sought, the use of single or multiple cycles can be performed.

During a potential sweep, the potentiostat measured the current that resulted due to applied voltage and the plot of current (ampere) vs potential (voltage) is dependent on time alongside myriad of other chemical and physical properties. A typical redox couple (reversible) for Hexaammine ruthenium(III) chloride vs a glassy carbon electrode is demonstrated showing the oxidation (Blue) and reduction (red) peaks in a reversable system (Fig. 1.8).
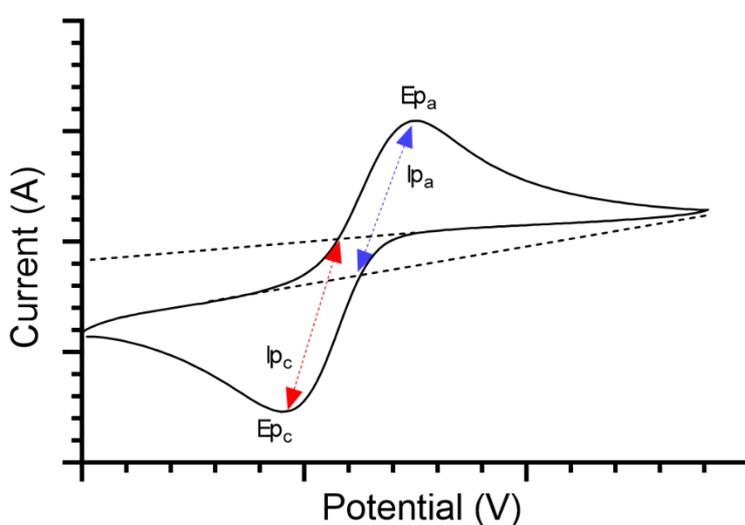
Figure 1. 8. A typical cyclic voltammogram for a reversable redox processes using 1 mM Hexaammine ruthenium(III) chloride in 0.1 M KCl using a standard glassy carbon electrode. Figure adapted from (Garcia-Miranda Ferrari et al., 2018).

There is a significant amount of information can be acquired from a cyclic voltammogram such as the electrochemical working area of the working electrodes and the overall heterogenous electron transfer rate kinetics. For this work, particular

interest was given to the onset potential, and the magnitude of the Faradaic redox peaks.

The current magnitude (i) which is produced in response to an electroactive species being oxidised, or reduced can be determined by the flux value given: (Fisher, 1996; Compton and Banks, 2011)

$$i = -nFAJ \qquad [2]$$

Where, n is the number of electrons involved in the reaction, F is the Faraday's constant, and A is the working electrode area. In this equation, J is the only value with variability, and co-dependant with current. J can thus be described as the number of molecules which are penetrating past the imaginary line to arrive at the surface of the working electrode as is denote with the units: mol s^{-1} cm^{-2}.

In cyclic voltammetry, there are three scenarios which determine the movement of molecules via mass transport within an electrolytic solution; 1) Convection which involves the force movement of the electrolyte through instances such as stirring, electrolyte temperature variations, and induced electrolyte flow. 2) Diffusion, which is the concentration gradient based movement of charged and uncharged ions through the electrolyte and 3) Migration, the induction of an electric field, which is generated by two electrodes at different potentials, attracting or repelling the charged ions. Electrochemical systems which are controlled by diffusional electron transport J can be elucidated using Fick's 1st law of mass transport, demonstrated by the following equation: (Bard and Faulkner, 2001; Compton and Banks, 2011)

$$J(x,t) = -D\frac{\partial c(x,t)}{\partial x} \qquad [3]$$

Where, $\frac{\partial c}{\partial x}$ is the concentration gradient at distance *x, t* is time, and D is the diffusional coefficient.

Time and distance to the concentration relationship are introduced by Fick's 2nd law:

$$\frac{\partial c}{\partial t} = D \frac{\partial 2c}{\partial x2} \qquad [4]$$

In the instance where convection, diffusion and migration are all occurring simultaneously within a system, different models of mass transport must be utilised. The relationship between the three transport mechanisms can be described using a one dimensional process using the Nernst-Planck equation: (Compton and Banks, 2011)

$$J(x,t) = -D \ \partial C(x,t)/\partial x - zFDC(x,t)/RT \ \partial \varphi(x,t)/\partial x \ \varphi + CV(x,t) \qquad [5]$$

Whereby, $\partial C(x,t)/\partial x$ demonstrates the potential gradient, z is the charge of the electroactive species and *V(x,t)* is the hydrodynamic velocity in aqueous media.

Finally, taking flux into consideration, it is possible to construct a general expression for the current response through the combination of the previous equations:

$$i = -nFAD \ \frac{\partial c(x,t)}{\partial x} \qquad [6]$$

Cyclic voltammetry offers an indispensable tool for the determination of the experimental electrochemical rate constants. Initial calculations devised by Nicholson provided a basis for the calculation of k^0, the electrochemical rate constant from the peak potential separation measured during a cyclic voltametric scan. This method is routinely utilised to determine the standard heterogenous electron transfer rates of quasi-reversable systems (Nicholson, 1965).

The distinguished peaks in a cyclic voltammogram are attributed to the diffusion layers which occur near the electrode surfaces. These resultant current peaks are a direct reflection of the continual change in the analyte concentration gradient over time. Thus, increasing and decreasing peak current can be attributed to the establishment of diffusion control.

A cyclic voltammogram characterises the voltametric response of two observed peak currents (I_p) and peak potentials (E_p) for the basis of this analysis. The resulting peak current for a reversible redox couple is determined by the *Randles-Sevcik* equation: (Brownson and Banks, 2014)

$$I_P = 2.65 \ x \ 10^5 n^{3/2} D^{1/2} v^{1/2} C A_{eff} \qquad [7]$$

Where, *I* is the experimentally determined peak current, *n*, is the number of electrons per molecule involved in the electrochemical process, *D* is the diffusion coefficient of the target analyte (in $cm^2 \ s^{-1}$), *u* is the applied voltametric scan rate ($V \ s^{-1}$), *C* is the concentration of the electroactive analyte (mol cm^{-3}) and A_{eff} is the electrochemical effective area. In this formula, the current is proportional directly to the analyte concentration, and is shown to increase, linearly with the scan rate. In simple redox reversable systems, the forward – reverse peak currents should be equivalent; however, these peak ratios can be rapidly influenced by chemical reactions which are in tune with the redox system (Brownson and Banks, 2014).

1.22.4 Determination of the Heterogeneous Electron Transfer Rate kinetics (K°)

The heterogeneous electron transfer kinetics rate constant values can be calculated using the Nicholson equation, should the reaction demonstrate an electrochemically *quasi*-reversible process (Nicholson, 1965).

$$\varphi = k^0 \left[(\pi D n v F)/(RT)\right]^{-1/2} \qquad [8]$$

Where, φ is the kinetic parameter which is represented as a function of peak to peak separation (ΔE_p) at a temperature of 298 K for a one step, one electron process.

1.23 Redox Probes

Outer sphere redox probes such as hexaamineruthenium(III) chloride are often described as surface insensitive thus, surface oxygen: carbon ratios alongside any other surface specific characteristics in relation to surface oxygen-carbon ratio, current surface state/ or cleanliness with respect to a monolayer film surface coating of uncharged absorbates, or any additional specific adsorption to surface groups, should not have a profound influence on the k^0 values determined. In these instances, the measured electrochemical response should only be dependent on the electrode material's electronic structure with the surface and should mainly serve as a source of electrons. As such, outer sphere systems are sensitive primarily to the electronic structure due to the density of electronic states near the Fermi level.

Inner sphere redox probes on the other hand, such as potassium ferrocyanide(II), are suggested as being more surface sensitive thus, result in k^0 values being more strongly influenced by the electrode if it is obscured by adsorbates or impurities. Moreover, such interactions may also depend heavily on the presence or absence of

specific oxygenated species which give rise to either beneficial or negative electrochemical effects (Elgrishi et al., 2017). In this instance, electrochemical systems are more strongly influenced by the surface state and possibly require specific surface functional groups rather than DOS as these systems have high reorganisation energies (Eckermann et al., 2010).

1.24 Instrumentation

Electrochemical amperometric sensors are operated in electrochemical non-equilibrium, and the simplest case is the polarisation of the working and a combined counter/reference electrode system. This is true for a significant majority of electrochemical devices whereby the potential difference is determined between the anode and cathode. As such it is denoted as a "two electrode system". However, in systems where a consistent applied potential is required, a three electrode system consisting of a working, reference and counter electrode is preferential. A three electrode system involves the use of a working, reference and counter electrode and is used and connected to a high input potentiostatic device. In this work, a 3-electrode system was opted for use, as the study aimed to use specific potential measurements at the surface of the electrode, which would enable the isolation of the oxidation and reduction peaks of the target biomolecule, cadaverine.

1.25 Limits of Detection

Limit of the blank (LOB), limit of detection (LOD) and limits of quantification (LOQ) are terms which describe the minimal concertation of a measured molecule, which can be effectively measured using an analytical technique (Armbruster et al., 1994). The

current guidelines of clinical laboratory measurement procedures EP17 demonstrate the standard methods for deducing the necessary values for what constitutes as the LOD (Armbruster and Pry, 2008). The limit of the blank is the maximum apparent concentration of the analyte determined when samples which contain no analyte are measured. Samples with no analyte are tested during LOB measurements, however, blank samples are able to produce analytical signals which many be demonstrative of low concentration analytes. The LOB demonstrates 95% of the measured values under the pretext of Gaussian distribution thus, the remaining 5% of the blank values demonstrate a potential response which may be replicable of a low concentration of analyte. The limit of detection is the minimum concentration of analyte which is to be distinguished from the LOB whereby detection is possible. The LOD is therefore always greater than the LOB.

In summary, periodontal disease is a major disease, with many systemic effects, and afflicts a major proportion of the global population. Current methods of assessment are insufficient thus, biosensing may be a solution to providing real-time, non-invasive measurements into the active disease status of periodontal disease.

CHAPTER 2

Materials and Methods

2.1 Materials

2.1.1 Biosensor Formulation and Testing

1-ethyl-3(3-Dimethylaminopropyl)Carbodiimide (Sigma-Aldrich, UK)

2-(N-morpholino)ethanesulfonic acid (Sigma-Aldrich, UK)

Ag/AgCl paste (product code C2040308D2; Gwent Electronic Materials Ltd., UK)

Carbon graphitic ink (Gwent Electronic Materials Ltd, UK)

Dielectric paste (Gwent Electronic Materials, UK)

Dimethylsulphoxide (Sigma-Aldrich, UK)

EmStat3 computer controlled potentiostat (Palmsens, Netherlands)

Ethanol (Sigma-Aldrich, UK)

Flexible polyester film (Autostat, Italy)

Glutaraldehyde (Sigma-Aldrich, UK)

H_2SO_4 (98%) (Sigma-Aldrich, UK)

HNO_3 (70%) (Sigma-Aldrich, UK)

HPLC grade water (BDH, UK)

Hydrogen chloride (Thermo Fisher Scientific, UK)

MWCNTs (Sigma-Aldrich, UK)

N-Hydroxysuccinimide (Sigma-Aldrich, UK)

pH meter (Hanna Instruments, UK)

Phosphate buffer (Sigma-Aldrich, UK)

Quartz glass high precision cuvette (Hellma Analyticis, UK)

Silicon wafer squares (Montco Silicon Technologies inc, USA)

2.1.2 Cell Biology

0.45 µm PTFE membrane filter (Thermo Fisher Scientific, UK)

Aluminium SEM mounts (Agar, Scientific, UK)

Bovine serum albumin (Fisher Scientific, UK)

Brain Heart infusion agar (Sigma-Aldrich, UK)

Brain heart infusion broth (Sigma-Aldrich, UK)

Cell counting kit-8 (Tebu-bio, UK)

Dulbecco's phosphate buffered saline (Sigma-Aldrich, UK)

Fluorescein isothiocyanate (FITC)-conjugated anti-human CD11c antibody (Clone

Bu15; BioLegend, UK)

Foetal bovine serum (Lonza, UK)

Haemin (Sigma-Aldrich, UK)

Horse Blood (TCS Biosciences, UK)

Immortalized Human Kidney proximal Tubule cells (ATCC, UK)

Interferon gamma (Sigma-Aldrich, UK)

Light microscope (Gtvision, UK)

Menadione (Sigma-Aldrich, UK)

Methanol (Thermo Fisher Scientific, UK)

Microplate reader (Thermo-Scientific Multiskan 60, UK)

Nutrient agar (Oxoid, UK)

Nutrient broth (Oxoid, UK)

Orbital shaker (New Brunswick Scientific, USA).

Paraformaldehyde (Sigma-Aldrich, UK)

Penicillin – streptomycin (Lonza, UK)

Phalloidin–tetramethylrhodamine B isothiocyanate conjugate from Amanita phalloides
(Fluka, Germany)

Phorbol 12-myristate 13-acetate (Applichem, Germany)

Saline tablets (Sigma-Aldrich, UK)

TC10 automated cell counter (Bio-Rad, USA)

Trypan blue (Lonza, UK)

Trypsin EDTA (Lonza, Belgium)

Tris base (Fisher Scientific, UK)

Tris hydrochloride (Fisher Scientific, UK)

Tris (hydroxymethyl) aminomethane (THAM) hydrochloride (Fisher Scientific, UK)

Triton X-100 (Lonza, Belgium)

Tween-20 (Fisher Scientific, UK)

U937 Human monocytic cell line (Health Protection Agency Culture Collections, UK)

Ultrasonic bath (Ultrawave, UK)

2.2 Methods

All chemicals used in this study were of analytical grade or higher unless stated otherwise. All solutions were prepared with Type 1 Milli-Q water with resistivity no less than 18.2 MΩ cm. This solution was vigorously degassed prior to electrochemical measurements with oxygen free nitrogen. This was carried out to ensure the removal of any trace levels of oxygen from the test solutions, which if present would convolute the electrochemical results.

2.2.1 Fabrication of Screen-Printed Electrodes (SPEs)

The screen-printed electrodes (SPEs) were fabricated in-house with stencil designs. A carbon graphitic ink formulation was screen-printed using a microDEK 1760RS screen printing machine (DEK, UK) onto a flexible polyester film (denoted throughout as SPE). The parameters used for the printing device were, print speed – 100 mm/s, flood speed – 100 mm/s, print gap – 0.05 mm. The layer of carbon graphitic ink was cured in a fan oven at 60 °C for 30 min. A silver/silver chloride reference electrode was incorporated onto the SPE by screen-printing Ag/AgCl paste onto the polyester substrate. A dielectric paste was printed onto the polyester flexible film substrate to cover the connections. The SPE was put through a second curing processes at 60 ℃ for 30 min. The SPEs were stored at 4 °C until ready for use. For the purpose of this work, electrochemical experiments were performed using the entire SPE with built in reference and counter electrodes, or only the working electrode with external reference and counter electrodes, which allowed for direct comparisons between all the electrodes used.

2.2.2 Multi-Walled Carbon Nanotube (MWCNT) Suspensions

Individual carbon nanotube suspensions were prepared in 1 mL aliquots for comparison purposes. MWCNTs were placed in a low retention Eppendorf tubes to minimise carbon complex formations. Two milligrams of MWCNT were added to each of 10 mL deionised H_2O (dH_2O), 100% ethanol, 2-(N-morpholino)ethanesulfonic acid (MES), and diamine oxidase solution in phosphate buffer (enzymatic solution) and ultra-sonicated at 42 KHz for 20 min to evenly disperse the MWCNTs.

2.2.3 Carboxylation of MWCNTs

An acidic solution containing 7.5 mL H_2SO_4 (98%) and 2.5 mL HNO_3 (70%) was used to incorporate carboxyl groups onto the MWCNTs outer surfaces. For complete carboxylation, 2 mg of MWCNTs were sonicated in acidic solution for 6h at 80 °C. After completion of the acid etching, the carboxylated MWCNTs (C-MWCNTs) were washed with dH_2O, and vacuum filtered until a pH of 7.2 was achieved to ensure removal of any residual acids and were dried in an oven at 90 °C overnight.

2.2.4 EDC-NHS Coupling of C-MWCNTs

To effectively couple the diamine oxidase enzyme to the C-MWCNTs, a two-step procedure was undertaken. Two milligrams of C-MWCNTs were suspended in 5 mL of water and sonicated for 10 min, followed by elution in 1 mL of MES buffer solution (pH 6.5) and a 2.2 mL of a 50 mg/ mL^{-1} NHS solution which was vortexed for 2 s. With

continual stirring at room temperature for 30 min, 1.2 mL of a 10mg/ mL^{-1} EDC solution was added to the C-MWCNT to complete the EDC-NHS coupling reaction. The C-MWCNT/EDC-NHS solution was filtered through a 0.45 μm PTFE membrane filter and rinsed using 5 mL of 50 mM MES buffer solution (pH 6.5) to remove any unconjugated EDC, NHS or cross linked urea. The C-MWCNTs were dried in a class II cabinet for one hour before being stored at 4 °C until required.

2.2.5 Preparation of DAO conjugated MWCNT/EDC-NHS

Two milligrams of MWCNTs/EDC-NHS in 2 mL of MES (50 mM at pH 6.5) were added into 1 mL of DAO solution (10 mg/ mL DAO in 0.1 M phosphate buffer) and the mixture was incubated at 37 °C for 1h under constant shaking (200 *rpm*) to allow for conjugation of the enzyme to preformed amine group complexes. Crosslinking was performed via the addition of 1 mL of a 0.2% glutaraldehyde solution to the C-MWCNT/EDC-NHS/DAO solution, and the suspension was incubated at room temperature under constant shaking for 30 min, followed by an overnight incubation at 4 °C. After the overnight incubation, the C-MWCNT/EDC-NHS/DAO/GA suspension was treated with Tris buffer (100 mM at pH 7.2) for 30 min and washed to remove unconjugated enzyme and glutaraldehyde. The crosslinked C-MWCNT/EDC-NHS/DAO/GA were suspended in 0.1 M MES buffer and stored at 4 °C until ready to use.

2.3 Surface Roughness Measurements

Optical Profilometry was used to obtain the surface topography (roughness parameters) of the carbon electrode surfaces pre- and post MWCNT conjugation. Analysis of the surface roughness was carried out qualitatively via images and quantitatively by using S values: S_a, S_q and S_{pv} (arithmetical mean height, mean square roughness and mean maximum height respectively) (Zemaps software [version 1.14.38]) ($n = 6$). The average peak and valley height and widths were also determined ($n = 10$).

2.4 Water contact angle measurements

Contact angle measurements of the carbon electrode surfaces pre- and post C-MWCNT/EDC-NHS/DAO/GA modification were determined at room temperate using the sessile drop technique (Amin et al., 2020). HPLC grade water at a droplet size of 5 µL was deposited onto the horizontally laid working electrode, and measurements were recorded using a goniometer with surface contact angle images being analysed using Kruss SW23 (DSA2) (Kruss, Germany) software ($n = 3$).

2.5 Fourier Transform Infra-Red Spectroscopy (FTIR)

MWCNTs which were unmodified and modified were analysed using FTIR to determine new bond formation. MWCNTs at a volume of 15 µL were deposed onto 10 mm x 10 mm silicon wafers and dried in a class II cabinet for 1 h. Samples were stored in a desiccator until ready for use. A Thermo-Winslet Continuum FTIR-ATR microscope was used for the analysis of the MWCNTs. The attachment used was a

type A MCT detector. The aperture was used at 200 mm × 200 mm, and the spectra of the unmodified and modified electrodes was acquired using Omnic 5.2 software.

2.6 Scanning Electron Microscopy (SEM) and Energy Dispersive X-Ray Spectroscopy (EDX)

MWCNT suspensions (unmodified MWCNT and C-MWCNT/EDC-NHS/DAO/GA) were prepared by pipetting 10 µL of the sample solution onto 10 mm x 10 mm silicon wafer squares (Montco Silicon Technologies inc, USA) and dried in a class II cabinet for 1 h. The dried samples were submerged in 4% *v/v* glutaraldehyde overnight, followed by dehydration of the MWCNT via an ethanol series of 30%, 50%, 70%, 90% and 100% *v/v*, respectively for 10 min. The electrodes were mounted on aluminium SEM mounts with double sided conducting carbon tabs (Agar Scientific, UK). Prior to imaging the electrode surfaces were sputter coated with gold-palladium and imaged using a Zeiss Supra 40VP field emission gun scanning electron microscope (Zeiss, UK) using the following parameters: acceleration voltage, 2.00 kV; working distance, 4.1−4.5 mm; SE2 detector, magnification at 10 000x. EDX analysis was also carried out alongside the SEM and was utilised to determine the chemical compositions of the carbon nanotube modifications. Measurements were made using an EDX Sapphire Si (Li) detector and quantified using a standardless ZAF algorithm. The chemical composition was calculated as an atomic percentage, giving the percentage of the atom relative to the total number of atoms per scan ($n = 3$).

2.7 Enzyme-Substrate Uptake

Increasing concentrations (0.25 U, 0.5 U, 1.0 U, 1.5 U, and 2 U) of diamine oxidase was added to a 96-well plate at a volume of 10 µL. To each well which contained enzyme, 10 µL of O-dianisidine dihydrochloride was added and mixed to allow for homogenisation into the wells. A microplate reader (Thermo-Scientific Multiskan 60, UK) was set up at an absorbance of 450 nm and was programmed to read each well in 4 s intervals over a 10 min duration. The 96-well plate was loaded into the microplate reader and 10 µL of a 30 µg/mL cadaverine suspension was added to each well, mixed ensuring no bubbles were introduced to the wells and the absorbance measured ($n = 3$).

2.8 UV-Vis Spectroscopy

Bulk MWCNTs and C-MWCNTs were prepared in 2 mg aliquots and suspended in 2 mL of 100% ethanol prior to UV-Vis analysis. A quartz glass high precision cuvette (Hellma Analyticis, UK) was used for all absorbance readings and 2 mL of 100% ethanol was used for calibrations. For the UV-Vis analysis of the MWCNT a Thermo scientific Evolution^{TM} 201 UV-Visible spectrophotometer was used, and spectra were recorded using the INSIGHT^{TM} software at the 1000 to 200 nm range ($n = 3$).

2.9 Raman Spectroscopy

Raman spectroscopy was performed on the MWCNT modifications using a DXR Raman microscope (Thermo scientific, UK) fitted with a 532 nm excitation laser at a low power of 3 mW to avoid heating effects. Spectra were recorded using a three second exposure time for three accumulations at each point ($n = 6$).

2.10 Electrochemical measurements

Electrochemical measurements of the modified carbon electrodes were carried out using an EmStat3 (Palmsens, Netherlands) computer controlled potentiostat, utilising the PStrace software. Measurements were taken using a three electrode system, with a nickel wire counter electrode, an Ag/AgCl reference electrode with the screen-printed modified carbon working electrode, completing the circuit. All measurements were made at room temperature in a cell consisting of a supporting electrolyte solution of 0.1 M KCl at pH 7.0 under continual stirring. In each instance of testing, 10 repeat SPEs were used per concentration of analyte, in each variable condition ($n = 10$).

2.10.1 Electrochemical Characterisation of the Modified SPEs

The redox probes used in this study were hexaamineruthenium(III) chloride and potassium ferrocyanide(II) which were prepared individually in solution at a concentration of 1 mM with 0.1 M KCl acting as a supporting electrolyte. The electrodes were initially characterised using cyclic voltammetry with the outer redox probe, $[Ru(NH_3)_6]^{3+/2+}$ at a concentration of 1 mM in 0.1 M KCl The following scan rates were used: 5 mV s, 10 mV s, 15 mV s, 25 mV s, 50 mV s, 75 mV s, 100 mV s, 150 mV s, 250 mV s and 500 mV s. The electrochemically effective area (A_{eff}) of the modified electrode was determined using the Randles-Ševčík equation for an electrochemically *quasi*-reversible process (Garcia-Miranda Ferrari et al., 2018) :

$$I_{p,f}^{quasi} = \pm 0.436\, nFA_{real}C\sqrt{\frac{nFDv}{RT}} \qquad [9]$$

Where, $I_{p,f}$ is the voltammetric peak current (analytical signal) determined using the forward peak for a *quasi*-reversable process, F is the Faraday constant in C mol^{-1}, n is the number of electrons per molecule involved, D is the diffusion coefficient in cm^2 s^{-1}, v is the voltammetric scan rate in V s^{-1}, R is the universal gas constant, T is the temperature in K, A_{real} is the electroactive area of the electrode in cm^2, and C is the concentration of the analyte.

The Heterogenous Electron transfer (HET) rate constant (k^0) was calculated using the Nicholson equation for an electrochemically *quasi*-reversable process, as described in the following equation:

$$\varphi = k^0 \left[(\pi D n v F)/(RT) \right]^{-1/2} \qquad [10]$$

Where, φ is the kinetic parameter which is represented as a function of peak to peak separation (ΔE_p) at a temperature of 298 K for a one step, one electron process.

The function of ΔE_p which fits the equation for practical by making the evaluation of the rate constant simpler and extends the Nicholson parameter towards significantly higher/lower peak potentials, as demonstrated by Metters et al., (2013) and Randviir (2018).

$$\varphi = (-0.6288 + 0.0021X)/(1 - 0.017X) \qquad [11]$$

Where, X is equal to ΔE_p and is used to determine φ as a function of ΔE_p from the experimentally measured voltammogram. As a result, φ against $[(\pi D n v F)/(RT)]^{-1/2}$ can be plotted, enabling the determination of k^0 from the gradient. The k^0 values were calculated assuming the diffusion coefficient for hexaammineruthenium(III) chloride was 9.10×10^{-6} cm^2 s^{-1}.

2.11 Human Kidney Proximal Tubule (HK-2) Cell Culture

Immortalized human kidney proximal tubule cells (HK-2) (ATCC, UK) were cultured in 50:50 glucose free DMEM (Invitrogen, UK) and Ham's F-12 medium (Lonza, UK) supplemented with 10% fetal bovine calf serum (Lonza, UK), 50 µg/mL streptomycin (lonza, UK), 50 µg/mL penicillin (Lonza, UK) and 2.5 mMol glutamine (Lonza, UK).

2.11.1 Maintenance of HK-2 Cells

HK-2 cells were maintained at 37 °C in a 5% CO_2 incubator. The cell culture media was changed every other day to produce cell confluency. When the required cell confluence was attained, trypsin-EDTA (Lonza, UK) was used to dislodge adherent cells from the cell culture flasks to allow for reseeding and continuation of culturing. To seed the cells, 0.4% trypan blue solution was used to determine cell viability at a 1:1 (*v/v*) ratio with the cell suspension. Cellular viability was measured using a TC10 automated cell counter, and the number of viable cells was used to calculate the number of seeded cells per well.

2.11.2 Preparation of RPMI 1640 Complete Medium

Foetal bovine serum was heat inactivated in a water bath maintained at 57 °C for 30 min. RPMI 1640 media (L-Glutamine and 25 mM HEPES) was supplemented with 10% FBS and 100 I.U/mL penicillin-streptomycin was prepared under aseptic conditions.

2.11.3 U937 Monocyte Cell Culture

U937 monocyte were cultured using RPMI-1640 complete medium at 37 °C and 5% CO_2. The U937 monocyte cell suspensions were centrifuged at 500 g for 7 min before media aspiration. The cells were maintained at 0.5 x 10^6 cells/mL by the resuspension in fresh RPMI-1640 media every second day. Cell viability was confirmed using sterile filtered trypan blue 0.4% using a 1:1 ratio of trypan blue to cell suspension, with non-viable cells absorbing the dye and being recoded using a TC10 automated cell counter (Bio-rad, USA). The required viability was above 80% for each experiment.

2.11.4 Monocyte Differentiation to M0 Macrophages

U937 monocytes were differentiated into macrophage-like cells by first incubating 1 x10^6 cells/mL with 50 ng/mL phorbol 12-myristate 13-acetate (PMA) in RPMI complete medium for 24 h at 37 °C in 5% CO_2. The cells were washed twice with RPMI complete medium and re-incubated for 48 h in PMA free RPMI complete media to fully differentiate the monocytes into inactivated M0 macrophages.

2.11.5 Flow Cytometry for Confirmation of Monocyte to M0 Macrophage Differentiation

Differentiation of U937 monocytes into M0 macrophages was confirmed by flow cytometry via analysis of CD11c+ surface marker expression. Monocytes and M0 macrophages were seeded in to 1 mL of RPMI 1640 complete medium at a density of 1 × 10^6 cells/mL in 12-well plates according to methods described in *Monocyte*

differentiation to M0 Macrophages. Adherent macrophages were detached from six replicate wells by removing the supernatant and adding 250 μL trypsin EDTA for 3 minutes at 37 °C and 5% CO_2. The trypsin EDTA was neutralized via addition 250 μL RPMI 1640 complete cell culture medium before being washed (centrifugation of well constituents at 500 g for 7 minutes and resuspension of the cell pellet) in 1 mL complete medium. Cells were washed twice in 200 μL DPBS. Half the fixed macrophage samples (n = 3) and half the fixed monocyte samples (n = 3) were stained for 30 minutes at RT with FITC-conjugated anti-human CD11c antibody diluted 1:40 with 10% FBS in DPBS. The remaining fixed monocyte (n = 3) and fixed macrophage (n = 3) samples were prepared as unstained negative controls by incubating at RT for 30 min with 10% FBS in DPBS lacking antibody. Unbound antibody was removed from samples by two sequential wash steps in DPBS, before resuspension in 500 μL DPBS. CD11c surface marker expression was assessed on 10,000 events (live, individual cells) using a BD Accuri C6F1 cytometer (BD Biosciences, USA). Data was analysed with BD Accuri C6 Software after gating events in the forward scattered channel (FSC)/side scattered channel (SSC) and fluorescence parameter 1 (FL1-A) windows. The average percentage CD11c+ cells (%) and median fluorescence intensity (MFI) were determined relative to unstained negative control U937 monocytes.

2.12 Bacterial Culture Media Preparation

Brain heart infusion agar (BHI) was used as a base for culturing bacteria for this work. To a 500 mL Duran of molten sterile BHI agar which had been cooled to under 50 °C, 10% (v/v) horse blood, 7.67 uM haemin, and 2.91 uM menadione was added to make the periodontal microorganism growth media. Similarly, BHI broth supplemented with

10% (v/v) horse blood, 7.67 uM haemin, and 2.91 uM menadione was used for inoculation of bacterial cultures prior to use for experimentation.

2.12.1 Preparation of Bacterial Cultures

Porphyromonas gingivalis (NCTC 11834) was cultured on BHI agar supplemented with 10% (v/v) horse blood, 7.67 uM haemin, and 2.91 uM menadione and incubated in an anaerobic cabinet at 37 °C in 5% CO_2 for 72 h or until colonies became apparent. The colony forming units (CFU) for *P. gingivalis* were counted on periodontal blood plates and used to calculate the density of bacteria (CFU/mL), taking into consideration the dilution factor.

When required for experimental procedures, *P. gingivalis* was cultured in periodontal blood broth for 48 h at 37 °C in an orbital shaker. The *P. gingivalis* broths were centrifuged at 3000 *g* for 10 min and, the supernatant discarded. The pelleted bacteria were washed twice with sterile water before re-suspending in 10 mL of sterile water. The bacteria were measured to an optical density of 1.0 ± 0.1 using a spectrophotometer, which was calibrated using water.

2.12.2 Colony Forming Units (CFU)

The CFU/mL of *P. gingivalis* was determined using the Miles-Misra droplet method (Miles et al., 1938). Serial dilutions were carried out up to 10^{-8} in triplicate with three replicate 20 μL droplets of each serial dilution was plated onto periodontal blood agar plates, which were divided into eight segments. The agar platea were incubated under anaerobic conditions at 37 °C in 5% CO_2 for up to 72 h, or until growth was apparent. The segment which the lowest dilution factor and countable colonies between 3 and

30 were chosen. The average number of colonies from replicate plates were recorded and used to calculate the CFU/mL [12] and standard error of the replicates using the following formulae [13]:

$$Colony\ Forming\ Units\ per\ mL = \frac{Number\ of\ colonies\ X\ Dilution\ factor}{Volume\ of\ culture\ plate} \qquad [12]$$

$$Standard\ Error = \frac{Standard\ deviation\ of\ samples}{\sqrt{Number\ of\ replicates}} \qquad [13]$$

2.13 M0 Macrophage Interaction with *P. gingivalis*

M0 macrophages, generated from U937 monocytes were prepared in 24-well plates as described in *Monocyte differentiation to M0 Macrophages*. Replicate control wells consisting of antibiotic-free RPMI-1640 medium but absent of macrophages was prepared and incubated for 24 h at 37 °C and 5% CO_2. Replicate negative control wells were prepared by treating macrophage-containing wells with 1 x 10^{-7} M bovine serum albumin in antibiotic-free RPMI-1640 medium and incubating for 24 h at 37 °C and 5% CO_2. The supernatant was removed from each well prior to inoculating the macrophages with 1 x 10^4 CFU of *P. gingivalis* in a total of 100 µL of antibiotic free RPMI-1640 containing 1 µg/mL LPS and 100 ng/mL IFN-y (1:1). The bacterially inoculated plates were incubated for 3 h at 37 °C and 5% CO_2 to allow for phagocytosis of the host-pathogen interaction to occur. After the incubation period, the supernatant from each well was collected.

2.13.1 Cell Viability Testing

To determine the effects of cadaverine on mammalian cell viability, concentrations of 3 µg/mL, 15 µg/mL and 40 µg/mL of cadaverine were tested. The cell viability of HK-

2 and U937 monocytes were tested using the cell counting kit-8 (Tebu-bio, UK). Cells were seeded into a 96-well plate at a density of 5 x10^3 cells per well and incubated for 24 h and 48 h at 37 °C in 5% CO_2, to allow for double dosing of the 48 h experiment. The cells were washed after incubation with phosphate buffered saline (PBS) (Lonza, UK) once 80% confluency of the cells had been attained. The cell media was replaced with serum free media for 24 h. After 24 h the serum free media was refreshed and cadaverine was added leaving the cells to incubate for a further 24 h. Controls for each timepoint were used and consisted of HK-2 and U937 monocyte cells exposed to serum free cell culture media, in the absence of cadaverine. The CCK-8 reagent was added to each well at a volume of 10 µL and left to incubate at 37 °C in 5% CO_2 for 1 h, 2 h and 3 h respectively. The absorbance of each well was measured at 450_{nm} and 600_{nm} using a microplate reader (Thermo-Scientific Multiskan 60, UK). For the 48 h incubations, the serum free media and cadaverine containing wells were refreshed after 24 h and re-incubated at 37 °C in 5% CO_2. After 48 h the CCK-8 dye was added and absorbance readings taken as mentioned previously.

2.13.2 Cell Viability Data Analysis

Cell absorbance data was exported to Microsoft excel and the absorbance values at 600_{nm} were deducted from the 450_{nm} absorbance values, and the control wells (CCK-8 reagent without cells) was standardised [14].

$$Cell\ Viability = \frac{((450\ ABS - 600\ ABS) - Blank\ Media\ with\ CCK-8)}{Cell\ Viability\ of\ Cell\ Culture\ Control}\ x\ 100 \qquad [14]$$

The individual standard error percentages were calculated, and graphs plotted using Prism GraphPad 9.1.1 [15]

$$\%\ Standard\ Error = \frac{(Standard\ Error\ of\ Samples)}{Cell\ Viabilty\ of\ Cell\ Culture\ Control}\ x\ 100 \qquad [15]$$

2.14 Cell Migration Assay

The *in vitro* cell migration/scratch assay was adapted (Liang et al., 2007) and was used to investigate the effects of cadaverine on the migration of M0 macrophages and HK-2 cells. M0 macrophages and HK-2 cells were seeded in separate 24-well plates and cultured in their respective growth media until 80% confluent. The growth media was removed from each well from each respective plate, and the cells were washed twice with PBS, after which 1 mL of serum free was media added. After 24 h incubation at 37 °C in 5% CO_2, a scratch was made using a sterile p200 pipette tip, directly across the centre of each well. Any detached cells were removed via sequential washing using serum free media. Cadaverine was prepared in concentrations of 3 µg/mL, 15 µg/mL, and 40 µg/mL using serum free media and 100 µL of each suspension was added to the cells. The cells were incubated at 0 h, 3 h, 6 h, 24 h, 48 h, and 72 h before being imaged using a GXCapture-T camera attached to a light microscope, to calculate the migration of cells over time. The images were analysed using Image J (Schneider et al., 2012), and the macro, MRI Wound Healing Tool (ImageJ) was used to estimate the area of each image, and the value was exported into Microsoft Excel. The percentage wound closure over time was calculated and corresponding graphs were plot.

2.15 Statistical Analysis

Statistical analysis of the results was carried out using Microsoft Excel and export into GraphPad Prism 9, and the unpaired t-tests and one way/two way ANOVA comparison tests were opted for use. In each instance a *p*<0.05 was deemed statistically significant.

CHAPTER 3

Biosensor Development and Characterisation

3.1 Introduction

Disposable screen-printed electrodes are widely utilised in many research fields due to their low costing and ability to be manipulated with ease (Garcia-Miranda Ferrari et al., 2018). Many research methods investigate varying the shape, size and modification of the electrode to achieve a desired effect, such as increased specificity, sensitivity or to eliminate a potential contaminant in the detection media. The use of disposable devices is gaining more traction due to their easy and rapid implication into daily life and has the potential to be implicated into the food and healthcare industries due to ease of use, low cost, and real-time readouts. This chapter elucidates the development of a screen-printed biosensor with a modified working electrode, which consists of MWCNTs which have been functionalised with the enzyme, diamine oxidase. Diamine oxidase was used not only for its selectivity towards cadaverine, but because of its amphiphilic nature, which was hypothesised to aid in the dispersion of MWCNTs in solution. Further work in this chapter determined the surface composition of the electrode and its topography, as these have been previously shown to affect the rate of electron transfer. The rate of electron transfer for the developed biosensor was measured using the known redox couple, ferrocene.

3.2 Results

3.2.1 Screen-Printing Process

The approach of developing biosensors using screen-printed technologies permits the mass production of highly reproducible configurations of electrodes which enable excellent scales of economy. The stencil designs used in the initial printing of the SPEs, consisted of the carbon channels (Fig. 3.1a), the Ag/AgCl reference electrodes (Fig. 3.1b), and the dielectric connection seal layer (Fig. 3.1c).
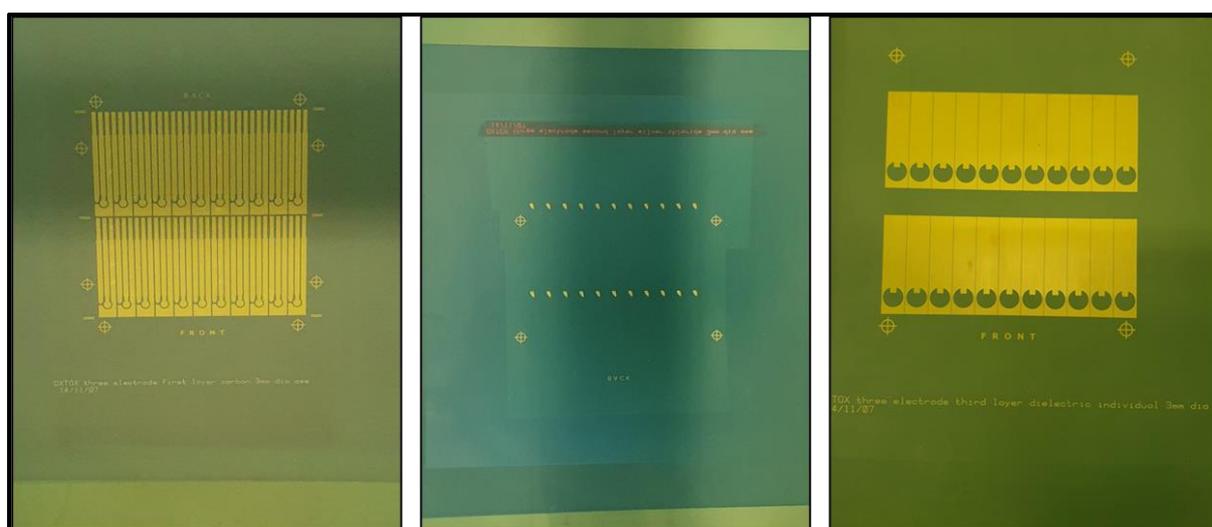
Figure 3. 1. Stencil designs which were used in the fabrication of the screen-printed electrodes a) carbon channels, b) Ag/AgCl reference electrode, and c) dielectric connection seal.

The process of screen-printing the SPEs starting from the initial carbon ink formulation being printed on the polyester flexible film substrate, was carried out using a microDEK 1760RS screen printing machine (Fig. 3.2). Using this process, a SPE with a working electrode diameter of 3 mm and a working area of 0.0707 cm^3 was produced.

Figure 3. 2. A microDEK 1760RS screen printing machine used for the fabrication of the screen-printed electrodes.

The print stencils were placed into the machine and loaded with the desired carbon paste formulation (Fig. 3.3). The squeegee passed the paste over the mesh, depositing the carbon paste onto the underlaying substrate. The squeegee pressure and speed parameters were consistent to maintain the replicability of the printed electrodes.
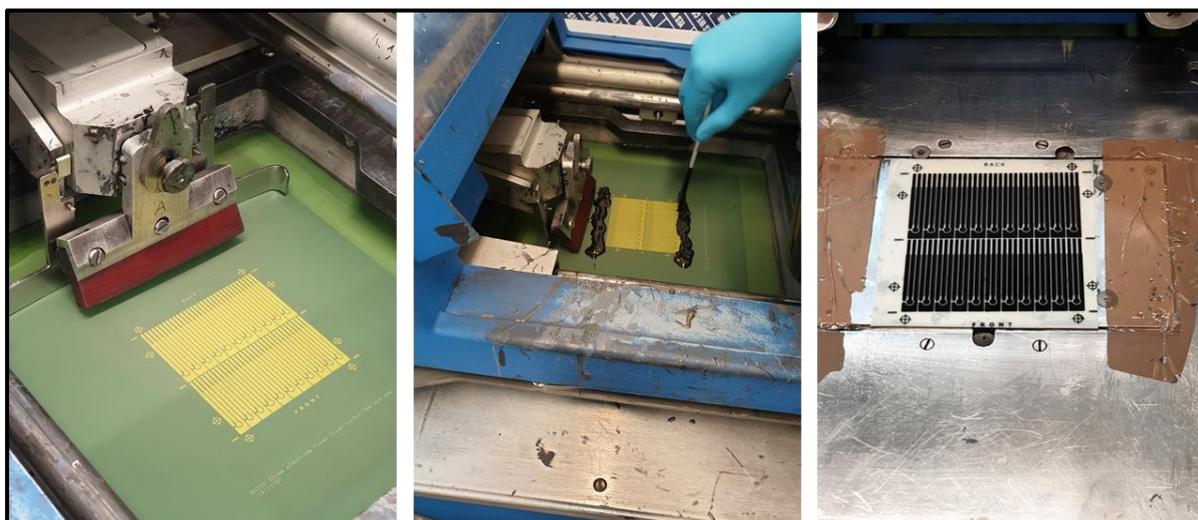
Figure 3. 3. Electrode channel stencil loaded into the microDEK 1760RS screen-printing machine (a) deposition of the carbon graphitic paste (b) to be printed onto the underlaying polyester flexible film substrate. c) The carbon electrode channels printed onto the polyester substrate and cured, ready for subsequent layers to be added.

The next stage involved the deposition of the Ag/AgCl reference electrodes over the existing carbon channels, ensuring the deposition occurred directly on top of the previous layer. A final dielectric sealant layer was applied to the electrode channels to seal the connections from interference, thus completing the electrode (Fig. 3.4).

Figure 3. 4. a) Ag/AgCl paste was deposited onto the mesh stencil and squeegeed across the membrane to allow for even coverage of the target area. b) Cured carbon channels (black) and Ag/AgCl reference electrodes (silver) on the polyester substrates. c) The final dielectric paste layer deposited onto the stencils and applied over the existing carbon electrode channels to seal the connections.

The final electrodes consisted of a carbon paste working electrode and electrode channels, an Ag/AgCl paste reference electrode and a carbon paste counter electrode (Fig. 3.5). The length of the finalised SPE was 43 mm, the width was 7 mm, and the diameter of the working electrode was 3 mm.
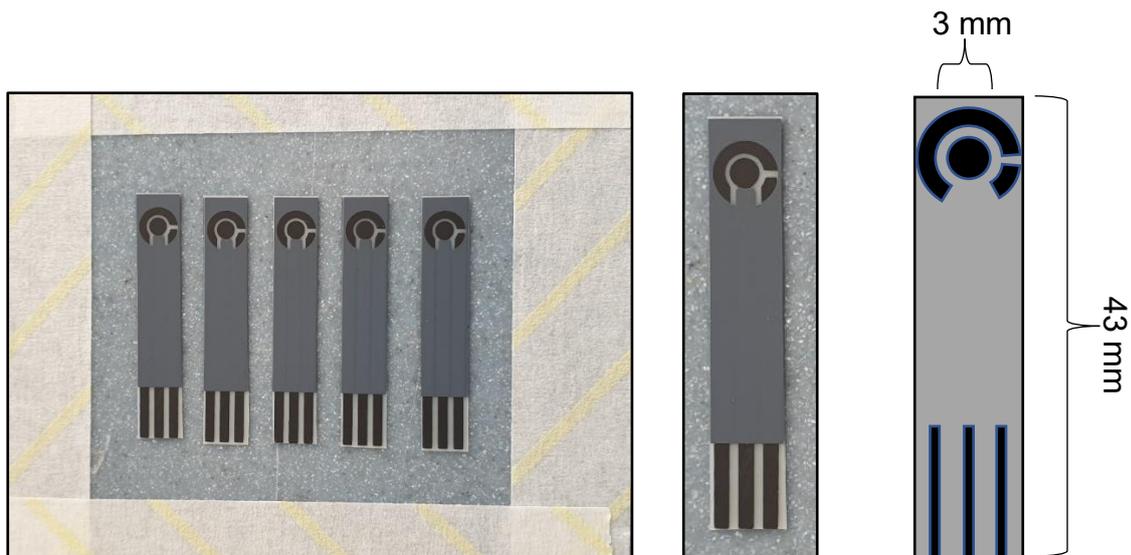
Figure 3. 5. The unmodified screen-printed electrodes. Schematic of the SPEs reproduced with permission from Amin et al., 2022.

3.2.2 MWCNT Suspensions

Since MWCNTs are by nature, hydrophbic and as a result rapidly form aggregates when exposed to water, they were pre- functionalised, or suspended in solvents to homogenously disperse. The inital disperability of MWCNTs in a) dH_2O, b) 100% ethanol, c) MES buffer, and d) enymatic solution consisting of 0.5 U of diamine oxidase in 0.1 M phosphate buffer pH 7.2 was determined (Fig. 3.6). The MWCNTs achived the most homogenous dispersion when suspended in the enzymatic solution (Fig. 3.6d) and remained evenly dispered over 24 h. Similarly, MES (Fig. 3.6c) showed effective initial dispersibility, however, once left unagitated overnight, the MWCNTs reformed aggregates and congregated at the bottom of the universal. The MWCNTs suspended in dH_2O and 100% ethanol solutions intially formed a homogenous solution under ultrasoniction, however, both solutions agrregated immediately and separated from the solution after ceasing soncation and within 2 h of being left undisturbed.
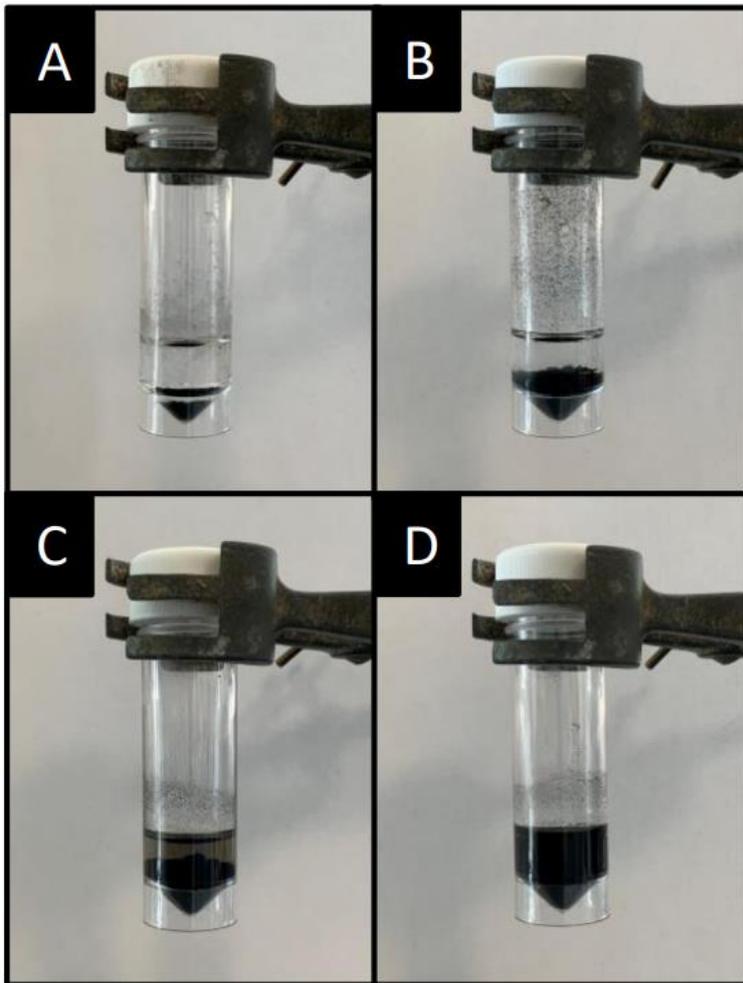
Figure 3. 6. MWCNT suspensions in 10 mL of a) dH$_2$O, b) 100% ethanol, c) MES buffer, and d) diamine oxidase enzymatic solution after ultrasonication for 20 min and left undisturbed for 2 h. Figure adapted from Amin et al., 2022.

3.2.3 UV-Vis Analysis

The UV-Vis spectra of pristine MWCNTs demonstrated absorbance peaks within the 240 nm – 265 nm range, characteristic of MWCNTs. An increase in a distinct peak intensity in the absorbance spectra was observed with the C-MWCNTs due to the increase in percentage surface oxygen, as a result of nanotube carboxylation. The increase in the degree of absorbance, reflected the increase in oxygenation on the

surface of the MWCNTs determined from the spectra (Fig. 3.7) enabled the C-MWCNTs from the carboxylated variants to be differentiated.
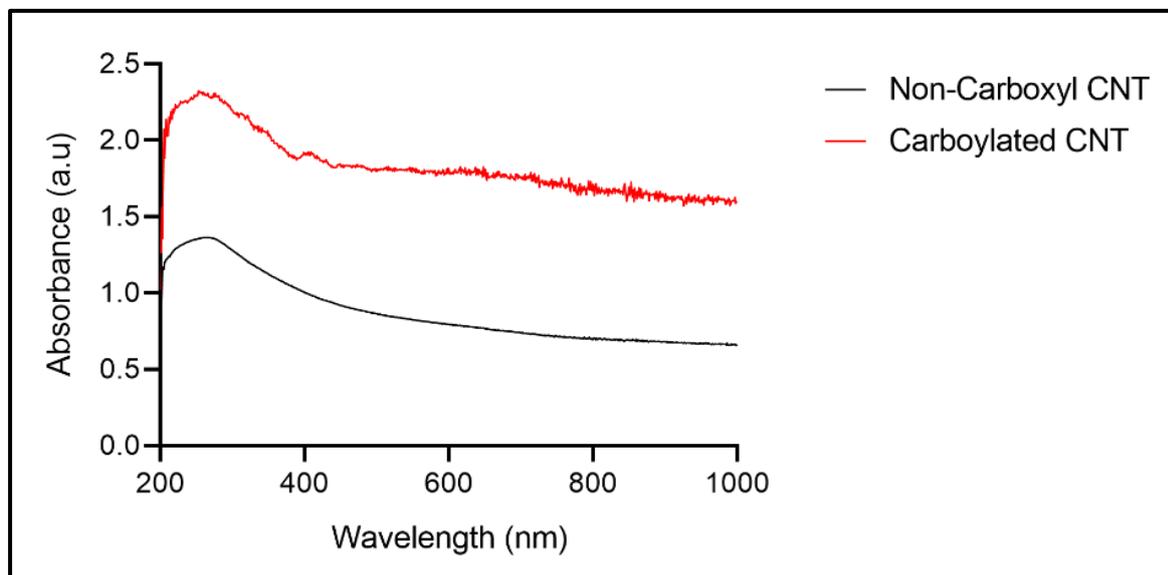
Figure 3. 7. UV-Vis absorption spectra demonstrating the peak intensity shift of MWCNTs (Black) and carboxylated MWCNTs (Red), measured in 100% ethanol.

3.2.4 Drop-Casting Modification of the Working Electrode

The modification of each electrode was carried out using a drop casting approach, whereby an aliquot of the enzyme-carbon nanotube formation was deposited onto the supporting electrode using a micropipette (Fig. 3.8). This deposition was allowed adequate drying time to factor in solvent evaporation. The electrodes were stored at 4 °C to maintain enzyme integrity for future experiments.
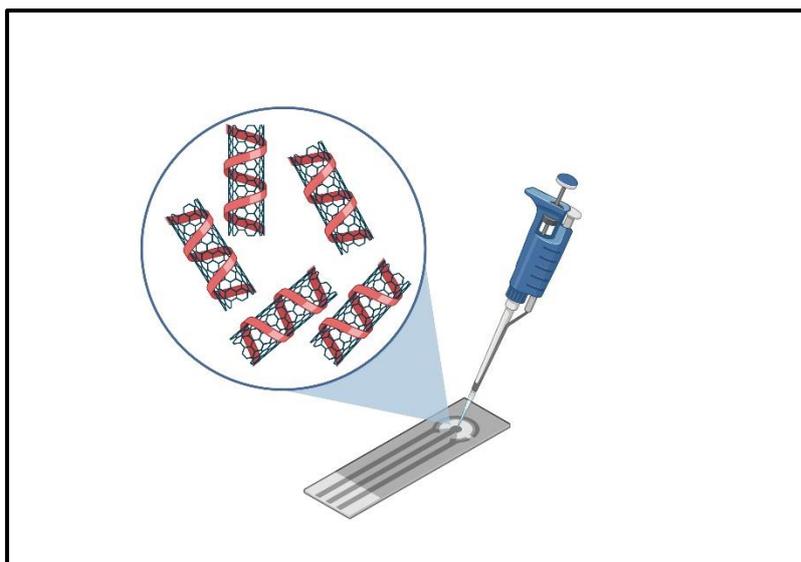
Figure 3. 8. Graphical representation of the drop casting procedure whereby, 10 µL of diamine oxidase-multi-walled carbon nanotube suspensions were pipetted onto the working electrode of the SPE.

3.2.5 Electrode Surface Topography

Surface roughness measurements using optical profilometry were carried out to evaluate the degree of roughness which was influenced by the deposition of the functionalised MWCNTs onto the electrode surfaces (Fig. 3.9). The pre- and post-modified surfaces showed an increase in overall S_a values (post-modified), although this was not significantly different ($p<0.05$). Similarly, the mean square roughness of the surface (S_q) demonstrated an increase in roughness on the SPE after addition of the MWCNT formulation, but again this was not found to be significantly different. However, the mean maximum height of the surface (S_{pv}) showed a significant increase ($p>0.05$) after the application of the MWCNT on to the SPEs due to MWCNT aggregate formation on the upper ridges of the carbon SPE surface. The line profiles for the electrodes were measured to assess the size of the surface features of the electrodes

pre- and post- modification across a normalised X and Y line profile. The results showed that the pre-modified electrode demonstrated the largest peaks and widest valleys at 2.68 µM and 123 nm for the X profile, and 1.04 µM and 58 nm for the Y profile (Fig. 3.10). On the other hand, the largest peaks and valleys on the post-modified electrodes were considerably smaller at, 796 nm and 72 nm for the X profile, and for the Y profile was 771 nm and 16 nm, respectively. However, the X and Y profiles for the post-modified electrodes (Fig. 3.11) demonstrated line profiles which were more homogenous in size and showed less pronounced hills and valleys due to the addition of the enzymatic MWCNT suspension. Overall, the addition of the modification to the electrodes increased surface height, and increased surface homogeneity in comparison to the pre-modified electrode surface.
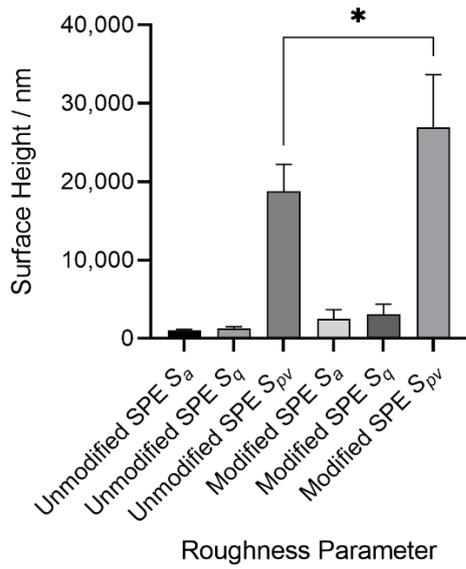
Figure 3. 9. a) Surface roughness measurements (S_a, S_q and S_{pv}) of carbon screen printed electrodes after drop casting of MWCNT formulation. *S* values were determined using optical profilometry. * and *** indicates a *p* value of < 0.05 and < 0.0001 respectively.
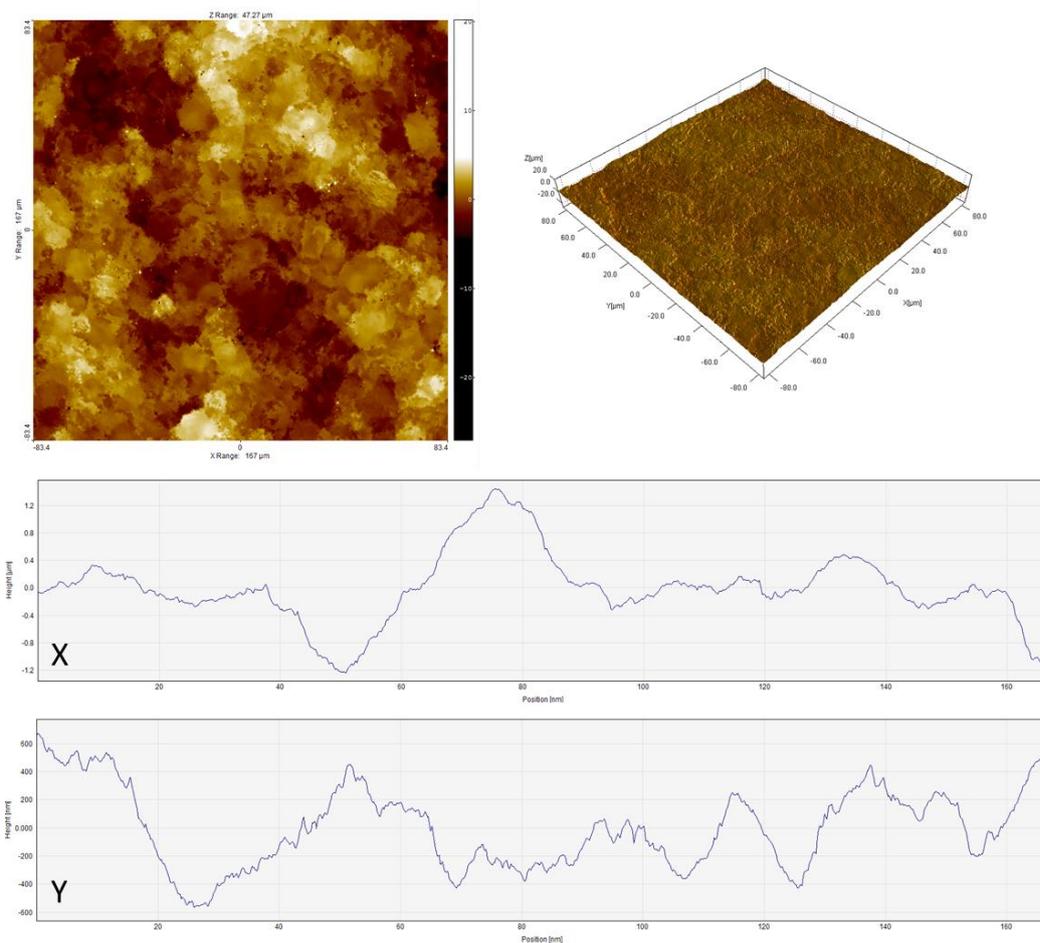
Figure 3. 10. Optical profiles demonstrating the surface topography of pre-modification screen-printed electrode surface. Line profiles of the X and Y axis display the cross-sectional profile of the widths and heights of the peaks and valleys of the surfaces.
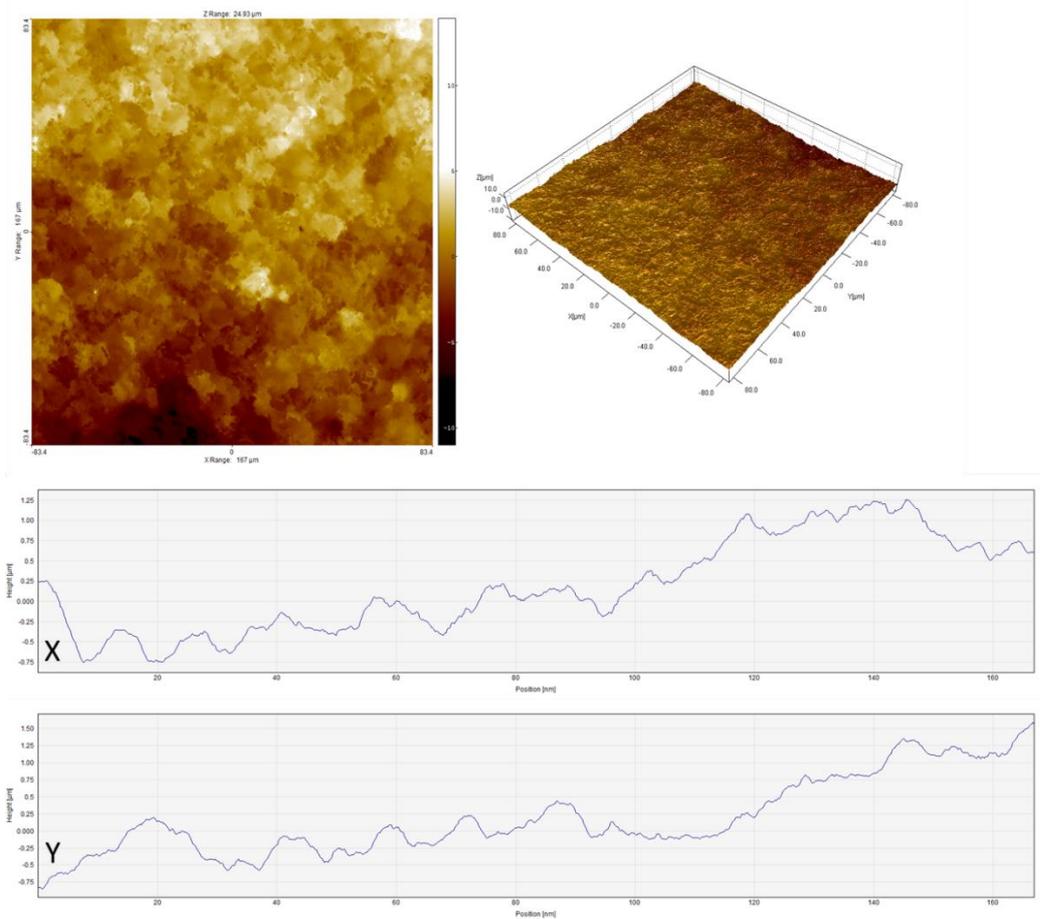
Figure 3. 11**.** Optical profiles demonstrating the surface topography of post-modification screen-printed electrode surface. Line profiles of the X and Y axis display the cross-sectional profile of the widths and heights of the peaks and valleys of the surfaces.

3.2.6 Electrode Wettability

Water contact angle measurements were carried out to determine to wettability changes the addition of the MWCNTs incurred on the carbon electrode surface (Fig. 3.12). The initial unmodified SPE demonstrated a water contact angle of 125.0° which subsequently decreased significantly ($p<0.0001$) with the deposition of the MWCNT formulation, resulting in a water contact angle of 23.5° and a more wettable, hydrophilic electrode surface.
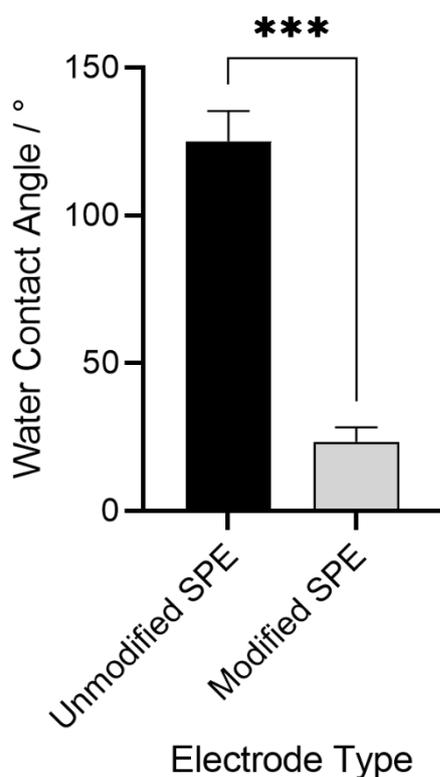
Figure 3. 12. Water contact angles of the unmodified carbon screen printed electrode and after the deposition of the MWCNT formulation. * and *** indicates a p value of < 0.05 and < 0.0001 respectively.

3.2.7 Fourier Transform Infra-Red Spectroscopy

FTIR spectra were carried out in the range of 400 – 4000 cm^{-1} to study the development of new bonds on the MWCNT surface due to the introduction of diamine oxidase and its crosslinkers (Fig. 3.13). The unmodified MWCNTs demonstrated typical characteristic bonds respective of the photon modes of carbon nanomaterials at 1600 cm^{-1}. For the functionalised MWCNTs, more bonds were measured relating to the organic bonds formed through the introduction of diamine oxidase and its associated conjugation biomolecules. At the 3500 cm^{-1} wavelength, O-H stretching bonds were measured indicating the presence of carbonyl groups. Functional groups at 2800 cm^{-1}, 2363 cm^{-1} and 1100 cm^{-1} demonstrated C-H stretching, $C=NH^{+}$ and C-N moieties, were shown to be respective of ionic amine groups of the enzyme, diamine oxidase. Further modifications to the MWCNTs in the form of direct nanotube carboxylation was presented at 1715 cm^{-1} and 1300 cm^{-1}, demonstrating O-H stretching and C-O bonds characteristic of the $COOH^{-}$ groups present in the carboxyl functional groups. C=O bonds were identified between 1750 cm^{-1} -1550 cm^{-1} which can be assigned to the carboxylic acid environment that was added when acid etching the nanotubes.
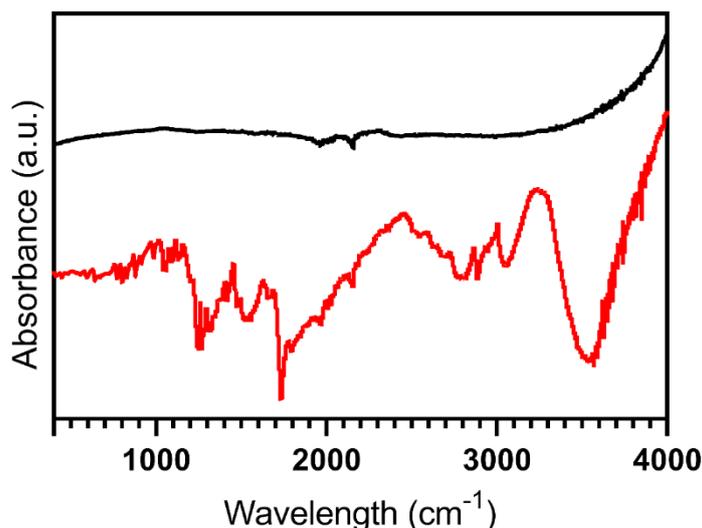
Figure 3. 13. FTIR spectra of unmodified multi-walled carbon nanotubes (Black), and diamine oxidase conjugated MWCNT (Red).

3.2.8 Scanning Electron Microscopy (SEM)

To evaluate the morphology of the electrode surface, SEM micrographs of the MWCNTs were used to verify and evaluate the changes the nanotubes had made on the SPE surfaces. The SEM images (Fig. 3.14) were taken of a) unmodified electrode surface, b) nonfunctionalized MWCNT on the electrode surface, and c) MWCNTs with complete enzyme cross-linking. The bare electrode surface (Fig. 3.14a) demonstrated an uneven heterogenous surface which is typical of carbon screen printed electrodes. Due to irregularities on the SPE surface, the addition of non functionalised MWCNTs resulted in the formation of irregular agglomerates. However, the enzyme cross-linked MWCNTs (Fig. 3.14c) demonstrated the opposite effect on the electrode surface whereby, more homogenous distribution was observed due to hydrophobic/hydrophilic interactions between MWCNTs and diamine oxidase.
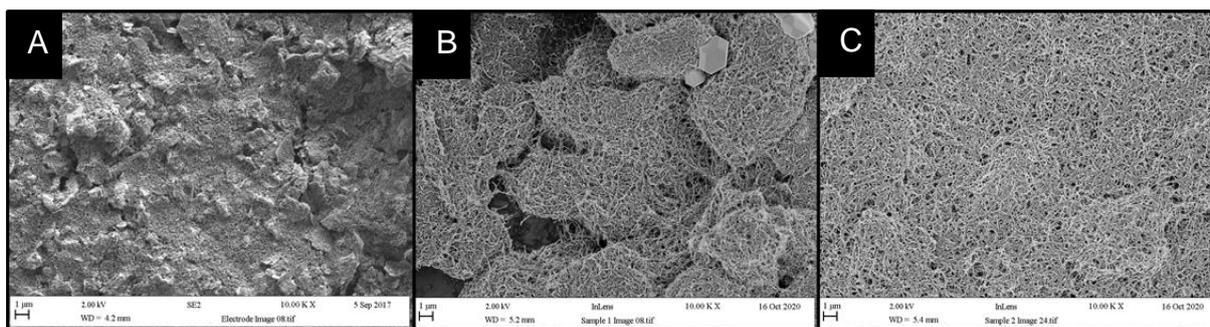
Figure 3. 14. SEM micrographs of MWCNTs in sonicated solutions of a) dH$_2$O, b) enzymatic solution, and c) MES buffer solution. Typical heterogenous surface demonstrated by carbon paste electrodes (a) contributing to MWCNT aggregate formation (b). Under enzymatic interaction MWCNTs demonstrate more homogenous dispersion with the electrode surface (c). Figure adapted from Amin et al., 2022.

3.2.9 Enzyme – Substrate Uptake Assay

The activity of the enzyme, DAO, was measured vs cadaverine in a concentration dependant assay (Fig. 3.15). Increasing concentrations of diamine oxidase (0.25 U, 0.5 U, 1.0 U, 1.5 U, and 2.0 U) were tested with 30 µg/mL of cadaverine using the colorimetric reagent O-dianisidine dihydrochloride. The results of this study demonstrated a concentration dependant increase in DAO activity in response to cadaverine oxidation. An increase in enzyme concentration from 0.25 U to 2.0 U demonstrated a positive correlation with average absorbance, indicating increased enzyme activity. It was determined that after 4 min, the reaction had completed and the number of active sites available for cadaverine on DAO had been up taken. This was demonstrated by the sharp increase in absorbance up to 4 min, followed by a plateau in absorbance.
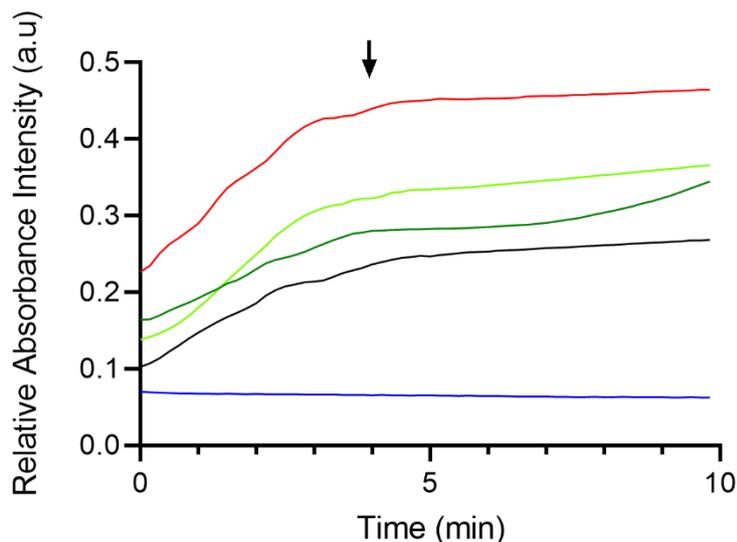
Figure 3. 15. Diamine oxidase enzyme activity response to cadaverine, measured over 10 min. Increasing concentration of cadaverine (0.25 U Blue, 0.5 U Black, 1.0 U Dark green, 1.5 U Light green, and 2.0 U Red) were used.

3.2.10 Raman Spectroscopy

Raman Spectroscopy was used to determine the spectral fingerprint of the unmodified and modified SPE surfaces. The Raman spectra of a) bulk MWCNT and b) enzyme functionalised MWCNTs was determined (Fig. 3.16). For both spectra, the radial breathing mode (RBM) was not present (100 cm^{-1} - 200 cm^{-1}), which is typical of multiwalled nanotube variants of carbon nanomaterials. The G band (identifiable at the 1875 cm^{-1} position) demonstrated the stretching mode of the C-C bonds which form the hexagonal lattice structure of all sp^2 carbon nanomaterials. Due the presence of defects on MWCNT surfaces, a D band (1350 cm^{-1}) was present on hexagonal sp^2 materials, with both unmodified and modified samples demonstrating these peaks. Furthermore, at the 2700 cm^{-1} wavelength, the vibrational mode characterised by the

breathing of six carbon atoms in a hexagonal lattice structure of graphene derivative molecules known as the G' (2D) band was observed.

The functionalised MWCNTs demonstrated (Fig. 3.16b) showed discrete Raman peaks additionally to those presented by unmodified MWCNTs. Peaks were measured at 2387 cm^{-1} which can be related to the D + D" band introduced by the presence of defective graphitic carbon. Further peaks at 2947 cm^{-1} were observed denote to CH stretching modes. At lower frequencies vibrational peaks at 2382 and 1783 cm^{-1} were observed and demonstrated C=C and C=O stretching bonds respectively. Finally, a protein identification vibrational mode at 719 cm^{-1} was determined as C-S bonds. From these spectra it was possible to determine the different vibrational modes of each MWCNT sample.
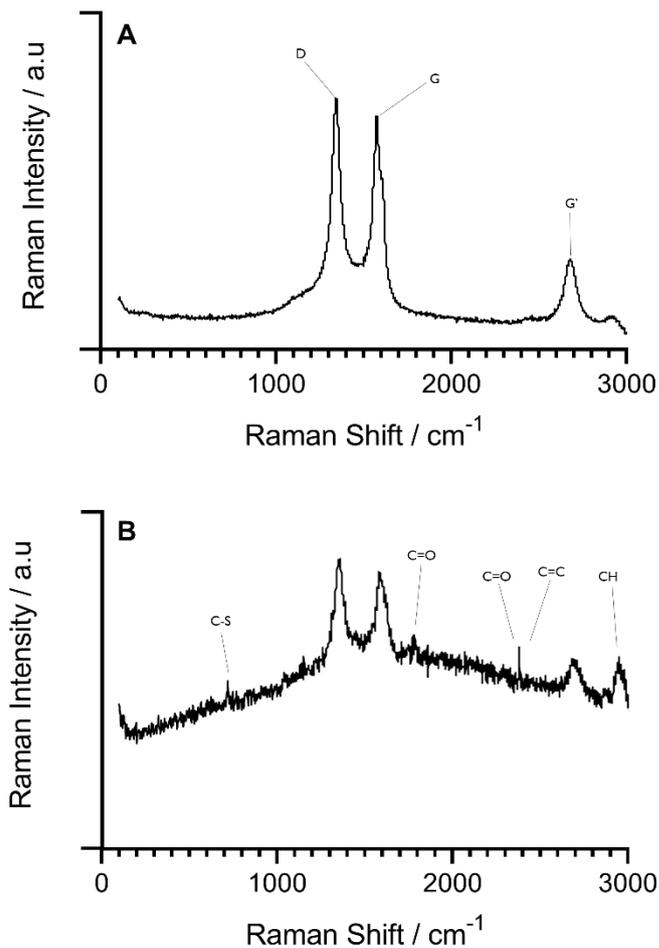
Figure 3. 16. Raman spectroscopy of A) bulk MWCNTs and B) functionalised MWCNTs. Figure reproduced with permission from (Amin et al., 2022)

3.2.11 Energy Diffraction X-Ray Spectroscopy

Energy diffraction x-ray spectroscopy was used to identity the elemental composition of the MWCNTs in bulk form and after enzyme conjugation. The presence of carbon oxygen, sodium, phosphorus and sulphur was demonstrated (Table 3.1). The addition of nitrogen, silicon, and chlorine were observed in the MWCNT formulations. The quantitative amounts of each element were calculated from the EDX data. In both samples that carbon was the most abundant element, followed by the presence of

oxygen. Differences could be observed in the pre- and post-conjugation samples due to the presence of EDC and NHS compounds and enzymes, as demonstrated by the additional presence of nitrogen, silicon, and chlorine groups in the post modified samples. Furthermore, the decreases on both weight percentage and atomic weight in the post modified samples were observed due to the increasing number of molecules present in each individual functionalisation stage.

Table 3. 1. Elemental composition EDX analysis of MWCNTs a) pre-modification and dispersed in DH_2O and b) enzymatic solution after complete enzyme conjugation.

Element	At % Unmodified MWCNT	At % Modified MWCNT
C	78.19	63.92
O	18.32	19.78
Na	1.68	2.14
P	0.20	0.18
S	1.71	4.78
N	N/A	6.87
Si	N/A	0.45
Cl	N/A	1.89

3.2.12 Voltammetric Studies of Modified SPE

The voltametric response of the MWCNT modified SPEs was evaluated electrochemically using the outer sphere redox probe, hexaammine-ruthenium(III) chloride. The voltametric peak to peak potential (ΔE_p) of the oxidation and reduction process of the redox couple was evaluated (Fig. 3.17a). The heterogenous electron

transfer rate was calculated for the MWCNT electrode and resulted in a k^0 value of 7.43x10^5 cm s^{-1} an A_{eff} of 0.658 cm^2, and A_{real} 87.70%. The ΔE_p for the MWCNT functionalised SPE was 62.5 mVs^{-1} at 100 mV s^{-1}. Furthermore, the peak current was plotted vs square root of the scan rate (Fig. 3.17b) to determine the linearity of the plot and results demonstrated a linear relationship with an R^2 = 0.9678.
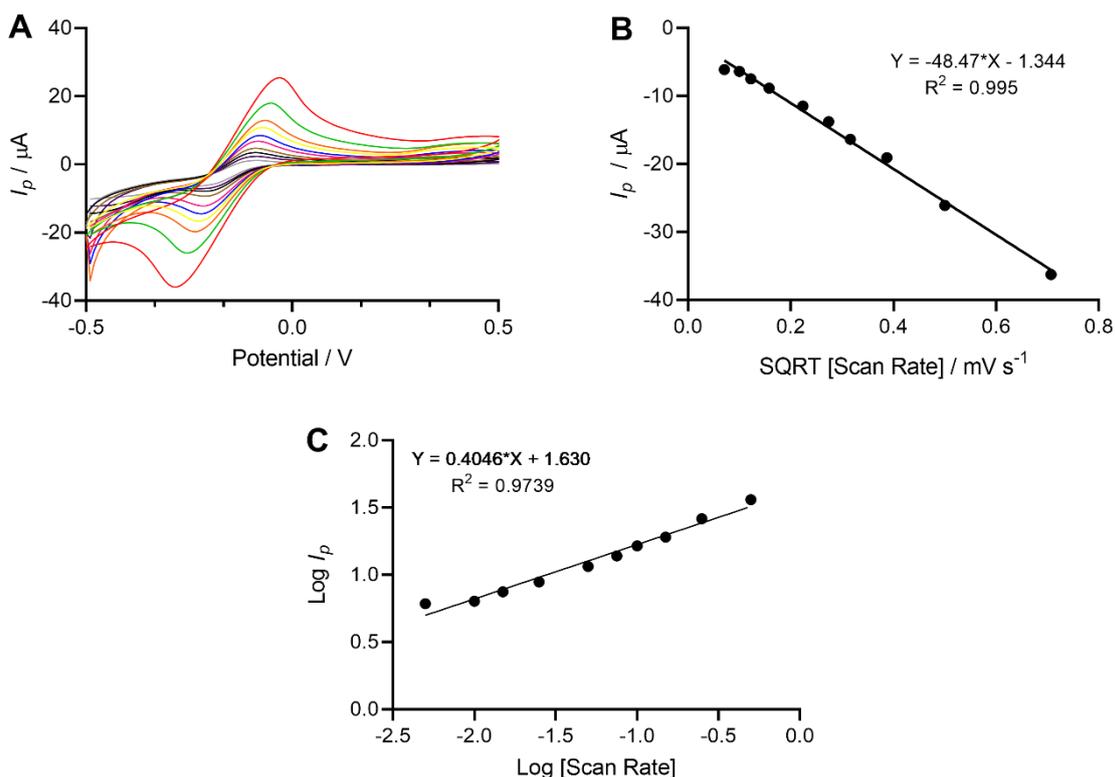
Figure 3. 17. A) Electrochemical effective area of MWCNT functionalised SPE determined using 1mM hexaammineruthenium(III) chloride within a potential window of -500 mV to +500 mV s-1 in 0.1 M KCl vs. Ag/AgCl reference electrode. B) Linearity of peak current vs square root of the scan rate with R2 of 0.995. C) Log of peak current as a function of log scan rate.

3.3 Discussion

This chapter developed screen-printed electrodes which, in later chapters, were used for the detection of bacterially derived toxins (as discussed in Chapter 1). Screen printing is a technique which has been studied and utilised for a long time and has shown to produce many effective sensing devices (Banks et al., 2016). Such technologies enable the development of sensor designs which offer various improvements in analytic sensitive, signal-noise ratios, and allow for the reduction of samples volumes, improving the portability of the biodevices and enabling the replacement of conventional electrode substrates. Furthermore, the mass producibility of such devices results in single-use applications, reducing potential contamination between samples and reduces the requirements of electrode pre-treatment, which is pre-requisite for conventional solid electrodes. Electrochemical analysis is a particularly effective analytical technique when it comes to evaluating sensors and biosensors. Previous studies have shown the analytical sensitively and specificity provided by using electrochemical sensors, in particular when investigating biological species (Rowley-Neale et al., 2020; Betlem et al., 2018). Thus, work disseminated in this chapter gives insight into some of the novel approaches taken in order to develop and analyse a functional cadaverine biosensor.

3.3.1 Proof of Concept

The bare SPEs used in this work have been previously utilised by the Banks group at Manchester Metropolitan University to a number of applications (Garcia-Miranda Ferrari et al., 2021; Crapnell et al., 2022). These application include biomarker

detection for cancer, cardiac and inflammatory infringements, and the success show in these studies have warranted their further investigation.

The electrode for the biosensor was modified using MWCNTs with covalently crosslinked DAO. An essential requirement for any enzymatic biosensing device is the immobilisation of the protein which in this instance, was achieved through covalent binding to reduce enzymatic response time and increase sensor shelf life (Campaña et al., 2019). In order to carry this out, 1-ethyl-3(3-Dimethylaminopropyl)Carbodiimide (EDC), a water soluble zero length crosslinker was used in the development of the sensing platform (Vashist, 2012). EDC is typically used in the coupling of carboxyl groups, which in this study, were acid etched onto the MWCNT surface, and used to conjugate EDC to primary amines. EDC undergoes nucleophilic substitution in the presence of strong nucleotides, such as primary amine molecules, and forms an unstable O-acylisourea intermediate (Wickramathilaka and Tao, 2019). This intermediate is readily hydrolysable, thus able to rapidly revert to its original carboxylate molecule. To overcome this, N-Hydroxysuccinimide (NHS) has been frequently utilised to develop a more stable intermediate prior to amine introduction (Staros et al., 1986; Fischer, 2010). This method also provides a greater effective area enabling increased protein loading for maximising the probability of enzyme substrate complex formation and overall increased sensitivity (Nejadnik et al., 2011).

3.3.2 MWCNT dispersibility

MWCNT suspensions are one method in which nanomaterials may be utilised in electrode modification for biosensor applications. Due to their biocompatibility,

MWCNTs are ideal candidates for biomolecule loading thus, significant research is being conducted into advancing this model, however, major challenges in the way of nanotube pre-processing remain. The formation of MWCNT agglomerations have been suggested to occur due to the hydrophobicity of the sp^2 carbon sidewalls and the strong π – π stacking interactions between individual carbon nanotubes (Zawawi et al., 2016). The surface of unmodified MWCNTs resulted in a shortage of hydrogen bonding with the water molecules which failed to facilitate stable MWCNT suspensions. This finding is in agreement with Alnarabiji et al (2016), who, using the sessile drop technique directly onto the surface of the MWCNTs, demonstrated that a water contact angle of 136° was obtained, indicating a hydrophobic structure (Alnarabiji et al., 2016). It has been suggested that the addition of the enzyme diamine oxidase utilised in this study resulted in improved carbon nanotube dispersion. Work by Kim et al (2017), suggested the amphiphilic nature of enzymes can be a key contributor in the facilitation of CNT dispersion as the hydrophobic moieties of the enzymes interact with the CNT surface and the hydrophilic enzyme residues interact with the dispersal solution, thus inhibiting nanotube aggregation and resulting in a homogenous CNT suspension (Kim et al., 2017). In agreement with this, the enzyme diamine oxidase used for the facilitation of the dispersion of MWCNTs demonstrated similar mechanisms thus, enabling a more uniformed drop cast on the electrode surface.

3.3.3 UV-VIS

The UV-Vis spectra of MWCNT and C-MWCNTs demonstrated two main absorption features. The π – plasmon absorption peaks at *ca.* 240 nm result from the excitation

of the π – electron systems which are apparent in all sp^2 – hybridised carbon materials (Braun et al., 2016). In agreement with the findings presented here, the relative increase in peak absorbance of the C-MWNCT in comparison to the MWCNTs was also determined in other work (Park et al., 2014; Fares, 2018). It was suggested that the increase in absorbance for the C-MWCNTs occurred due to the π – plasmon bands resonating free electrons in the C-MWCNT structures, resulting in increased absorbance intensities.

3.3.4 Scanning Electron Microscopy (SEM)

Carbon paste electrodes demonstrate 'flake like' morphologies under SEM imaging. These flakes which are embedded in the carbon graphitic ink used in their production have been evaluated previously (Slate et al., 2018). The characteristic flakes typical of MWCNT behaviour were observed on the electrode surfaces which has been previously shown to be due to the Van der Waals interactions between each nanotube (Chaisiwamongkhol et al., 2017). However, after MWCNT functionalisation the arrangement of MWCNT structures on the electrode surfaces decreased the amount of aggregation present and resulted in an improved MWCNT arrangement due to the hydrophobic interactions between the nanotubes (Brito et al., 2020). The resultant 'thread like' woven mesh morphology arises due to functionalisation steps taken on MWCNTS and resulted in less aggregated, more homogenous complexes after drop casting on to the electrodes, and this has been shown to contribute towards a larger effective electrochemical surface area (Chaisiwamongkhol et al., 2017).

3.3.5 Enzyme Activity

The enzymatic activity of diamine oxidase was tested in response to cadaverine, to determine the most effective concentration for use on the biosensor surface. The colorimetric reagent, O-dianisidine dihydrochloride was used as an indicator of enzymatic activity and has been shown to previously work to effectively catalyse the formation of H_2O_2 production as a result of biochemical oxidation (Stepien and Guy, 2017). The experiment was conducted on a timescale of up to 10 min. It was calculated that based off the catalytic activity rate of DAO, in order for it to catalyse the respective cadaverine concentration, it would require at least 4 min of reactivity time. This was confirmed by the experiment, in that after 4 min the absorbance intensity for each concentration tested stopped increasing, instead demonstrating a plateau, which would be indicative of a reaction endpoint. At this point it would be possible to suggest any cadaverine in the system would have formed enzyme substrate complexes with DAO thus, ceasing further enzyme activity.

3.3.6 Surface Roughness and Wettability

Screen-printed electrode surfaces have irregular featured surfaces due to the presence of peaks and valleys of graphitic carbon originating from the initial printing processes in their development. The surface profiles of the unmodified electrodes were measured to determine if roughness of the surface changed with the deposition of the MWCNT formulation. The unmodified carbon working electrodes initially presented with a less rough surface, which could be attributed to the binder utilised in their production filling in the surface features resulting in a smoother surface profile (Fanjul-Bolado et al., 2008). In contrast, the MWCNT functionalised electrodes

demonstrated significantly increased roughness profiles due to the possible formation of MWCNT aggregates upon interaction with the carbon paste substrate. MWCNTs have been shown to accumulate on surface peaks and features thus, exaggerating surface peak height increasing overall roughness profiles as observed in our work (Stueckle et al., 2017). An increase in electrode roughness as a result of carbon nanotube deposition was similarly observed by Ziyatdinova et al, (2010), whereby the modification of glassy carbon electrodes led to a significant increase in surface roughness which has been suggested to be due to the formation of CNT aggregates on the carbon electrode surface (Ziyatdinova et al., 2012). Sun et al, (2015) demonstrated the application of CNTs to a graphene surface not only increased the surfaces overall roughness, but also improved the electrical conductivity between the surface and the CNTs via the introduction of a greater number of enzyme active sites for increased biocatalytic activity (Feng and Ji, 2011; Sun et al., 2015). This was particularly important, as this has been suggested to increase the conductivity which aids in the measurements of lower analyte concentrations therefore, increasing overall device sensitivity (Jessl et al., 2018). Increases in surface wettability were demonstrated by the modified electrode and were possibly a result of the introduction of more polar head groups of -COOH on the electrode, thus presenting as a more hydrophilic surface (Kamra et al., 2016). It has been shown in previous works that increases in the hydrophilicity of electrodes resulted in more efficient analyte detection at the electrode interface (Meng et al., 2017).

3.3.7 Raman Spectroscopy

Raman spectroscopy is an effective technique in the characterisation of carbon materials due to its non-destructive nature and its sensitively to structural changes at the molecular level. Raman analysis of MWCNTs within this study was conducted on samples with the same concentration of nanotubes. The predominant features of carbon nanomaterials were the presence of the G and D peaks which were evident around the 1560 cm^{-1} and 1360 cm^{-1} respectively for visible excitation (Mohamed Saheed et al., 2013). Two different formations of nanotubes were evaluated, non functionalised MWCNT without further modification, and C-MWCNT/EDC-NHS/DAO/GA. The Raman analysis demonstrated typical spectra for MWCNTs in their bulk form, with D bands (A_{1g} mode) corresponding to the sp^3 disorder carbon – carbon rings of defective graphene structures, and the G band (E_{2g} mode) characteristic of graphitic layers in the planar sp^2 bonded stretching configuration carbon (Karimi-Maleh et al., 2020). The second harmonic order G'-band (2D band) was also observed within the unmodified MWCNT Raman spectra. The presence of these two bands determined the presence of semiconducting and metallic MWCNTs within the observed samples and is in agreement with previous characterisation of MWCNTs (Zdrojek et al., 2004; Rebelo et al., 2016; Xiong et al., 2017). C-MWCNT/EDC-NHS/DAO/GA characterisation showed additional Raman peaks that denoted the presence of diamine oxidase, EDC – NHS and GA. The presence of the protein crosslinking reagent, GA was observed through the presence of C-S (organosulfur) bonds and C=O which were demonstrated in GA's structure (Chauhan et al, 2014). Identification of the enzyme diamine oxidase was also determined by the presence of C-H stretching bands at the 2947 cm^{-1} range. Work by Sebek et al., (2011), also determined that within the 2900 cm^{-1} range, C-H stretching bands were

dominantly present in aliphatic molecules as proteins, thus confirming the detection of the aliphatic enzyme, diamine oxidase (Sebek et al., 2011). The structure of the MWNCTs was impacted by the numerous stages of modification thus, the D + D" band was observed as an indicator of inactive modes of defective graphitic carbon, with the D + D" band seen as the combination of the inactive D photon within a further inactive D" mode (Couzi et al., 2016).

3.3.8 Electrochemical analysis

The electrochemical behaviour of the MWCNT modified electrodes was investigated pre- and post-modification to determine the ability of the MWCNT formulation to amplify the electrochemical response. SPEs with a MWCNT formulation consisting of C-MWCNTs with crosslinked diamine oxidase enzyme were used to detect cadaverine in solution. The voltammetric response of the modified SPE was investigated via the commonly utilised redox probe, hexaammine-ruthenium(III) chloride (Alwarappan et al., 2009). The observed redox behaviour of the SPE was recorded as voltammetric peak to peak potential (ΔE_p) of the oxidation and reduction (Rahim et al., 2018). The reversible limit, which was at ΔE_p 59 mV (298 K) and smaller potentials up to this limit demonstrated a more reversible electrochemical processes (EP et al., 2014). The voltammetric analysis of the profiles demonstrated an ΔE_p of 62.5 mV s^{-1}. The increase in peak to peak separation was potentially due to the percentage of binder used in the electrode's fabrication, which has been shown to reduce fast electron transport at the carbon structure (Mikysek et al, 2012). Further analysis of the SPEs via the deduction of the heterogenous electron transfer rate constant, k^0 of hexaammine-ruthenium(III) chloride for the modified SPE corresponded to 7.43x10^5 cm. To evaluate the MWCNT

structure of the electrode and to confirm its non-porous nature, scan rate studies were carried out whereby the peak current was measured as a function of the scan rate and the plot was determined to be linear, which indicated an electron process which was diffusional and on a non-porous structure (Figueredo-Filho et al., 2013).

3.4 Conclusion

Screen-printing was used to fabricate the SPE and modification with DAO and MWCNTs enabled the development of a highly specialised working electrode for the detection of periodontal disease biomarkers. The homogenous dispersion of MWNCTs was achieved through the manipulation of the hydrophobic/hydrophilic interactions of DAO to enable a more uniformed nanotube solution. Following the fabrication of a screen-printed carbon paste electrode, its surface properties were evaluated which demonstrated that following the addition of the enzyme, the surface demonstrated increased wettability and roughness, which enhanced electron transfer to the electrode. SEM, EDX analysis and Raman spectroscopy confirmed the identity of the MWCNTs and the electrode surface. Electrochemical voltammetric analysis of the modified electrode demonstrated efficient electron transfer kinetics and a linear range vs the scan rate, which resulted in a non-porous electrode surface. Overall, this chapter demonstrated the production of screen-printed electrodes with a novel DAO-MWCNT surface modification for use as biosensors for the potential detection of cadaverine to be used as a means of periodontal disease evaluation.

CHAPTER 4

Electrochemical Determination of Cadaverine

4.1 Introduction

In this chapter, the electrochemical properties of the C-MWCNT-EDC-NHS-DAO-GA were assessed as a means to detect cadaverine. Cyclic voltammetry and differential pulse voltammetry were used to initially see if cadaverine could be measured electrothermally, and then to identify the redox peaks for cadaverine and to isolate the active oxidisation peak for a more detailed assessment. The aim for the work in this chapter was to determine the applicability of the biosensor as a means to determine the presence of cadaverine. This was carried out in standard solution and compared with artificial saliva to determine the biosensors applicability in more 'real-world' samples.

4.2 Results

4.2.1 Unmodified SPE Interaction

To provide an initial base line for cadaverine detection, an unmodified carbon graphitic ink SPE was used. The SPE was cycled with cadaverine at a concentration of 30 µg/mL in order to establish a base means of detection. Following 10 cycles at a scan rate of 100 mV s^{-1}, cadaverine demonstrated no redox peaks when using an unmodified SPE vs Ag/AgCl reference electrode in Britton-Robinson Buffered KCl (Fig. 4.1).
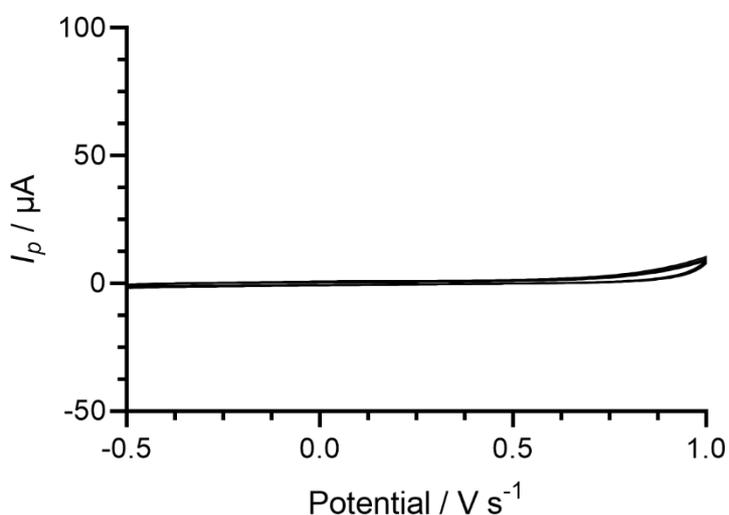
Figure 4. 1. Cyclic voltammogram obtained using an unmodified carbon SPE in the presence of 30 µg/ mL of cadaverine solution in Britton-Robinson buffer at a scan rate of 100 mV s^{-1}. Potential window 0.5 to 1.0 V s^{-1} vs Ag/AgCl reference electrode.

4.2.2 C-MWCNT/DAO/EDC-NHS/GA SPE Interaction with Cadaverine

The voltammetric response of cadaverine vs the modified C-MWCNT/DAO/EDC-NHS/GA SPE was investigated, ensuring the same conditions were held as when

measuring the unmodified SPEs (Fig. 4.2). In contrast to the unmodified electrode, the results demonstrated a pair of redox peaks which denoted the electrochemical oxidation and reduction of cadaverine and H_2O_2 respectively, at the working electrode of the C-MWCNT/DAO/EDC-NHS/GA SPE.
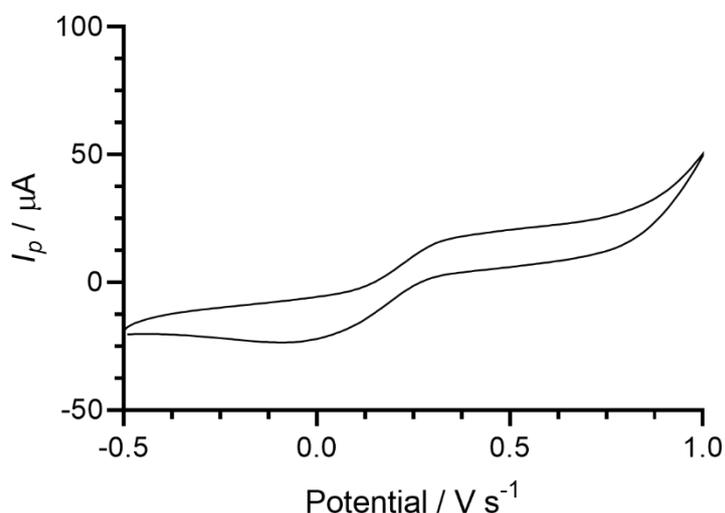
Figure 4. 2. Cyclic voltammogram of cadaverine recorded utilising a C-MWCNT/DAO/EDC-NHS/GA working electrode vs Ag/AgCl reference electrode at a scan rate of 100 mV s^{-1}. Voltammetric oxidation (anodic) and reduction (cathodic) peaks corresponded to 19.49 and -0.180 V s^{-1} respectively.

The height of the oxidation peak, which corresponded to the electrochemical oxidation of cadaverine as a result of enzyme-substrate interaction at the site of the working electrode, was analysed as a function of scan rate, whereby the anodic peak height (I_p) vs the square root of scan rate was plotted. This initially presented with a linear correlation with increasing scan rate, showing a larger peak current response. However, at the higher scan rates, this trend was no longer linear, possibly due to the availability of cadaverine in the system. Further analysis depicted in the form of log peak current vs log scan rate (Fig. 4.3) demonstrated a gradient of 0.29, which was

found to be within the theoretical expected value of 0.5 for a diffusional controlled process at the surface of the working electrode, indicating an electrode structure which was non-porous.
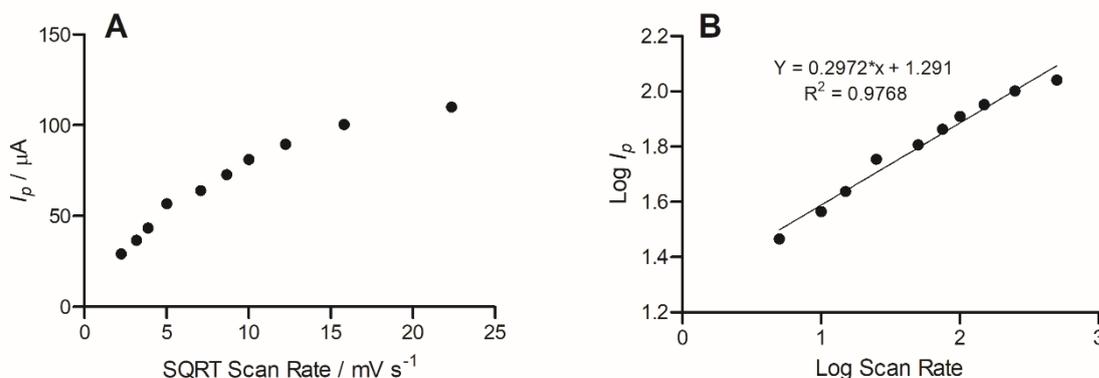
Figure 4. 3. a) Voltammetric anodic peak height of cadaverine expressed as a function of the square root of the scan rate. b) Log peak current vs log scan rate.

4.2.3   C-MWCNT/DAO/EDC-NHS/GA   SPE   vs Cadaverine Concentration

The electrochemical responses of the modified C-MWCNT/DAO/EDC-NHS/GA SPE were evaluated as a function of cadaverine concentration. The single anodic peak of cadaverine in response of the C-MWCNT/DAO/EDC-NHS/GA SPE was utilised and a DPV plot of cadaverine concentration vs peak current was constructed (Fig. 4.4). A peak current range of 140 – 204 µA vs Ag/AgCl was determined at an increasing concentration of cadaverine (3 µg/mL (red), 15 µg/mL (green), 40 µg/mL (yellow), 65 µg/mL (orange), 100 µg/mL (black) and, 150 µg/mL (blue)).
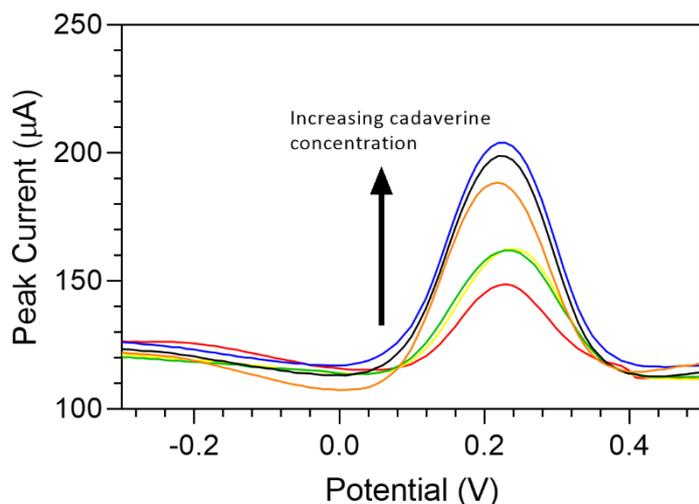
Figure 4. 4. Differential pulse voltammogram of cadaverine (3 – 150 µg/ mL) using MWCNT/DAO/EDC-NHS/GA SPE with resulting peak current range of 140 – 204 µA vs Ag/AgCl reference electrode in supporting Britton-Robinson buffer and 0.1M KCl at pH 6.0.

The concentration of cadaverine was plotted vs peak current (Fig. 4.5) and demonstrated a linear increase in analytical signal in response to increased cadaverine concentration. When the unmodified carbon SPE was used, little or no cadaverine was detected, similar to the cyclic voltammetric analysis demonstrated previously.
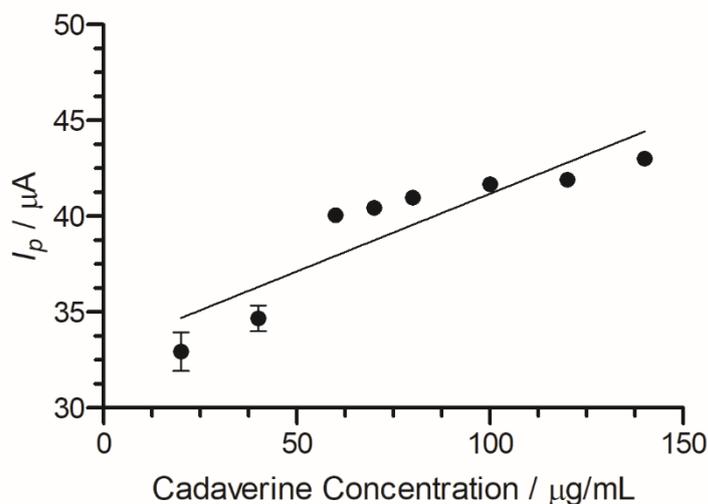
Figure 4. 5. A plot demonstrating cadaverine concentration (3 – 150 μg/ mL) vs I_p at C-MWCNT/DAO/EDC-NHS/GA SPE, with linear ranges identified at low and high concentrations of cadaverine.

Using this information, the limit of detection for the C-MWCNT/DAO/EDC-NHS/GA SPE could be determined. The limit of the blank was the initial measurement used to identify the minimum concentration which could be reliably measured using analytical techniques. The limit of the blank is defined as the highest concentration of apparent expected analyte concentration of replicates whereby no test analytes are to be found. The mean blank value was obtained from the voltammetric response of a C-MWCNT/DAO/EDC-NHS/GA SPE in the absence of cadaverine. Changes to the current were recorded within the expected potential window (-0.3 – 0.5 V s^{-1}) whereby the electrochemical oxidation and reduction of cadaverine would be expected to occur.

Next, the limit of detection (LOD) was determined. The LOD is defined as the lowest concentration of analyte measured, which is reliably distinguishable from the LOD and

was determined by calculating three times the standard deviation of the blank and for cadaverine this was 0.8 µg/mL (28 µM).

The effect of pH on the electrochemical system was determined. The C-MWCNT/DAO/EDC-NHS/GA SPE was measured against a pH range of 2 - 12 and cyclic voltammetric profiles of cadaverine were assessed as a function of pH by plotting the oxidation peak of cadaverine vs pH (Fig. 4.6). It should be noted that the pK$_a$ of cadaverine is 10.25 at 25°C. A linear correlation was demonstrated between the increasing pH and the peak potential of cadaverine. The linearity of the system past the pK$_a$ of cadaverine ceased, causing a shift in E_p towards higher values. The performance of the enzyme was strongly dependant on pH and varied significantly on the pH of the buffer solution, showing an increase in peak potential with an increase in pH.
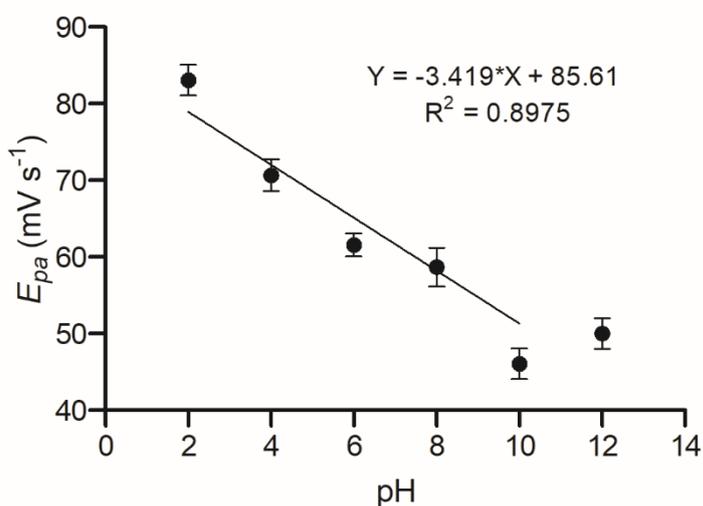
Figure 4. 6. A plot of E$_{pa}$ vs pH at a range of 2 to 12 in Britton-Robinson Buffered KCl solution.

To better emulate the environment of the oral cavity, artificial saliva was used to evaluate the C-MWCNT/DAO/EDC-NHS/GA biosensor. The peak response of the cadaverine using the C-MWCNT/DAO/EDC-NHS/GA biosensor within an artificial saliva was determined using DPV (Fig. 4.7). When using the saliva, a narrower potential range was observed with a similar peak current response over multiple repeat measurements.
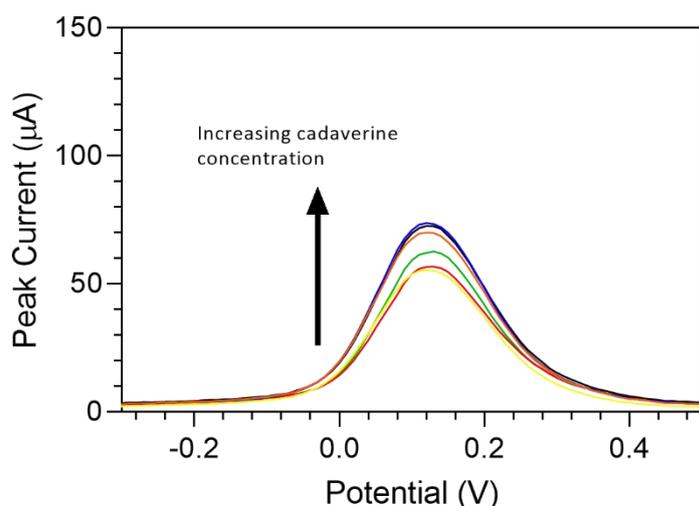
Figure 4. 7. DPV response of cadaverine (30 µg/mL) vs C-MWCNT/DAO/EDC-NHS/GA SPE in artificial saliva at a pH of 7.2 vs Ag/AgCl reference electrode.

The biosensors shelf-life was measured using repeat SPEs which had been stored at 4°C in 0.1M phosphate buffer over a period of 40 days. In each instance 10 repeat SPEs were used, and their efficacy tested using 3µg/mL of cadaverine as the measured concentration. The biosensor demonstrated no degradation over the first five days, maintaining a 100% efficacy over 10 repeats. However, on the 10th day of testing, the efficacy of the biosensor reduced to 99.71%, and continued to decrease on days 15 (99.1%), 20 (98.53%), 30 (98.19%), and day 40 (97.88%). Overall, the

biosensor after 40 days demonstrated a total decline in efficacy of 2.12% vs 3μg/mL

of cadaverine.
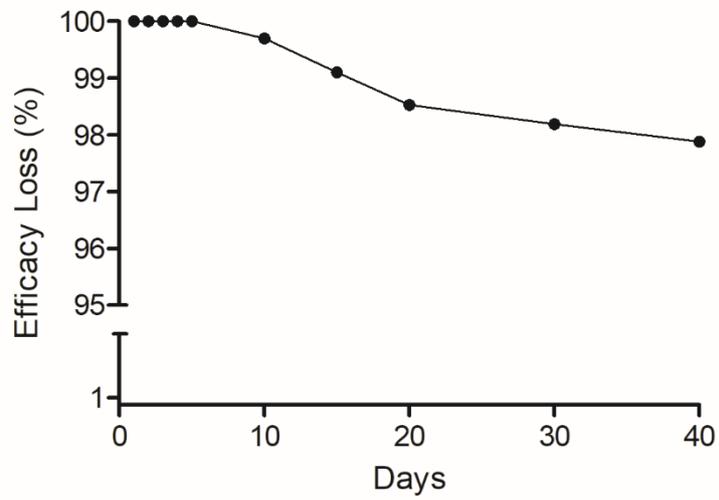
Figure 4. 8. Total percentage loss of biosensor efficacy when stored at 4°C in 0.1M

phosphate buffer over a period of 40 days.

4.3 Discussion

The electrochemical detection of cadaverine as a potential biomarker for the indication of periodontal disease was elucidated. Work by Sakanaka et al, (2016), previously demonstrated the effects of increased levels of cadaverine correlating to poor patient oral health and deemed cadaverine as an important predictive periodontal biomarker. The current measurement techniques for such biomolecules utilised chromatography methods which remain an expensive and time consuming practice, requiring ample sample derivatisation prior to any measurements being obtained. Within the clinical dental environment, periodontal disease assessment remains a dated practice whereby the traditional techniques of clinical attachment level, bleeding on probing and pocket depth measurements encompass the golden standard of periodontal disease diagnostics (Ramenzoni et al., 2021). However, these traditional techniques only enable clinicians to identify the course of the disease, failing to provide information on the disease activity, information on the patient's current oral health, or the risk of potential future periodontal breakdown (Srivastava et al., 2017). Thus, the requirement for periodontal disease analysis and monitoring is of the utmost importance, with this study demonstrating a means of real-time periodontal disease monitoring using cadaverine as a key indicator of oral disease state. Thus, the use of biosensors that detect cadaverine that can be used in point-of-care devices would enable the current state of oral health of a patient to be established, without the need of clinical invasive analysis or expensive chromatography based analysis.

4.3.1 SPE Electrochemical Analysis

An unmodified carbon graphitic paste SPE was used for the purpose of providing a comparison against the modified enzyme biosensor. Following the electrochemical analysis carried out in this work, cadaverine demonstrated no redox peaks at a concentration of 30 μg/ mL using the unmodified SPE vs Ag/AgCl reference electrode. It has been previously reported that cadaverine demonstrates a pair of redox peaks during cyclic voltammetric analysis at concentrations ranging from 19.6 μM - 100 mM (Henao-Escobar et al., 2013; Spehar-Délèze et al 2015). However, this may have been due to cadaverine presenting as an electrochemically inert molecule without the presence of an active site of a conjugated enzyme. Thus, under these operational conditions, the cadaverine molecule would not undergo a redox reaction under standard conditions with a changing potential.

The voltammetric response of cadaverine vs the modified C-MWCNT/DAO/EDC-NHS/GA SPE was investigated, ensuring the same conditions were held as the previous unmodified electrode. In contrast to the unmodified electrode, the results demonstrated a pair of redox peaks which denoted the electrochemical oxidation and reduction of cadaverine and H_2O_2 respectively, at the working electrode of the C-MWCNT/DAO/EDC-NHS/GA SPE. The demonstration of the peaks may have occurred in this instance, as cadaverine had a target binding site, which was the active site of the conjugated DAO enzyme located at the working electrode interface. Thus, the facilitation of the transport of electrons from the enzyme active site to the surface of working electrode would be enabled, resulting in the electrochemical measurements recorded.

The height of the oxidation peak which corresponded to the electrochemical oxidation of cadaverine as a result of enzyme-substrate interaction at the site of the working electrode was evaluated and were thereby measured as a function of scan rate. The measurement of the anodic peak height (I_p) vs the square root of scan rate was plotted as it was the key peak of interest for the oxidation of cadaverine. The log peak current vs log scan rate and demonstrated a gradient of 0.29, which was found to be within the theoretical range of 0.1 to 0.5 (Compton and Banks, 2010). This indicated a diffusional controlled process at the surface of the working electrode which would suggest a non-porous electrode structure (Figueredo-Filho., et al 2013). Similar work has been demonstrated by Heano-Escobar et al., (2013), whereby the electrochemical oxidation of cadaverine was achieved via the active redox centre of the enzyme, monoamine oxidase, a less specific polyamine oxidising enzyme than the enzyme utilised in this study. The enzyme DAO demonstrated a much stronger affinity towards cadaverine than other similar biomolecules, which potentially may result in increased sensitivity of the sensor in more complex solutions such as human saliva.

4.3.2 Cadaverine Electrochemistry

To determine the effectiveness of the C-MWCNT/DAO/EDC-NHS/GA biosensor, the sensor must be able to successfully measure differing concentrations of cadaverine and provide discreet peak values for each. Thus, the electrochemical responses of the modified C-MWCNT/DAO/EDC-NHS/GA SPE platform were evaluated as a function of cadaverine concentration. The single anodic peak of cadaverine in response of the C-MWCNT/DAO/EDC-NHS/GA SPE, and a DPV plot of cadaverine concentration vs peak current was determined. The peak current range using the modified biosensor was 32.22 – 43.13 µA vs Ag/AgCl and demonstrated an increasing concentration of

cadaverine (3 – 150 µg/mL), which was shown to be linear. This was in contrast to the unmodified carbon SPE, where little or no cadaverine was detected. This suggests that the sensor could detect cadaverine, but also was responsive to the amount of analyte present in the solution.

The LOD for the C-MWCNT/DAO/EDC-NHS/GA SPE was determined. The limit of the blank is the initial measurement used to identify the minimum concentration which can be reliably measured using analytical techniques (Armbruster and Pry, 2009). The mean blank value was obtained from the voltammetric response of a C-MWCNT/DAO/EDC-NHS/GA SPE in the absence of cadaverine. Changes to the current were recorded within the expected potential window (-0.5 – 1.0 V s^{-1}) where the electrochemical oxidation and reduction of cadaverine would occur. Next, the LOD was determined, and for cadaverine this was 0.8 µg/mL (28 µM). The results demonstrated an LOD which was equal to or lower than the previous works of Henao-Escobar et al., (2013) which detected cadaverine using a monoamine oxidase biosensor at 19.99 µM. Work by Vanegas et al., (2018) demonstrated a linear range of 50 µM – 1.6 mM for cadaverine and similar biogenic amines for a biosensor used for the detection of fish sample decay (Vanegas et al., 2018). The increased sensitivity of the device presented in this thesis may be hypothesised to be due to the modified enzyme/carbon nanotube surface of the working electrode allowing for an increased surface area to enable the enzyme - cadaverine interactions. This resulted in the ability of the C-MWCNT/DAO/EDC-NHS/GA SPE to detect the electron transfer of the concentrations of the cadaverine at lower levels than previously reported.

The effect of pH on the electrochemical system was determined as it had been shown in previous works that pH could significantly alter the affinity of an enzyme to its substrate. The C-MWCNT/DAO/EDC-NHS/GA SPE was measured against a pH range of 2 - 12 and voltammetric profiles of cadaverine were assessed as a function of pH. Noting that the pK_a of cadaverine is 10.25 at 25°C, a linear correlation was demonstrated with respect to increasing pH and cadaverine peak potential. This suggested that the performance of the enzyme was strongly dependant on pH and varied significantly on the pH of the buffer solution.

The future application of this device would be as a diagnostic tool for the early detection of periodontal disease as cadaverine has been shown a concentration dependant correlation with the severity of periodontal disease. Thus, simply testing the biosensor in model media would not give an accurate representation of its efficacy in real world solutions. To better emulate the environment of the oral cavity, artificial saliva was used to evaluate the C-MWCNT/DAO/EDC-NHS/GA biosensor within a simulated real world environment. Following testing of the C-MWCNT/DAO/EDC-NHS/GA biosensor within an artificial saliva environment, a narrower potential range was observed with a similar peak current response over multiple repeat measurements. This suggested that the biosensor would not be inhibited by interfering molecules present in human saliva. Thus, the biosensor demonstrated good efficacy when used in a simulated real world environment, as the saliva of individuals may be used to potentially detect the level of cadaverine in the body as a non-invasive means rapid, potential disease identification.

The life span of the C-MWCNT/DAO/EDC-NHS/GA was evaluated and determined that after a duration of 40 days, the biosensor resulted in only a 2.12% efficacy loss. This is of importance particularly considering the application of such devices, as tools which are required to be transported and stored until required for use. It has been previously shown that under normal storage conditions of non-functionalised enzymatic electrodes, the systems struggle to operate after storage, resulting in poor working lifespans (Crapnell et al., 2022). The increase in shelf-life of the C-MWCNT/DAO/EDC-NHS/GA biosensor may be attributed to its modification, in particular its crosslinking using glutaraldehyde. Numerous previous works have demonstrated the effects of glutaraldehyde fixation and its ability to increase the shelf-life of enzymes via intermolecular crosslinking (Ritter et al., 2014; Migneault et al., 2018).

This work demonstrated the development of a MWCNT and DAO modified biosensor as an inexpensive and rapid alternative method to detect cadaverine. In addition, using this method precluded the requirement for samples pre-processing, a major advantage to current polyamine detection methods. This biosensor utilised DAO, a polyamine specific enzyme which was covalently crosslinked to MWCNTs and selectively detects cadaverine due to enzyme substrate specificity.

This method of detection can be compatible with a range of biomolecules by simply altering the detection enzyme in the biosensor system. The simplicity of fabrication and application lends itself to great interest within the healthcare environment due to low operational potentials, costs, and the benefit of real time analysis, making it a potentially suitable alternate device to current detection strategies.

4.4 Conclusion

The C-MWCNT/DAO/EDC-NHS/GA biosensor had been successfully developed for use in an electrochemical detection system for cadaverine. The incorporation of DAO onto C-MWCNTs demonstrated a viable method to measure the concentrations of cadaverine in both stock solutions and artificial saliva, using an enzyme-substrate complex reaction. Using electroanalytical techniques such as DPV and CV, the C-MWCNT/DAO/EDC-NHS/GA biosensor demonstrated the ability to measure concentrations of cadaverine to as low as 0.8 µg/mL, which was measured in real-time and shows limits of detection lower than that of current devices. Furthermore, the device was shown to respond to small changes in cadaverine concentrations, which would be indicative of periodontal disease state changes within afflicted individuals. The ability of the device to operate in an artificial saliva environment was determined to be successful and provides possibilities for this device to be developed further to increase its technological readiness level. Thus, such a biosensor which is cheap to produce, readily and rapidly producible, and provides measurements in real-time for cadaverine detection, has the potential to be developed for use in the early detection of disease.

CHAPTER 5

Cytotoxicity of Cadaverine and *P. gingivalis*

5.1 Introduction

P. gingivalis is one of the main microorganisms responsible for electing the inflammatory disease states seen in periodontitis and has a myriad of virulence factors including the production of gingipains which result in evasion of host cell recognition and destruction (Xu et al., 2020). Gingipains have been shown to contribute significantly towards *P. gingivalis* highly resistant bactericidal efficacy through degradation of human complement components. The methods used in this chapter were to evaluate the cytotoxic profiles of *P. gingivalis* and cadaverine and were measured using host pathogen interactions and *via* cell viability and migration assays. The aim of this chapter was to determine if *P. gingivalis* and cadaverine elicited a detrimental effect towards human cell lines and to visualise the killing of *P. gingivalis* by host immune cells.

5.2 Results

5.2.1 Monocyte to Macrophage Differentiation

The changes in morphology of U937 monocytes after the cells were treated with PMA at a concentration of 50 ng/mL for 24 h (Fig. 5.1). Spherical floating monocytes (Fig. 5.1a) were transformed into macrophage cells (Fig. 5.1b) which were characterized by increased adherence, ruffled cell membranes and the formation of cell clusters.
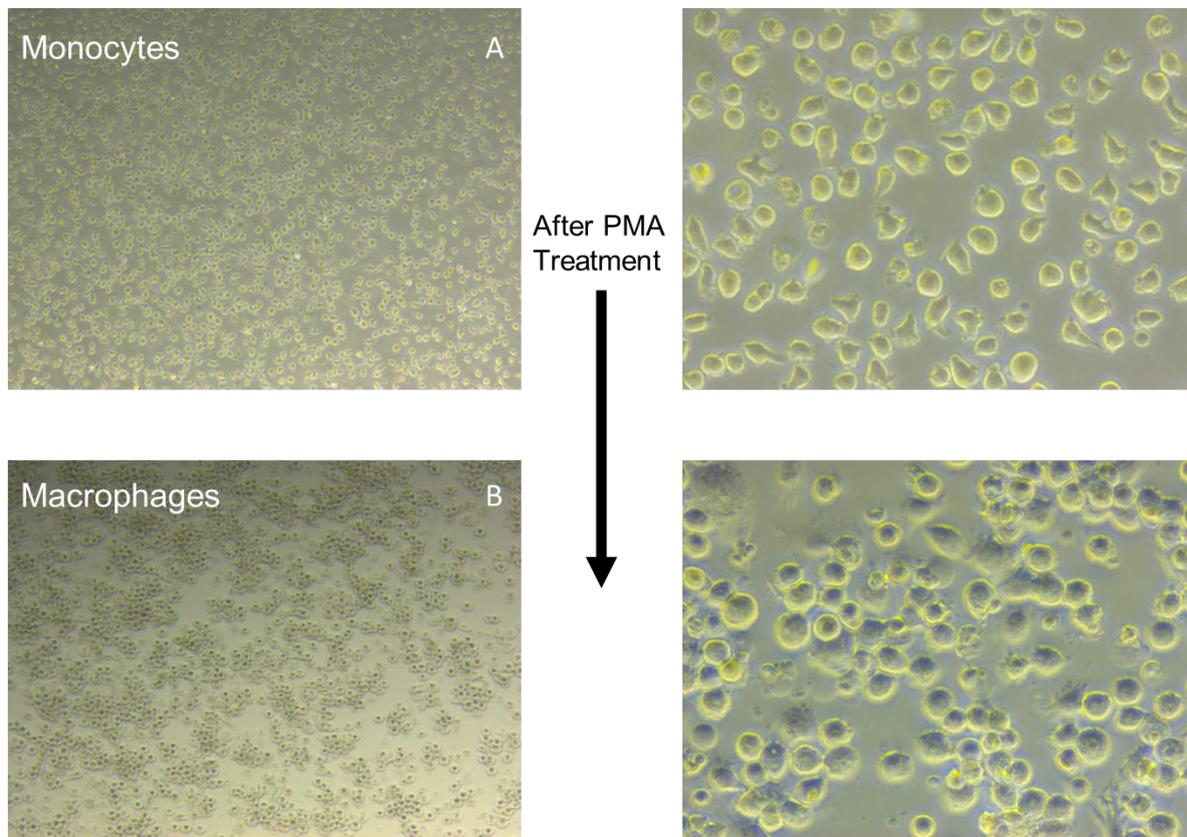
Figure 5. 1. Morphological changes of U937 monocytes after 24 h Phorbil 12-myristate 13-acetate treatment at a concentration of 50 ng/ L. Spherical unadhered monocytes (A) were differentiated into adherent macrophage cells (B) which formed aggregations and clusters. Macrophages showed ruffled cell membranes.

5.2.2 Flow Cytometry

The differentiation of U937 monocytes to distinct macrophage populations were confirmed using flow cytometry via the detection of FTIC-conjugated anti-human CD11C surface marker expression. The U937 PMA-differentiated macrophages were almost entirely CD11c$^+$ (Fig. 5.2), whereas untreated U973 monocyte controls primarily lacked the CD11c surface marker. The CD11c MFI was significantly increased in the PMA-treated U937 cells in comparison to the untreated U937 monocyte controls. This confirmed the PMA treatment differentiated the U937 monocytes into adherent U937 M0 macrophages.
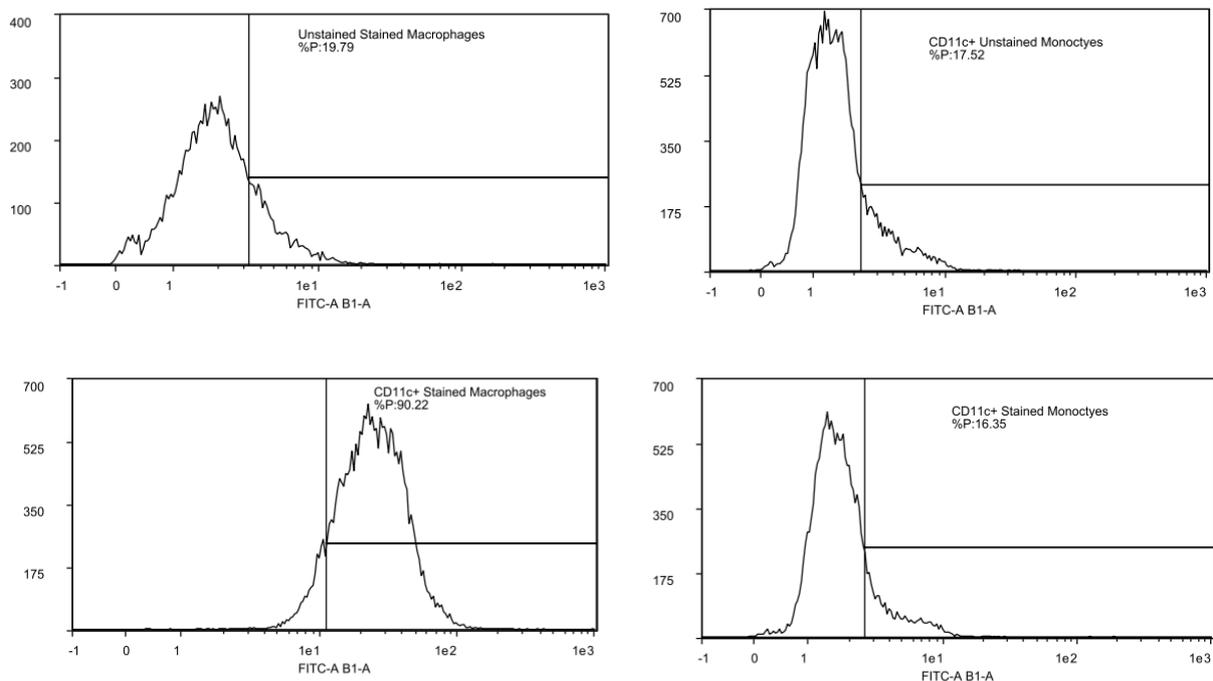
Figure 5. 2. Flow cytometry confirming the differentiation of U937 monocytes into M0 macrophages. Phorbol 12-myristate 13-acetate- differentiated cells evidently and exclusively expressed the Cd11c surface macrophage marker, whereas monocytes were absent of CD11c.

5.2.3 Bacterial Cultures

The microorganism *P. gingivalis* was cultured initially in liquid media and streaked onto solid BHI with supplementation agar plates and demonstrate the black pigmented *P. gingivalis* streaked on solid medium (Fig 5.3).
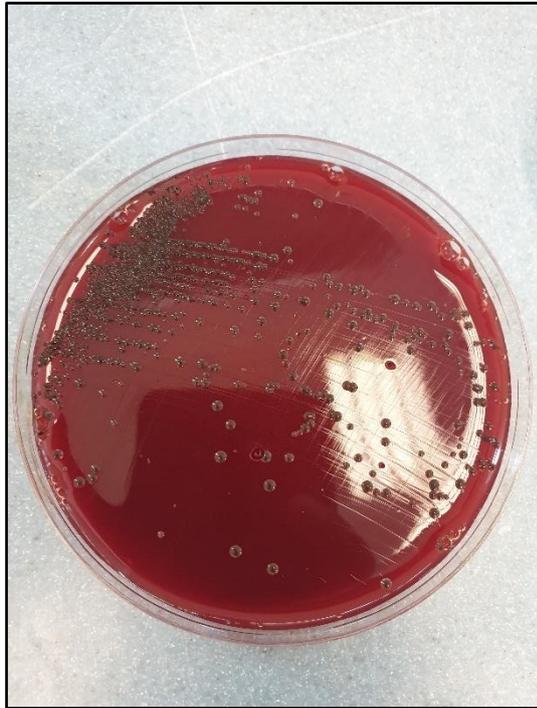
Figure 5. 3**.** *P. gingivalis* streaked onto brain heart infusion agar supplemented with 10% (v/v) horse blood, 7.67 uM haemin, and 2.91 uM menadione.

5.2.4 Scanning Electron Microscopy

To visualise and make comparisons between the host pathogen interaction of U937 derived M0 macrophages and *P. gingivalis*, the samples were visualised using SEM (Fig. 5.4). The point at which the M0 macrophages extend their pseudopodia appendages to entrap localised bacteria was demonstrated in image a, b and d (red arrow), with a large number of membrane extensions being observed. The engulfed

bacteria (Fig. 5.4b) were also seen in all images and show internalised *P. gingivalis* as the macrophage membrane encloses them for phagocytosis.
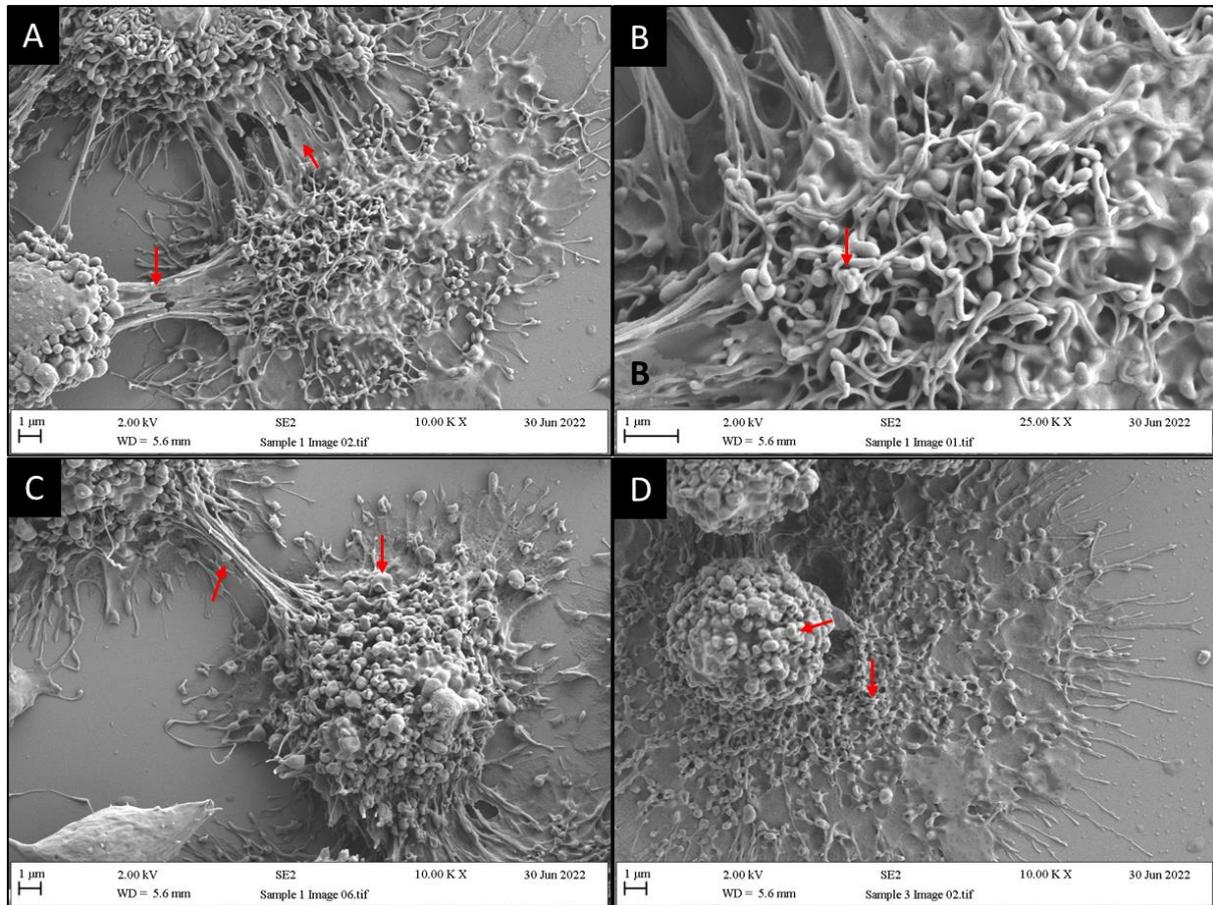
Figure 5. 4**.** Scanning electron micrograps showing the morphological changes in U937 derrived M0 macrophages after host pathogen interaction with *P. gingivalis*. The M0 macrophage extends its psudopodia-like membrane to engage and engulf surrounding invading bacteria (a, c, d). The internalisation of the *P. gingivalis* was observed (b) and shows the macrophage membrane engulfing the bacteria by spreading its appendages over the localised bacteria.

5.2.5 HK-2 Cell Viability

Immortalized renal human proximal tubule cell viability was tested against cadaverine to determine the detrimental effects cadaverine would have towards renal cell lines

(Fig. 5.5). Cell viability was undertaken following the exposure of HK-2 cells for 24 h and 48 h to cadaverine at concentrations of 3 µg/mL, 15 µg/mL, and 40 µg/mL. These concentrations were chosen with in accordance with the three periodontal disease states of mild, moderate, and advance periodontitis (Fig.5.5). Following the addition of CCK-8 reagent, timepoints of 24 h, 25 h, and 26 h, were measured to assess cell viability. The results after 24 h (a) and 25 h (b) of cadaverine incubation demonstrated a reduction in cellular viability in comparison to the control of HK-2 cells in serum free media. The reduction in viability was consistent with the increase in cadaverine concentration from 3 – 40 µg/mL, however, the reduction was statistically not significant. After 26 h of incubation a significant reduction in cellular viability was determined at 40 µg/mL. This effect was also observed after 48 h of incubation with cadaverine whereby, the 48 h, 49 h and 50 h timepoints each demonstrated significant reductions in HK-2 cell viability at each concentration of cadaverine tested (3, 15 and 40 µg/mL) with the exception of the 3 µg/mL cadaverine concentration at the 48 h timepoint. Up to 50% reductions in viability were observed, in particular after the 26 h timepoint, indicating a significant loss in cellular viability.
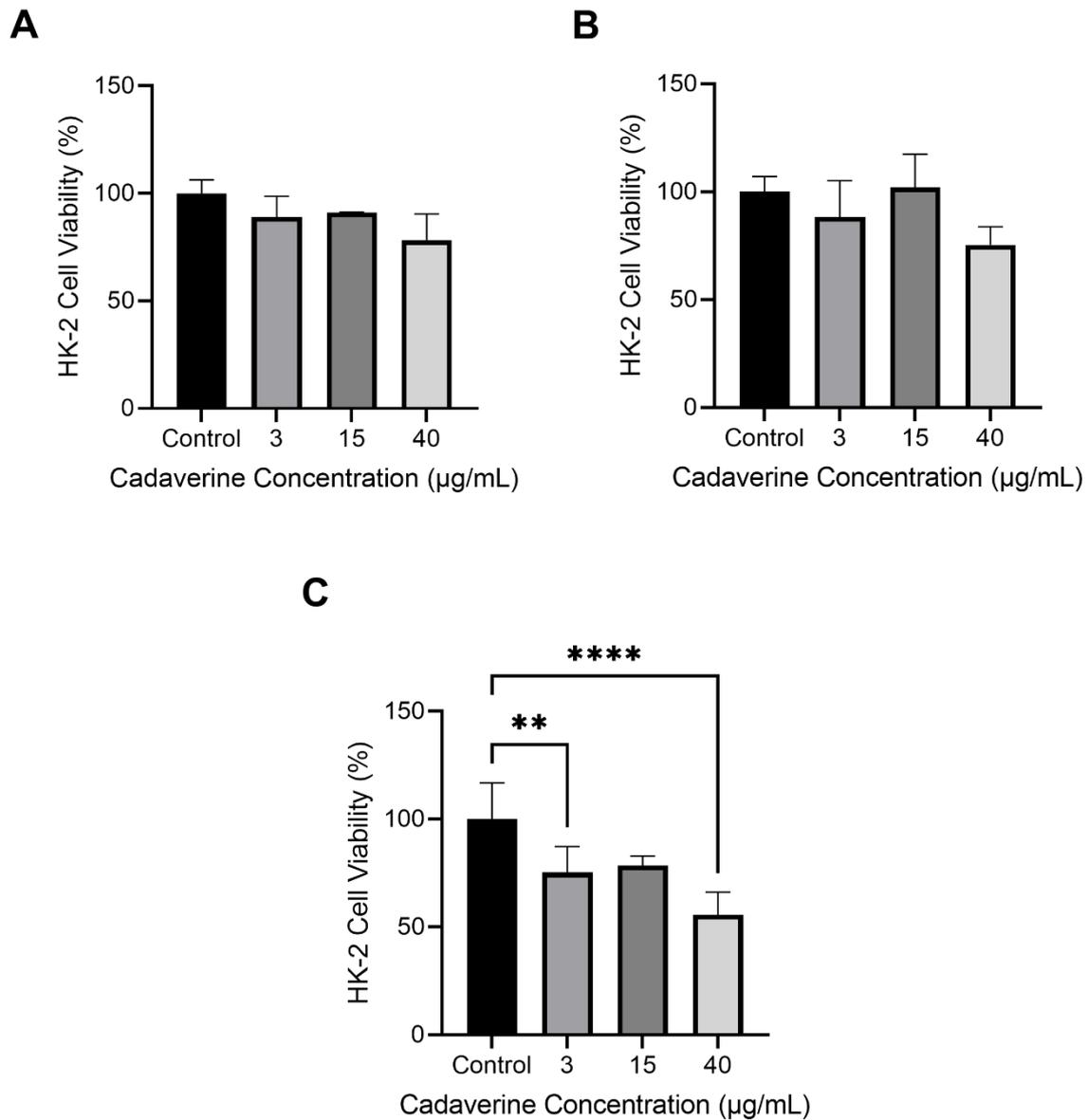
Figure 5. 5. Cell viability of HK-2 cells after A) 24 h, B) 25 h, and C) 26 h of incubation with cadaverine concentrations of 3 µg/mL, 15 µg/mL, and 40 µg/mL. The error bars represent standard error of the mean. $*p \leq 0.05$, $**p \leq 0.01$, $***p \leq 0.001$, $****p \leq 0.0001$ ($n=6$).

The cytotoxic effects of cadaverine after 48 h of incubation with HK-2 cells was investigated (Fig. 5.6). Significant detrimental effects of HK-2 cells were observed after

48 h of incubation whereby, the 48 h (a), 49 h (b) and 50 h (c) timepoints each demonstrated significant reductions in HK-2 cell viability at each concentration of cadaverine tested (3, 15 and 40 µg/mL), with the exception of the 3 µg/mL cadaverine concentration at the 48 h timepoint. Upwards of a 50% reduction in overall cell viability was observed, suggesting that cadaverine showed significant cytotoxicity towards HK-2 cells after being incubated with the cells for at least 48 h.
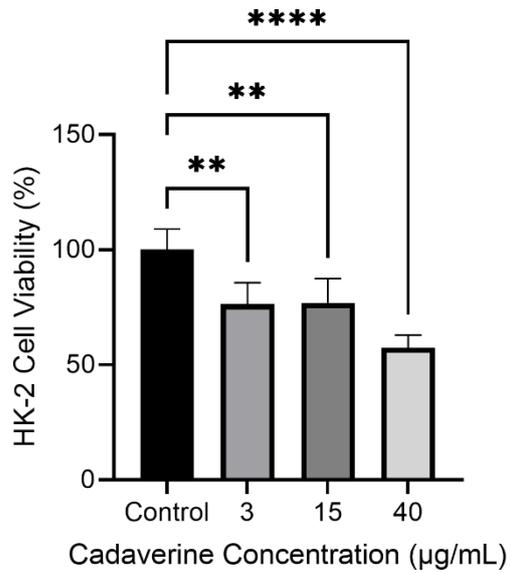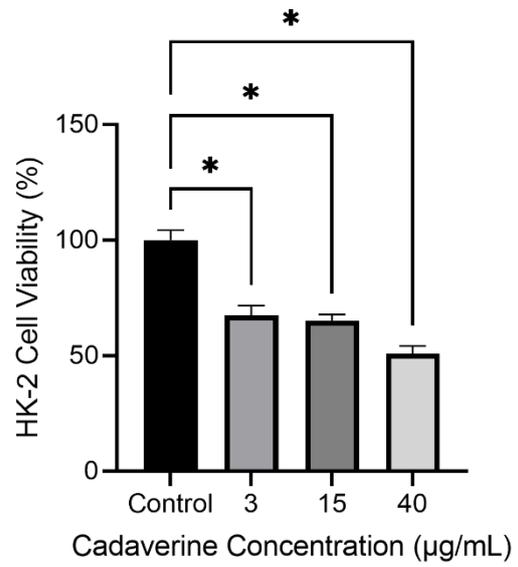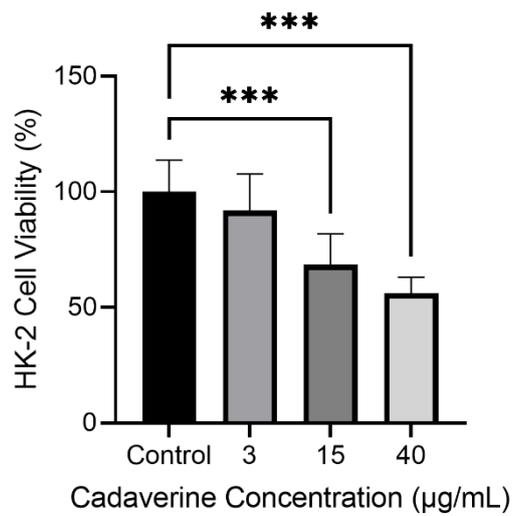
Figure 5. 6. Cell viability of HK-2 cells after A) 48 h, B) 49 h, and C) 50 h of incubation with cadaverine concentrations of 3 µg/mL, 15 µg/mL, and 40 µg/mL. The error bars represent standard error of the mean. $*p \leq 0.05$, $**p \leq 0.01$, $***p \leq 0.001$, $****p \leq 0.0001$ ($n=6$).

5.2.6 M0 Macrophage Cell Viability

M0 macrophage cell viability was investigated following the exposure of cadaverine for 24 h and 48 h (Fig. 5.7). After 24 h (a) of exposure, cadaverine at each tested concentration (3 µg/mL, 15 µg/mL, and 40 µg/mL) showed no significant differences between M0 macrophages viability when treated with cadaverine in comparison with the control. However, after 25 h (b), the highest concentration of cadaverine tested, 40 µg/mL, a significant reduction in cellular viability was determined. In contrast to the previous timepoints tested, after 26 h (c), all three concentrations of cadaverine (3 µg/mL, 15 µg/mL, and 40 µg/mL) demonstrated significant reductions in M0 macrophage cell viability when compared to the control.
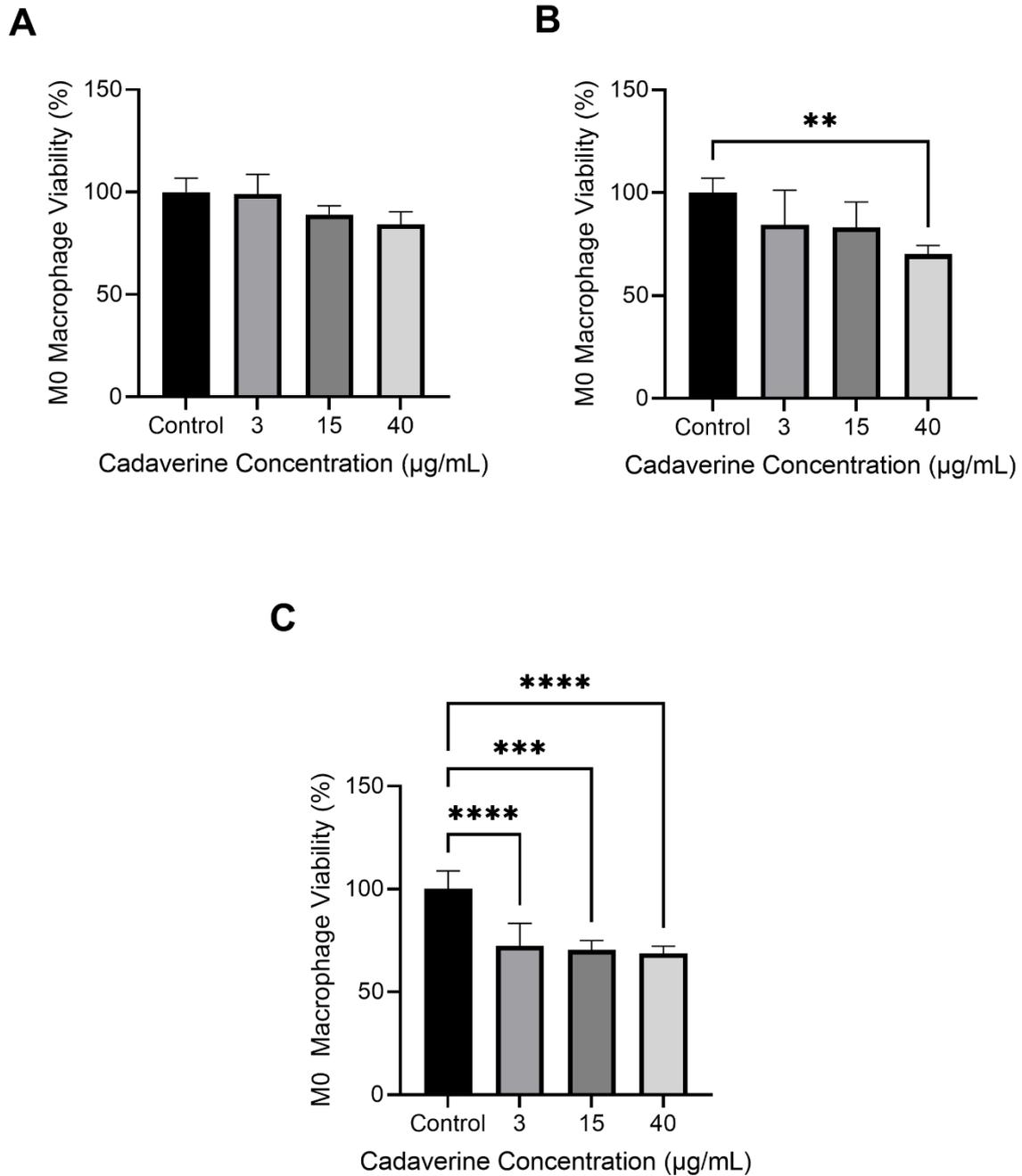
Figure 5. 7. Cell viability of M0 macrophage cells after A) 24 h, B) 25 h, and C) 26 h of incubation with cadaverine concentrations of 3 µg/mL, 15 µg/mL, and 40 µg/mL. The error bars represent standard error of the mean. $*p \leq 0.05$, $**p \leq 0.01$, $***p \leq 0.001$, $****p \leq 0.0001$ ($n=6$).

The viability of M0 macrophage cells was tested following 48 h of exposure to cadaverine at concentrations of 3 µg/mL, 15 µg/mL, and 40 µg/mL (Fig. 5.8). After 48 h (a), statistical analysis showed significant differences in M0 macrophage viability when compared to untreated cells. Furthermore, the viability of the cells decreased further with increases in the concentration of cadaverine to a maximum 51% reduction in total viable cells, at the highest concentration.
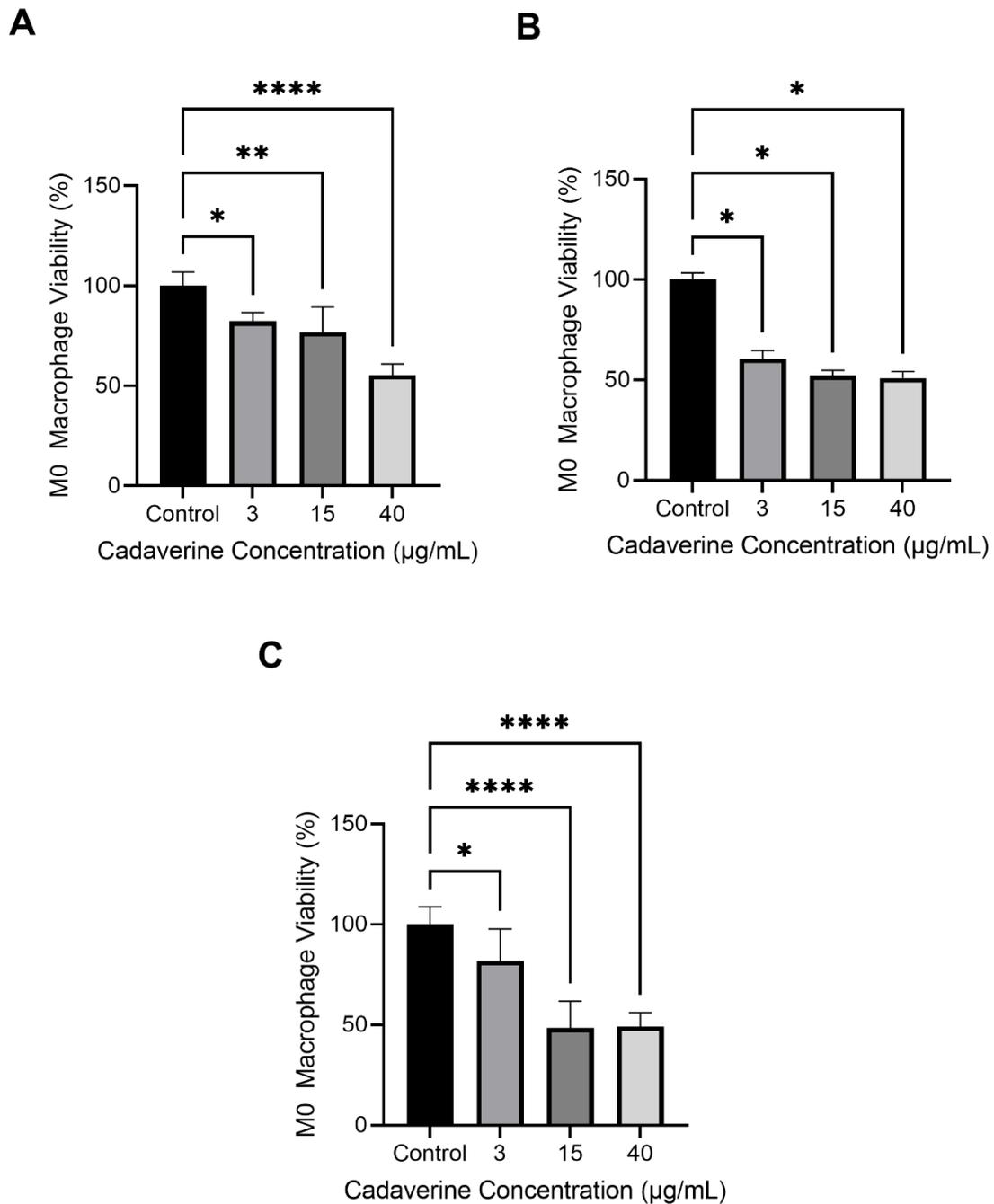
Figure 5. 8. Cell viability of M0 macrophage cells after A) 48 h, B) 49 h, and C) 50 h of incubation with cadaverine concentrations of 3 µg/mL, 15 µg/mL, and 40 µg/mL. The error bars represent standard error of the mean. *$p \leq 0.05$, **$p \leq 0.01$, ***$p \leq 0.001$ (n=6).

5.2.7 Cell Migration and Wound Healing Assay

The cell migration assay was carried out to determine the effects cadaverine, over 72 h, had on the migratory and wound closure outcome of M0 macrophage cells (Fig. 5.9). Measurements were taken at 0 h, 3 h, 6 h, 24 h, 48 h and 72 h, and the mean of each timepoint was compared to the control using a two-way ANOVA with multiple comparisons. The results showed that after 72 h, all samples tested achieved 100% wound closure. At the 3 h, 6 h, 24 h, and 48 h timepoints, all concentrations of cadaverine demonstrated significant reductions in wound closure in comparison to the control, with the exception of 3 µg/mL cadaverine at 3 h which showed no significant reduction in migration.
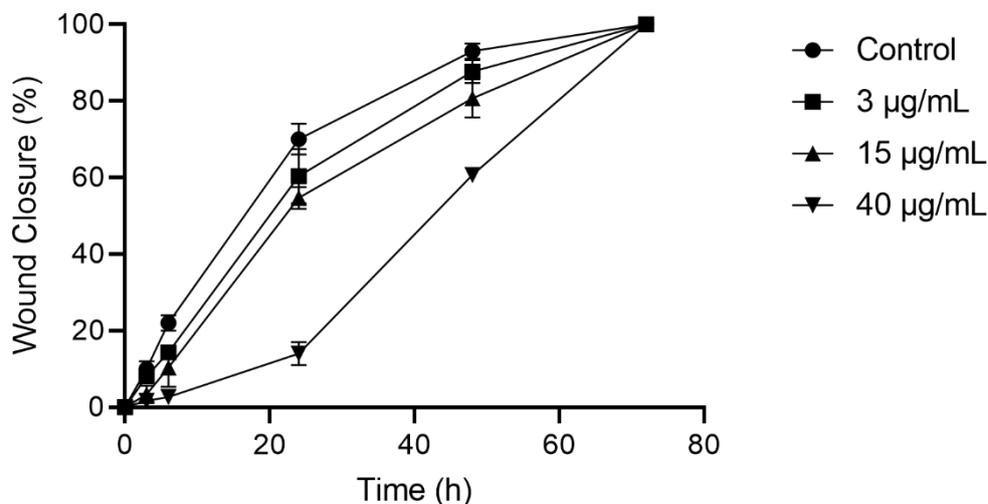
Figure 5. 9. Percentage wound closure of M0 macrophage cells after 24 h exposure to serum free media (control), 3 µg/mL of cadaverine, 15 µg/mL of cadaverine, and 40 µg/mL of cadaverine. Wound was made and expressed as a percentage of total closure of the individual wells. Error bars show standard error of the mean (n=3).

5.3 Discussion

5.3.1 Flow Cytometry

The *in vitro* stimulation of monocytes into macrophage cells is one of the essential requirements to carry out host-pathogen interactions. The differentiation of monocytes has been reported to be successfully achieved using PMA. This has been previously shown that PMA it induces monocytes to undergo transformation through the up-regulation of cell adhesin molecules such as CD11b, CD11c, and CD18, which enables the *in vitro* cells to become adherent to cell culture flasks (Martinez et al., 2006; Luscinskas et al., 1994). Flow cytometry was used in this study to confirm the successful differentiation of monocytes to macrophages via CD11c marker expression. The significantly high abundance of PMA-differentiated macrophages which express the CD11c surface marker when compared to non expressing monocytes, in the absence of PMA, were used to confirm the differentiation of U937 monocytes into M0 macrophage cells.

5.3.2 SEM of Host Pathogen Interaction

The SEM images demonstrated the morphological changes which macrophages undergo when arriving at the sight of infection. Whilst these images demonstrate the late effects of macrophages towards a bacterial infection, in the earlier stages of infection, *P. gingivalis* has been reported to demonstrate a myriad of host immune cell evading mechanisms which result in its continual survival and higher CFU counts in periodontitis than other competing oral microorganisms (Werheim et al., 2020). The establishment of a large number of pseudopodal appendages for the purpose of bacterial engulfment and subsequent phagocytosis is the common process of

inflammatory infections. These findings suggest that *P. gingivalis* is phagocytosed by macrophages during infection.

5.3.3 Cell Viability

The results of the cell viability assays indicated that prolonged exposure to cadaverine had a statistically significant effect on the cell viability of HK-2 and M0 macrophage cells. These results correspond with previous evidence, suggesting that cadaverine shows a dose dependant cytotoxic effect towards human cell lines (Del Rio et al., 2019). The method by which cadaverine causes its cytotoxic effects had also been suggested, which being similar to other polyamines. Cadaverine produces a necrotic effect towards the tested cell lines and may suggest a possible mode of action in which cadaverine after 24 h exposure elicits on HK-2 and M0 macrophage cells. This work corresponds which previous evidence of the cytotoxicity of *P. gingivalis* supernatants as cytotoxicity measurements against gingival fibroblast cells were carried out and showed significant reductions in cellular viability (Yamasaki et al., 1998; Morioka et al., 1993).

5.3.4 Cell Migration Assay

The results of the cell migration/wound healing assay demonstrated that after incubation with cadaverine, the motility and migration of M0 macrophage cells significantly decreased in comparison to the serum free media controls. These reductions in migration may be due to the cytotoxic effects elicited by cadaverine. It has been previously shown that cadaverine can react with nitrates within the cellular

environment and produce nitrosamines, compounds which have a long history of being toxic carcinogens and may be a reason for the effects seen in this work (Del Rio et al., 2019; Ladero et al., 2010). However, there is little previous evidence to show that cadaverine is able to disrupt the migration of cells, however, similar polyamine compounds in putrescine and spermine have been investigated. These polyamines have been shown to inhibit cell migration of keratinocytes and fibroblast cell lines (Lim et al., 2018). Whilst the presence of physiological levels of polyamines are required for normal cellular function and growth, increased levels have shown to adversely affect the migration of cells by means of apoptosis and necrosis and may be a similar active mechanism for anti-migratory effects determined by cadaverine (Costa et al., 2021).

5.4 Conclusion

P. gingivalis and cadaverine cytotoxicity was investigated towards HK-2 and M0 macrophage cells to determine possible detrimental effects they incur during periodontitis. The results from this chapter demonstrated a linear relationship between concentration of the respective toxin and the extent of the cytotoxic effects incurred by the cells. *P. gingivalis* supernatants were tested as they relay the metabolites responsible for the effects seen during periodontal disease. Cadaverine was found to induce anti-migratory effects on M0 macrophages, and these effects were more evident as the concentrations of cadaverine increased.

CHAPTER 6

Summary of Findings, Future work, and Limitations

6.1 Summary of Findings

Periodontal disease is a very common disease within human populations (Nazir et al., 2017). It has been shown that periodontitis is frequently co-morbid with other diseases such as CKD, with a significant number of overlapping risk factors (Sharma et al., 2016). In addition, periodontitis has been shown to have coinciding systemic effects on distal locations in the body sourcing from the bacterium of microbial products in the bloodstream, with numerous studies linking its involvement in a number of other diseases such as cardiovascular disease. *P. gingivalis* one of the keystone microorganisms in periodontitis has a number of pathogenic mechanisms in which it exacerbates a periodontitis infection, with one being the release of metabolites, in particular, cadaverine. The effects of cadaverine in periodontal disease have been investigated previously, and suggestions have been made into its concentration dependant isolation in each respective periodontitis disease stage. This effect of cadaverine had led to further investigation into the current methods of periodontitis diagnostics and resulted determining that current techniques provide insufficient information of the active state of the disease (Armitage, 2003; Srivastava et al., 2017).

One of the main objectives of this study was to initially identify a potential biomarker which would provide a means detection for periodontitis, along with serving as a target molecule for developing a biosensor towards. The number of periodontal microorganisms is complex, however, the bacteria which has been most implicated in periodontal disease and has been studied extensively is *P. gingivalis*. Of the metabolome which *P. gingivalis* possesses, cadaverine has been linked with increased periodontal disease state and perpetuating tissue destruction (Sakanaka et al., 2017), and thus this molecule, provided an ideal candidate for targeted detection.

One of the key challenges in this study was to identify a way to selectively detect cadaverine as the oral cavity provides an environment which is complex in nature and is host to a myriad of potential interference molecules (Han et al., 2022). As such, the enzyme, diamine oxidase, was selected due to its polyamine specific active site, and enabling for enzyme-substrate specific interactions (Sessa and Perin, 1994). It has been shown extensively in literature that the addition of biological layers to an electrode surface slow down electron transfer rates, however, the method in which they are deposited and formulated may reduce the inference which they incur (Mikysek et al, 2012). Thus, physical adsorption, one of the main methods in enzyme immobilisation was opted against for this work, in preference to focusing on covalent attachment with the aid of nanotube scaffold structures. The insoluble nature of carbon nanotubes has long since provided a challenge for biosensor development, since these eliminate the use of common harsh solvents which cannot be used since they damage the enzyme. Thus, the EDC-NHS carbodiimide couple provided the most suitable method of conjugation, by not only maintaining the enzyme integrity, but also by aiding in the homogenous dispersion of the CNTs, though the amphiphilic action of the enzymes (Kim et al,. 2017).

The detection of a modified biosensor to detect cadaverine, showed that unmodified SPEs were unable to relay any electrochemical signals for cadaverine detection and this was in part due to the unavailability of any cadaverine oxidising elements on the bare SPE surface. The modified biosensor demonstrated good efficiency in cadaverine detection, showing linear correlations between cadaverine concentration and peak currents. Further results disseminated the pH dependency on the system and functioned linearly also, towards the pKa of cadaverine. One of the aims of this

work was to determine if the developed device would operate in nonstandard solutions, thus demonstrating it had applicability in real world applications. Thus, testing of the biosensor in simulated human saliva was of major importance, and showed the sensor maintained its efficacy towards cadaverine, being unhindered by interfering biomolecules.

The conversion of monocytes into macrophage like cells *in vitro* was an essential requirement to conduct all of the host pathogen assays used in this study as they are the primary host defence cells in a peritonitis infection. PMA throughout the literature has been shown to induce the differentiation of monocytes into M0 resting macrophages *in vitro* through the upregulation of adhesin molecules such as CD11a, CD11b and CD11c (Martinez et al., 2006l; Luscinskas et al., 1994). This enables the cells to adhere to their respective culture flasks. The use of flow cytometry was used to confirm the differentiations of the monocytes into macrophages using CD11c surface marker expression as an indicator of successful differentiation. The high expression levels of CD11c in the macrophages after PMA differentiation, in comparison to the monocytes, confirmed the successful differentiation of U937 monocytes into M0 macrophages.

An objective of this work was to determine if cadaverine is able to induce cytotoxic and migratory effects in human cells. This was carried out using the incubation of cadaverine against human kidney and macrophage cells lines and the assessment of cellular biochemical activity over 24 and 48 h, whilst also investigating the migratory effects induced by determining the wounding healing effects overtime. This work presents novel data in that *P. gingivalis* and cadaverine both exhibited cytotoxic effects

against human kidney and macrophage cells, accompanying a strong anti-migratory effect. The anti-migratory effect of cadaverine presented in this work after 24 h may be due to the cytotoxic effect of slowing cell migration, as previous work reports of anti-migratory effects which occur due to degradation of adhesin molecules, resulting in impaired cellular function (Costa et al., 2021). This is an important finding as it may suggest one of the mechanisms in which a periodontitis infection is maintained, as host cells exhibit impaired migration to the site of infection.

Overall, the main findings of this study are that the developed biosensor was able to detect cadaverine, at concentrations indictive of periodontal disease in both stock and simulated real-world solutions. Furthermore, *P. gingivalis* and its derived metabolite, cadaverine, were able to elicit a cytotoxic and anti-migratory response towards HK-2 and U937 derived M0 macrophage cells.

6.2 Conclusion

This thesis reports a body of experimental evidence which contributes to the fields of electrochemistry and biosensor design, in particular the electrochemical detection of cadaverine using an enzyme modified multi-walled carbon nanotube screen-printed biosensor. Furthermore, this study also investigated the detrimental effects of oral bacterial toxins on host cells. When translating these findings to the context of disease detection, they provide a potential alternative to traditional periodontal disease diagnostic techniques, which remain a dated and inefficient practice.

The successful modification of a carbon paste screen-printed electrode with a novel diamine oxidase and multi-walled carbon nanotube formulation was demonstrated. This formulation was shown to conjugate diamine oxidase to the nanotubes successful and demonstrate more homogeneous dispersion properties than previous works and overall contributed to developing faster electron transfer rates for the biosensor.

The biosensor's efficacy towards its target substrate, cadaverine showed a concentration dependant association of cadaverine detection and was able to successfully electrochemically detect the key periopathogen toxin, cadaverine.

This work also disseminated the cytotoxic effects which cadaverine and *P. gingivalis* induces towards human cells. Methods such as flow cytometry and scanning electron microscopy confirmed the successful differentiation of monocytes to macrophages and the host pathogen interaction model demonstrated significant cytotoxic and migration effects of cadaverine and *P. gingivalis* towards human kidney and human monocytic cell lines.

Based on the findings in this thesis, the developed biosensing device which is able to detect cadaverine at concentrations indicative of periodontal disease and also showed efficacy to operate in simulated human saliva.

Further continuation of this work has been developed by the submission of a £1.4 Million EPSRC grant to translate the biosensor into related technologies and into a potential prototype, working with industrial partners. Moreover, this work has future studies being developed in collaboration with the University of Glasgow whereby, trials into the biosensors efficacy in saliva taken from patients with periodontal disease are also being considered.

This thesis thereby, met the aims and objectives initially proposed, and may go on to provide an effective tool for determining the extent of an individual's periodontitis using a rapid, cost effective, point of care biosensor.

6.2.1 Limitations and Future Work

Following on from the findings presented in this thesis, it would be of interest to further investigate the properties of the carbon nanotubes which provide the foundation of the biosensor. Investigating the properties of the CNTs by trying different variations of nanotube may increase sensor sensitivity and selectivity. Due to the MWCNT analysis limitations in this work, further testing in the form of XPS characterisation, for analysis of the MWCNTs surface chemistry would provide important information regarding confirmation of chemically functionalised CNTs. Moreover, when developing the carbon nanotube modification, this work utilised analytical means to determine if carboxylation of the nanotubes had taken place. Transmission scanning electron microscopy would be a further option of obtaining qualitative data on the carboxylation of the nanotubes as numerous studies have shown previously (Martin et al., 2013; Masytin et al., 2018).

A key process during the development of the sensor is the method in which the nanotubes are incorporated on the working electrode. Drop-casting, albeit efficient and cost effective has many shortcomings. This is of particular importance when considering the future implications of this work and to further increase the technological readiness level of the device, more efficient methods of nanotube to surface deposition would be required. Thus, investigating new methods such as spin coating and electrodeposition would be worth pursuing to unify the homogeneity of the electrode surface and to give a more replicable modification.

After enzyme modifications of the biosensor, it was evident that further analysis would be needed to obtain further information on its interactions with cadaverine. Utilising

electrochemical impedance spectroscopy and chronoamperometry would be an effective means of investigating the frequency dependant properties of the electrode, in addition phenomena such as the adsorption properties of cadaverine vs the biosensor could be investigated. Moreover, it would be of interest to analyse the analytical properties of other electrodes and make comparisons. Since the electrochemical study of cadaverine is still in its infancy, it would be worthwhile to assess a combination of different electrodes when determining the most suitable for its application.

This study used artificial saliva as a means of replicating the oral environment. The oral cavity and its corresponding biofluid are host to over 500 bacterial species and a significantly higher number of metabolites and other biological components. Thus, using artificial saliva may not provide a complete replica of what would be isolated in a real human saliva. Having a significantly higher number of possible interference molecules may convolute the results and efficacy of the device. As to date, no cadaverine study using biosensors has taken place using real human saliva. Thus, continuation into investigating the real world applicability of the biosensor would include determining its efficacy in real human saliva.

The host pathogen interaction findings in this study were obtained from experiments which using *in vitro* and *ex vivo* macrophages. Repeating these experiments *in vivo* would provide evidence to confirm the detrimental effects of cadaverine and *P. gingivalis* on the oral environment and its surroundings tissues. Investigating the effects of cadaverine on such a model would provide further insight into the progression of the disease and may potentially result in different biosensors or

biosensor arrays being developed which are able to monitor the progression of the disease upon its initial discovery in a host.

The distinct morphological changes which occur in macrophages as a result of incubation with *P. gingivalis* requires future work to disseminate the physical and biochemical effects which are induced in response to the pathogen interaction. A spectrometric means of quantification could be used such as FTIR spectroscopy or Raman analysis for the identification of functional group changes on the cell membranes during the host pathogen interaction.

In this study, the cells lines used to investigate the cytotoxic and migratory effects of the periodontal toxin, cadaverine, was HK-2 and U937 monocytes. Human gingival fibroblast/ epithelial cells would be used for further testing albeit their availability in an immortalised state is a rarity since primary cells introduce the difficulty of prolonged cultivation. Repeats of the cytotoxicity experiments which more strongly represent the tissues of oral cavity which microbial toxins are more likely to infect would be beneficial to further elucidate the potential effects of cadaverine.

The use of the colorimetric tetrazolium based CCK-8 reagent for the viability assays also represents a potential limitation for this work. The key issue arising from the nature of these reagents and their ability to become convoluted with interaction from external compounds and interact with the readings. This tetrazolium based compounds assess cellular viability through biochemical activity, which gives and indirect measure of cellular viability in proportion to the absorbance at two wavelengths. To provide a more accurate and specific measure of cell death, flow

cytometry using Annexin V/Propidium iodide could be used as they provide direct indication of the cells apoptotic and necrotic states.

References

Ai, J., Smith, B. and Wong, D.T., (2010) Saliva Ontology: an ontology-based framework for a Salivaomics Knowledge Base. *BMC Bioinformatics*, 11, p.302.

Alexi, N., Hvam, J., Lund, B.W., Nsubuga, L., de Oliveira Hansen, R.M., Thamsborg, K., Lofink, F., Byrne, D. V. and Leisner, J.J., (2021) Potential of novel cadaverine biosensor technology to predict shelf life of chilled yellowfin tuna (Thunnus albacares). *Food Control*, 119, p.107458.

Alhogail, S., Suaifan, G.A.R.Y., Bizzarro, S., Kaman, W.E., Bikker, F.J., Weber, K., Cialla-May, D., Popp, J. and Zourob, M., (2018) On site visual detection of Porphyromonas gingivalis related periodontitis by using a magnetic-nanobead based assay for gingipains protease biomarkers. *Mikrochim Acta*, 1852, p.149.

AlMoharib, H.S., AlMubarak, A., AlRowis, R., Geevarghese, A., Preethanath, R.S. and Anil, S., (2014) Oral fluid based biomarkers in periodontal disease: part 1. Saliva. *J Int Oral Health*, 64, pp.95–103.

Alpuim Costa, D., Nobre, J.G., Batista, M.V., Ribeiro, C., Calle, C., Cortes, A., Marhold, M., Negreiros, I., Borralho, P., Brito, M., Cortes, J., Braga, S.A. and Costa, L., (2021) Human Microbiota and Breast Cancer—Is There Any Relevant Link?—A Literature Review and New Horizons Toward Personalised Medicine. *Frontiers in Microbiology*, 12.

Alwarappan, S., Erdem, A., Liu, C. and Li, C.-Z., (2009) Probing the Electrochemical Properties of Graphene Nanosheets for Biosensing Applications. *Journal of Physical Chemistry C*, 11320, pp.8853–8857.

Amano, A., (2007) Disruption of epithelial barrier and impairment of cellular function by Porphyromonas gingivalis. *Frontiers in Bioscience*, 1210, pp.3965–3974.

Amin, M., Abdullah, B.M., Rowley-Neale, S.J., Wylie, S., Slate, A.J., Banks, C.E. and Whitehead, K.A., (2022) Diamine Oxidase-Conjugated Multiwalled Carbon Nanotubes to Facilitate Electrode Surface Homogeneity. *Sensors*, 222, p.675.

Amin, M., Abdullah, B.M., Wylie, S.R., Rowley-Neale, S.J., Banks, C.E., Whitehead K.A., (2022) The Voltammetric Detection of Cadaverine Using a Diamine Oxidase and Multi-Walled Carbon Nanotube Functionalised Electrochemical Biosensor. *Nanomaterials* (*Basel*), 13(1), p.36.

Amin, M., Rowley-Neale, S., Shalamanova, L., Lynch, S., Wilson-Nieuwenhuis, J.T., El Mohtadi, M., Banks, C.E. and Whitehead, K.A., (2020) Molybdenum Disulfide Surfaces to Reduce Staphylococcus aureus and Pseudomonas aeruginosa Biofilm Formation. *ACS applied materials & interfaces*, 1218, pp.21057–21069.

Amin, M., Tang, S., Shalamanova, L., Taylor, R.L., Wylie, S., Abdullah, B.M. and Whitehead, K.A., (2021) Polyamine biomarkers as indicators of human disease. *Biomarkers*, 262, pp.77–94.

Andörfer, L., Holtfreter, B., Weiss, S., Matthes, R., Pitchika, V., Schmidt, C.O., Samietz, S., Kastenmüller, G., Nauck, M., Völker, U., Völzke, H., Csonka, L.N., Suhre, K., Pietzner, M. and Kocher, T., (2021) Salivary metabolites associated with a 5-year tooth loss identified in a population-based setting. *BMC Medicine*, 191, p.161.

Ariyamuthu, V.K., Nolph, K.D. and Ringdahl, B.E., (2013) Periodontal disease in chronic kidney disease and end-stage renal disease patients: a review. *Cardiorenal Med*, 31, pp.71–78.

Armbruster, D.A., Tillman, M.D. and Hubbs, L.M., (1994) Limit of detection (LQD)/limit of quantitation (LOQ): comparison of the empirical and the statistical methods exemplified with GC-MS assays of abused drugs. *Clinical chemistry*, 407 Pt 1, pp.1233–8.

Armbruster, D.A. and Pry, T., (2008) Limit of Blank, Limit of Detection and Limit of Quantitation. *The Clinical Biochemist Reviews*, 29Suppl 1, p.S49.

Asha, K., Satsangi, V.R., Shrivastav, R., Kant, R. and Dass, S., (2020) Effect of morphology and impact of the electrode/electrolyte interface on the PEC response of Fe2O3 based systems – comparison of two preparation techniques. *RSC Advances*, 1069, pp.42256–42266.

Asikainen, S., Doğan, B., Turgut, Z., Paster, B.J., Bodur, A. and Oscarsson, J., (2010) Specified species in gingival crevicular fluid predict bacterial diversity. *PLoS One*, 510, p.e13589.

Babbar, N., Murray-Stewart, T. and Casero, R.A., (2007) Inflammation and polyamine catabolism: the good, the bad and the ugly. *Biochem Soc Trans*, 35Pt 2, pp.300–304.

Bai, Y., Huang, H., Meng, K., Shi, P., Yang, P., Luo, H., Luo, C., Feng, Y., Zhang, W. and Yao, B., (2012) Identification of an acidic α-amylase from Alicyclobacillus sp. A4 and assessment of its application in the starch industry. *Food Chemistry*, 1314, pp.1473–1478.

Banks, C.E., Foster, C.W. and Kadara, R.O., (2016) Screen-Printing Electrochemical Architectures.

Bard, A.J. and Faulkner, L.R., (2001) Basic Potential Step Methods. *Electrochemical Methods: Fundamentals and Applications*, pp.156–225.

Barnes, V.M., Kennedy, A.D., Panagakos, F., Devizio, W., Trivedi, H.M., Jönsson, T., Guo, L., Cervi, S. and Scannapieco, F.A., (2014) Global metabolomic analysis of human saliva and plasma from healthy and diabetic subjects, with and without periodontal disease. *PLoS One*, 98, p.e105181.

Barnes, V.M., Teles, R., rivedi, H.M.T., Devizio, W., Xu, T., Mitchell, M.W., Milburn, M. V and Guo, L., (2009) Acceleration of Purine Degradation by Periodontal Diseases. *Journal of dental research*, 889, pp.851–855.

Barros, S.P., Williams, R., Offenbacher, S. and Morelli, T., (2016) Gingival crevicular fluid as a source of biomarkers for periodontitis. *Periodontol 2000*, 701, pp.53–64.

Bartlett, P.N., Bradford, V.Q. and Whitaker, R.G., (1991) Enzyme electrode studies of glucose oxidase modified with a redox mediator. *Talanta*, 381, pp.57–63.Bartold, P.M. and Van Dyke, T.E., (2013) Periodontitis: a host-mediated disruption of microbial homeostasis. Unlearning learned concepts. *Periodontology 2000*, 621, pp.203–217.

Berezow, A.B. and Darveau, R.P., (2011) Microbial shift and periodontitis. *Periodontol 2000*, 551, pp.36–47.

Berlaimont, V., Pauwels, O., Dubois, J. and Hanocq, M., (1997) Evidence of difference between cytotoxicity, cell cycle and morphonuclear effects of polyamines on sensitive and multidrug resistant P388 cell lines. *Anticancer Res*, 173C, pp.2057–2064.

Betlem, K., Down, M.P., Foster, C.W., Akthar, S., Eersels, K., Van Grinsven, B., Cleij, T.J., Banks, C.E. and Peeters, M., (2018) Development of a Flexible MIP-Based Biosensor Platform for the Thermal Detection of Neurotransmitters. *MRS Advances*, 328, pp.1569–1574.

Bik, E., Dorosz, A., Mateuszuk, L., Baranska, M. and Majzner, K., (2020) Fixed versus live endothelial cells: The effect of glutaraldehyde fixation manifested by characteristic bands on the Raman spectra of cells. *Spectrochimica Acta Part A: Molecular and Biomolecular Spectroscopy*, 240, p.118460.

Bisswanger, H., (2014) Enzyme assays. *Perspectives in Science*, 11–6, pp.41–55.Bollella, P. and Katz, E., (2020) Enzyme-Based Biosensors: Tackling Electron Transfer Issues. *Sensors (Basel, Switzerland)*, 2012, pp.1–32.

Bosshardt, D.D., (2018) The periodontal pocket: pathogenesis, histopathology and consequences. *Periodontol 2000*, 761, pp.43–50.

Brownson, D.A.C. and Banks, C.E., (2014) The Handbook of Graphene Electrochemistry. *The Handbook of Graphene Electrochemistry*, pp.1–201.

Cammarata, C.R., Hughes, M.E. and Ofner, C.M., (2015) Carbodiimide induced cross-linking, ligand addition, and degradation in gelatin. *Molecular Pharmaceutics*, 123, pp.783–793.

Cartwright, M., Rottman, M., Shapiro, N.I., Seiler, B., Lombardo, P., Gamini, N., Tomolonis, J., Watters, A.L., Waterhouse, A., Leslie, D., Bolgen, D., Graveline, A., Kang, J.H., Didar, T., Dimitrakakis, N., Cartwright, D., Super, M. and Ingber, D.E., (2016) A Broad-Spectrum Infection Diagnostic that Detects Pathogen-Associated Molecular Patterns (PAMPs) in Whole Blood. *EBioMedicine*, 9, pp.217–227.

Castagnola, M., Scarano, E., Passali, G.C., Messana, I., Cabras, T., Iavarone, F., Di Cintio, G., Fiorita, A., De Corso, E. and Paludetti, G., (2017) Salivary biomarkers and proteomics: future diagnostic and clinical utilities. *Acta Otorhinolaryngol Ital*, 372, pp.94–101.

Castro, S.A., Collighan, R., Lambert, P.A., Dias, I.H., Chauhan, P., Bland, C.E., Milic, I., Milward, M.R., Cooper, P.R. and Devitt, A., (2017) Porphyromonas gingivalis gingipains cause defective macrophage migration towards apoptotic cells and inhibit phagocytosis of primary apoptotic neutrophils. *Cell Death & Disease 2017 8:3*, 83, pp.e2644–e2644.

Cekici, A., Kantarci, A., Hasturk, H. and Van Dyke, T.E., (2014) Inflammatory and immune pathways in the pathogenesis of periodontal disease. *Periodontol 2000,* 641, pp.57–80.

Chaisiwamongkhol, K., Batchelor-McAuley, C., Sokolov, S. V., Holter, J., Young, N.P. and Compton, R.G., (2017) Optimising carbon electrode materials for adsorptive stripping voltammetry. *Applied Materials Today*, 7, pp.60–66.

Champigneux, P., Delia, M.L. and Bergel, A., (2018) Impact of electrode micro- and nano-scale topography on the formation and performance of microbial electrodes. *Biosensors and Bioelectronics*, 118, pp.231–246.

Chan, Y.Y., Eng, A.Y.S., Pumera, M. and Webster, R.D., (2015) Assessments of Surface Coverage after Nanomaterials are Drop Cast onto Electrodes for Electroanalytical Applications. *ChemElectroChem*, 27, pp.1003–1009.

Chen, C., Li, X., Wen, Y., Liu, J., Li, X., Zeng, H., Xue, Z., Zhou, X. and Xie, X., (2019) Noncovalent engineering of carbon nanotube surface by imidazolium ionic liquids: A promising strategy for enhancing thermal conductivity of epoxy composites. *undefined*, 125.

Chen, L., Deng, H., Cui, H., Fang, J., Zuo, Z., Deng, J., Li, Y., Wang, X. and Zhao, L., (2018) Inflammatory responses and inflammation-associated diseases in organs. *Oncotarget*, 96, pp.7204–7218.

Chen, T.K., Knicely, D.H. and Grams, M.E., (2019) Chronic Kidney Disease Diagnosis and Management. *JAMA*, 32213, p.1294.

Cho, M.I. and Garant, P.R., (2000) Development and general structure of the periodontium. *Periodontol 2000*, 24, pp.9–27.

Choong, M.K. and Tsafnat, G., (2012) The implications of biomarker evidence for systematic reviews. *BMC Med Res Methodol*, 12, p.176.

Colburn, A.W., Levey, K.J., O'Hare, D. and Macpherson, J. V., (2021) Lifting the lid on the potentiostat: a beginner's guide to understanding electrochemical circuitry and practical operation. *Physical Chemistry Chemical Physics*, 2314, pp.8100–8117.

Compton, R., (2011) *Understanding voltammetry*. 2nd ed. ed. London: Imperial College Press.Cornejo Ulloa, P., van der Veen, M.H. and Krom, B.P., (2019) Review: modulation of the oral microbiome by the host to promote ecological balance. *Odontology*, 1074, pp.437–448.

Costalonga, M. and Herzberg, M.C., (2014) The oral microbiome and the immunobiology of periodontal disease and caries. *Immunol Lett*, 1622 Pt A, pp.22–38

Couzi, M., Bruneel, J.L., Talaga, D. and Bokobza, L., (2016) A multi wavelength Raman scattering study of defective graphitic carbon materials: The first order Raman spectra revisited. *Carbon*, 107, pp.388–394.

Crane, B., Hughes, J.P., Rowley Neale, S.J., Rashid, M., Linton, P.E., Banks, C.E. and Shaw, K.J., (2021) Rapid antibiotic susceptibility testing using resazurin bulk modified screen-printed electrochemical sensing platforms. *The Analyst*, 14618, pp.5574–5583.

Crapnell, R., Garcia-Miranda Ferrari, A., Dempsy, N., Banks, C.E., (2022) Electroanalytical overview: screen-printed electrochemical sensing platforms for the detection of vital cardiac, cancer and inflammatory biomarkers. *Sen. Diagn*, 1, pp.405-428.

Damian, C.M., Garea, S.A., Vasile, E. and Iovu, H., (2012) Covalent and non-covalent functionalized MWCNTs for improved thermo-mechanical properties of epoxy composites. *Composites Part B: Engineering*, 438, pp.3507–3515.

Darveau, R.P., Arbabi, S., Garcia, I., Bainbridge, B. and Maier, R. V, (2002) Porphyromonas gingivalis lipopolysaccharide is both agonist and antagonist for p38 mitogen-activated protein kinase activation. *Infect Immun*, 704, pp.1867–1873.

de Almeida, P. e. V, Grégio, A.M., Machado, M.A., de Lima, A.A. and Azevedo, L.R., (2008) Saliva composition and functions: a comprehensive review. *J Contemp Dent Pract*, 93, pp.72–80.

de Brito, A.R., Tavares, I.M. de C., de Carvalho, M.S., de Oliveira, A.J., Salay, L.C., Santos, A.S., dos Anjos, P.N.M., Oliveira, J.R. and Franco, M., (2020) Study of the interaction of the lactase enzyme immobilized in a carbon nanotube matrix for the development of the chemically modified carbon paste electrode. *Surfaces and Interfaces*, 20, p.100592.

Del Rio, B., Redruello, B., Linares, D.M., Ladero, V., Ruas-Madiedo, P., Fernandez, M., Martin, M.C. and Alvarez, M.A., (2019) The biogenic amines putrescine and cadaverine show in vitro cytotoxicity at concentrations that can be found in foods. *Sci Rep*, 91, p.120.

Delbove, T., Gueyffier, F., Juillard, L., Kalbacher, E., Maucort-Boulch, D., Nony, P., Grosgogeat, B. and Gritsch, K., (2021) Effect of periodontal treatment on the glomerular filtration rate, reduction of inflammatory markers and mortality in patients with chronic kidney disease: A systematic review. *PLOS ONE*, 161, p.e0245619.

Denny, P., Hagen, F.K., Hardt, M., Liao, L., Yan, W., Arellanno, M., Bassilian, S., Bedi, G.S., Boontheung, P., Cociorva, D., Delahunty, C.M., Denny, T., Dunsmore, J., Faull, K.F., Gilligan, J., Gonzalez-Begne, M., Halgand, F., Hall, S.C., Han, X., Henson, B., Hewel, J., Hu, S., Jeffrey, S., Jiang, J., Loo, J.A., Ogorzalek Loo, R.R., Malamud, D., Melvin, J.E., Miroshnychenko, O., Navazesh, M., Niles, R., Park, S.K., Prakobphol, A., Ramachandran, P., Richert, M., Robinson, S., Sondej, M., Souda, P., Sullivan, M.A., Takashima, J., Than, S., Wang, J., Whitelegge, J.P., Witkowska, H.E., Wolinsky, L., Xie, Y., Xu, T., Yu, W., Ytterberg, J., Wong, D.T., Yates, J.R. and Fisher, S.J., (2008)

The proteomes of human parotid and submandibular/sublingual gland salivas collected as the ductal secretions. *J Proteome Res*, 75, pp.1994–2006.

Deo, P.N. and Deshmukh, R., (2019) Oral microbiome: Unveiling the fundamentals. In: *J Oral Maxillofac Pathol*. pp.122–128.

Di Crescenzo, A., Ettorre, V. and Fontana, A., (2014) Non-covalent and reversible functionalization of carbon nanotubes. *Beilstein J Nanotechnol*, 5, pp.1675–1690.

Dodds, M., Roland, S., Edgar, M. and Thornhill, M., (2015) Saliva A review of its role in maintaining oral health and preventing dental disease. *BDJ Team*, 21, pp.11–13.

Dye, B.A., Herrera-Abreu, M., Lerche-Sehm, J., Vlachojannis, C., Pikdoken, L., Pretzl, B., Schwartz, A. and Papapanou, P.N., (2009) Serum antibodies to periodontal bacteria as diagnostic markers of periodontitis. *J Periodontol*, 804, pp.634–647.

Dzyadevych, S. V., Arkhypova, V.N., Soldatkin, A.P., El'skaya, A. V., Martelet, C. and Jaffrezic-Renault, N., (2008) Amperometric enzyme biosensors: Past, present and future. *IRBM*, 292–3, pp.171–180.

Eatemadi, A., Daraee, H., Karimkhanloo, H., Kouhi, M., Zarghami, N., Akbarzadeh, A., Abasi, M., Hanifehpour, Y. and Joo, S.W., (2014) Carbon nanotubes: properties, synthesis, purification, and medical applications. *Nanoscale Res Lett*, 91, p.393.

Eckermann, A.L., Feld, D.J., Shaw, J.A. and Meade, T.J., (2010) Electrochemistry of redox-active self-assembled monolayers. *Coordination Chemistry Reviews*, 25415–16, pp.1769–1802.

Elgrishi, N.N., Rountree, K.J., Mccarthy, B.D., Rountree, E.S., Eisenhart, T.T. and Dempsey, J.L., (2017) A Practical Beginner's Guide to Cyclic Voltammetry.

EP, R., DA, B., JP, M., RO, K. and CE, B., (2014) The fabrication, characterisation and electrochemical investigation of screen-printed graphene electrodes. *Physical chemistry chemical physics : PCCP*, 1610, pp.4598–4611.

Erdely, A., Wagner, L., Muller, V., Szabo, A. and Baylis, C., (2003) Protection of wistar furth rats from chronic renal disease is associated with maintained renal nitric oxide synthase. *J Am Soc Nephrol*, 1410, pp.2526–2533.

Estrela, P., Bhalla, N., Jolly, P., (2016) Introduction to biosensors. *Essays Biochem* 60 1 pp. 1–8.

Fagúndez, P., Botasini, S., Tosar, J.P. and Méndez, E., (2021) Systematic process evaluation of the conjugation of proteins to gold nanoparticles. *Heliyon*, 76, p.e07392.

Fanjul-Bolado, P., Hernández-Santos, D., Lamas-Ardisana, P.J., Martín-Pernía, A. and Costa-García, A., (2008) Electrochemical characterization of screen-printed and conventional carbon paste electrodes. *Electrochimica Acta*, 5310, pp.3635–3642.

Fares, M.M., (2018) π-Plasmon absorbance films of carboxylic functionalized CNTs coupled with renewable PGP platforms. *Polymers for Advanced Technologies*, 296, pp.1861–1869.

Fayazfar, H., Afshar, A. and Dolati, A., (2013) Controlled Growth of Well-Aligned Carbon Nanotubes, Electrochemical Modification and Electrodeposition of Multiple Shapes of Gold Nanostructures. *Materials Sciences and Applications*, 0411, pp.667–678.

Ferrari, A.G.M., Foster, C.W., Kelly, P.J., Brownson, D.A.C. and Banks, C.E., (2018) Determination of the Electrochemical Area of Screen-Printed Electrochemical Sensing Platforms. *Biosensors 2018, Vol. 8, Page 53*, 82, p.53.

Figueiredo-Filho, L.C.S., Silva, T.A., Vicentini, F.C. and Fatibello-Filho, O., (2014) Simultaneous voltammetric determination of dopamine and epinephrine in human body fluid samples using a glassy carbon electrode modified with nickel oxide nanoparticles and carbon nanotubes within a dihexadecylphosphate film. *The Analyst*, 13911, pp.2842–2849.

Figueredo, C.M., Lira-Junior, R. and Love, R.M., (2019) T and B Cells in Periodontal Disease: New Functions in A Complex Scenario. *International Journal of Molecular Sciences*, 2016.

Fisher, A., (1996) *Electrode dynamics*.

Fogo, A.B., (2007) Mechanisms of progression of chronic kidney disease. *Pediatr Nephrol*, 2212, pp.2011–2022.

Fons-Badal, C., Fons-Font, A., Labaig-Rueda, C., Fernanda Solá-Ruiz, M., Selva-Otaolaurruchi, E. and Agustín-Panadero, R., (2020) Analysis of Predisposing Factors for Rapid Dental Calculus Formation. *Journal of Clinical Medicine*, 93, p.858.

Ford, P.J., Gamonal, J. and Seymour, G.J., (2010) Immunological differences and similarities between chronic periodontitis and aggressive periodontitis. *Periodontol 2000*, 53, pp.111–123.

Forner, L., Larsen, T., Kilian, M. and Holmstrup, P., (2006) Incidence of bacteremia after chewing, tooth brushing and scaling in individuals with periodontal inflammation. *J Clin Periodontol*, 336, pp.401–407.

Fujita, T., Yoshimoto, T., Kajiya, M., Ouhara, K., Matsuda, S., Takemura, T., Akutagawa, K., Takeda, K., Mizuno, N. and Kurihara, H., (2018) Regulation of defensive function on gingival epithelial cells can prevent periodontal disease. *Jpn Dent Sci Rev*, 542, pp.66–75.

Fung, E. and Kurella Tamura, M., (2016) Epidemiology and Public Health Concerns of CKD in Older Adults. *Adv Chronic Kidney Dis*, 231, pp.8–11.

Gadekar, N.B., Hosmani, J. V, Bhat, K.G., Kotrashetti, V.S., Nayak, R.S., Babji, D. V, Pattanshetty, S.M., Joshi, V.M. and Bansode, R.A., (2018) Detection of antibodies against Aggregatibacter actinomycetemcomitans in serum and saliva through ELISA

in periodontally healthy individuals and individuals with chronic periodontitis. *Microb Pathog*, 125, pp.438–442.

Gao, L., Xu, T., Huang, G., Jiang, S., Gu, Y. and Chen, F., (2018) Oral microbiomes: more and more importance in oral cavity and whole body. *Protein Cell*, 95, pp.488–500.

Gemünde, A., Lai, B., Pause, L., Krömer, J., Holtmann, D. and Chemelectrochem,], (2022) Redox Mediators in Microbial Electrochemical Systems.

Ghallab, N.A., (2018) Diagnostic potential and future directions of biomarkers in gingival crevicular fluid and saliva of periodontal diseases: Review of the current evidence. *Arch Oral Biol*, 87, pp.115–124.

Giannobile, W. V., (2012) Salivary diagnostics for periodontal diseases. *The Journal of the American Dental Association*, 143, pp.6S-11S.

Goek, O.N., Prehn, C., Sekula, P., Römisch-Margl, W., Döring, A., Gieger, C., Heier, M., Koenig, W., Wang-Sattler, R., Illig, T., Suhre, K., Adamski, J., Köttgen, A. and Meisinger, C., (2013) Metabolites associate with kidney function decline and incident chronic kidney disease in the general population. *Nephrol Dial Transplant*, 288, pp.2131–2138.

Guo, Y., Nguyen, K.A. and Potempa, J., (2010) Dichotomy of gingipains action as virulence factors: from cleaving substrates with the precision of a surgeon's knife to a meat chopper-like brutal degradation of proteins. *Periodontol 2000*, 541, pp.15–44.

Hajishengallis, G. and Lamont, R.J., (2012) Beyond the red complex and into more complexity: the polymicrobial synergy and dysbiosis (PSD) model of periodontal disease etiology. *Mol Oral Microbiol*, 276, pp.409–419.

Hajishengallis, G., (2015) Periodontitis: from microbial immune subversion to systemic inflammation. *Nature Reviews Immunology*, 151, pp.30–44.Hakala, T.K., Liitiä, T. and

Suurnäkki, A., (2013) Enzyme-aided alkaline extraction of oligosaccharides and polymeric xylan from hardwood kraft pulp. *Carbohydrate Polymers*, 931, pp.102–108.

Han, Z.-J., Yabuuchi, N., Hashimoto, S., Sasaki, T. and Komaba, S., (2013) Cross-Linked Poly(acrylic acid) with Polycarbodiimide as Advanced Binder for Si/Graphite Composite Negative Electrodes in Li-Ion Batteries. *ECS Electrochemistry Letters*, 22, pp.17–20.

Hayat, A. and Marty, J.L., (2014) Disposable Screen Printed Electrochemical Sensors: Tools for Environmental Monitoring. *Sensors (Basel, Switzerland)*, 146, p.10432.

Heresztyn, T., Worthley, M.I. and Horowitz, J.D., (2004) Determination of l-arginine and NG, NG - and NG, NG' -dimethyl-L-arginine in plasma by liquid chromatography as AccQ-Fluor fluorescent derivatives. *J Chromatogr B Analyt Technol Biomed Life Sci*, 8052, pp.325–329.

Hernández, M., Dutzan, N., García-Sesnich, J., Abusleme, L., Dezerega, A., Silva, N., González, F.E., Vernal, R., Sorsa, T. and Gamonal, J., (2011) Host-pathogen interactions in progressive chronic periodontitis. *J Dent Res*, 9010, pp.1164–1170.

Hess, P., Altenhöfer, A., Khan, A.S., Daryab, N., Kim, K.S., Hacker, J. and Oelschlaeger, T.A., (2004) A Salmonella fim Homologue in Citrobacter freundii Mediates Invasion In Vitro and Crossing of the Blood-Brain Barrier in the Rat Pup Model. *Infection and Immunity*, 729, p.5298.

Hickey, N.A., Shalamanova, L., Whitehead, K.A., Dempsey-Hibbert, N., van der Gast, C. and Taylor, R.L., (2020) Exploring the putative interactions between chronic kidney disease and chronic periodontitis. *Crit Rev Microbiol*, pp.1–17.

Higgins, M.L., Tillman, M.C., Rupp, J.P. and Leach, F.R., (1969) The effect of polyamines on cell culture cells. *J Cell Physiol*, 742, pp.149–154.

Holden, J.A., Attard, T.J., Laughton, K.M., Mansell, A., O'Brien-Simpson, N.M. and Reynolds, E.C., (2014) Porphyromonas gingivalis Lipopolysaccharide Weakly Activates M1 and M2 Polarized Mouse Macrophages but Induces Inflammatory Cytokines. *Infection and Immunity*, 8210, pp.4190–4203.

Holmstrup, P., Damgaard, C., Olsen, I., Klinge, B., Flyvbjerg, A., Nielsen, C.H. and Hansen, P.R., (2017) Comorbidity of periodontal disease: two sides of the same coin? An introduction for the clinician. *Journal of Oral Microbiology*, 91.

House, J.L., Anderson, E.M. and Ward, W.K., (2007) Immobilization techniques to avoid enzyme loss from oxidase-based biosensors: a one-year study. *Journal of diabetes science and technology*, 11, pp.18–27.

How, K.Y., Song, K.P. and Chan, K.G., (2016) Porphyromonas gingivalis: An Overview of Periodontopathic Pathogen below the Gum Line. *Frontiers in Microbiology*, 7FEB, p.53.

Humphrey, S.P. and Williamson, R.T., (2001) A review of saliva: normal composition, flow, and function. *J Prosthet Dent*, 852, pp.162–169.

Hwang, H., Hwang, B.Y. and Bueno, J., (2018) Biomarkers in Infectious Diseases. *Dis Markers*, 2018, p.8509127.

Ibáñez-Redín, G., Wilson, D., Gonçalves, D. and Oliveira, O.N., (2018) Low-cost screen-printed electrodes based on electrochemically reduced graphene oxide-carbon black nanocomposites for dopamine, epinephrine and paracetamol detection. *Journal of Colloid and Interface Science*, 515, pp.101–108.

Igarashi, K. and Kashiwagi, K., (2000) Polyamines: mysterious modulators of cellular functions. *Biochem Biophys Res Commun*, 2713, pp.559–564.

Igarashi, K., Ueda, S., Yoshida, K. and Kashiwagi, K., (2006) Polyamines in renal failure. *Amino Acids*, 314, pp.477–483.

J Pytko-Polonczyk, J., Jakubik, A., Przeklasa-Bierowiec, A. and Muszynska, B., (2017) Artificial saliva and its use in biological experiments. *Journal of physiology and pharmacology : an official journal of the Polish Physiological Society*, 686, pp.807–813.

J. Slate, A., C. Brownson, D.A., Dena, A.S.A., C. Smith, G., A. Whitehead, K. and E. Banks, C., (2018) Exploring the electrochemical performance of graphite and graphene paste electrodes composed of varying lateral flake sizes. *Physical Chemistry Chemical Physics*, 2030, pp.20010–20022.

Jagadish, K., Srikantaswamy, S., Byrappa, K., Shruthi, L. and Abhilash, M.R., (2015) Dispersion of Multiwall Carbon Nanotubes in Organic Solvents through Hydrothermal Supercritical Condition. *Journal of Nanomaterials*, 2015.

Jaros, D. and Rohm, H., (2011) Enzymes Exogenous to Milk in Dairy Technology: Transglutaminase. *Encyclopedia of Dairy Sciences: Second Edition*, pp.297–300.

Jastrzebska, M., Wrzalik, R., Kocot, A., Zalewska-Rejdak, J., Cwalina, B. and Zalewska-rejdak, J., (2003) Raman spectroscopic study of glutaraldehyde-stabilized collagen and pericardium tissue. *J. Biomater. Sci. Polymer Edn*, 142, pp.185–197.

Jessl, S., Beesley, D., Engelke, S., Valentine, C.J., Stallard, J.C., Fleck, N., Ahmad, S., Cole, M.T. and De Volder, M., (2018) Carbon nanotube conductive additives for improved electrical and mechanical properties of flexible battery electrodes. *Materials Science and Engineering: A*, 735, pp.269–274.

Jiang, K. and Gerhardt, R.A., (2021) Fabrication and Supercapacitor Applications of Multiwall Carbon Nanotube Thin Films. *C*, 74, p.70.

Kang, M., Fang, J., Li, S., Liu, T., Wang, C. and Tan, L., (2013) Effect of Electrode Morphology on the Electrochemical Performance of Pt/YSZ Electrodes. *Int. J. Electrochem. Sci*, 8, pp.12757–12768.

Katz, J., Sambandam, V., Wu, J.H., Michalek, S.M. and Balkovetz, D.F., (2000) Characterization of Porphyromonas gingivalis-induced degradation of epithelial cell junctional complexes. *Infect Immun*, 683, pp.1441–1449.

Kayal, R.A., (2013) The Role of Osteoimmunology in Periodontal Disease. *BioMed Research International*, 2013, p.12.

Khan, Z. and Pandey, M., (2014) Role of kidney biomarkers of chronic kidney disease: An update. *Saudi J Biol Sci*, 214, pp.294–299.

Kharlamova, M. V., Paukov, M. and Burdanova, M.G., (2022) Nanotube Functionalization: Investigation, Methods and Demonstrated Applications. *Materials*, 1515, p.5386.

Khurshid, Z., Mali, M., Naseem, M., Najeeb, S. and Zafar, M.S., (2017) Human Gingival Crevicular Fluids (GCF) Proteomics: An Overview. *Dent J (Basel)*, 51.

Kilian, M., Chapple, I.L.C., Hannig, M., Marsh, P.D., Meuric, V., Pedersen, A.M.L., Tonetti, M.S., Wade, W.G. and Zaura, E., (2016) The oral microbiome – an update for oral healthcare professionals. *British Dental Journal*, 22110, pp.657–666.

Kim, B.C., Lee, I., Kwon, S.-J., Wee, Y., Kwon, K.Y., Jeon, C., An, H.J., Jung, H.-T., Ha, S., Dordick, J.S. and Kim, J., (2017) Fabrication of enzyme-based coatings on intact multi-walled carbon nanotubes as highly effective electrodes in biofuel cells. *Scientific Reports 2017 7:1*, 71, pp.1–10.

Kim, J. and Amar, S., (2006) Periodontal disease and systemic conditions: a bidirectional relationship. *Odontology / the Society of the Nippon Dental University*, 941, p.10.

Kivimäki, M. and Steptoe, A., (2018) Effects of stress on the development and progression of cardiovascular disease. *Nat Rev Cardiol*, 154, pp.215–229.

Knight, E.T., Liu, J., Seymour, G.J., Faggion, C.M. and Cullinan, M.P., (2016) Risk factors that may modify the innate and adaptive immune responses in periodontal diseases. *Periodontol 2000*, 711, pp.22–51.

Kovács, T., Mikó, E., Vida, A., Sebő, É., Toth, J., Csonka, T., Boratkó, A., Ujlaki, G., Lente, G., Kovács, P., Tóth, D., Árkosy, P., Kiss, B., Méhes, G., Goedert, J.J. and Bai, P., (2019) Cadaverine, a metabolite of the microbiome, reduces breast cancer aggressiveness through trace amino acid receptors. *Scientific Reports*, 91.

Kuboniwa, M., Sakanaka, A., Hashino, E., Bamba, T., Fukusaki, E. and Amano, A., (2016) Prediction of Periodontal Inflammation via Metabolic Profiling of Saliva. *J Dent Res*, 9512, pp.1381–1386.

Kucherenko, I.S., Soldatkin, O.O., Kucherenko, D.Y., Soldatkina, O. V. and Dzyadevych, S. V., (2019) Advances in nanomaterial application in enzyme-based electrochemical biosensors: a review. *Nanoscale Advances*, 112, pp.4560–4577.

Kudo, H., Yagi, T., Chu, M.X., Saito, H., Morimoto, N., Iwasaki, Y., Akiyoshi, K. and Mitsubayashi, K., (2008) Glucose sensor using a phospholipid polymer-based enzyme immobilization method. *Analytical and Bioanalytical Chemistry 2007 391:4*, 3914, pp.1269–1274.

Kurihara, S., Oda, S., Kato, K., Kim, H.G., Koyanagi, T., Kumagai, H. and Suzuki, H., (2005) A novel putrescine utilization pathway involves gamma-glutamylated intermediates of Escherichia coli K-12. *J Biol Chem*, 2806, pp.4602–4608.

Kurzawa, C., Hengstenberg, A. and Schuhmann, W., (2002) Immobilization method for the preparation of biosensors based on pH shift-induced deposition of biomolecule-containing polymer films. *Analytical chemistry*, 742, pp.355–361.

Kusano, T., Berberich, T., Tateda, C. and Takahashi, Y., (2008) Polyamines: essential factors for growth and survival. *Planta*, 2283, pp.367–381.

Ladero, V., Calles-Enriquez, M., Fernandez, M. and A. Alvarez, M., (2010) Toxicological Effects of Dietary Biogenic Amines. *Current Nutrition & Food Science*, 62, pp.145–156.Levey, A.S., (1990) Measurement of renal function in chronic renal disease. *Kidney Int*, 381, pp.167–184.

Li, N. and Collyer, C.A., (2011) Gingipains from Porphyromonas gingivalis - Complex domain structures confer diverse functions. *Eur J Microbiol Immunol (Bp)*, 11, pp.41–58.

Lim, H.K., Rahim, A.B., Leo, V.I., Das, S., Lim, T.C., Uemura, T., Igarashi, K., Common, J. and Vardy, L.A., (2018) Polyamine Regulator AMD1 Promotes Cell Migration in Epidermal Wound Healing. *Journal of Investigative Dermatology*, 13812, pp.2653–2665.

Lim, S.A. and Ahmed, M.U., (2019) CHAPTER 1:Introduction to Immunosensors. *RSC Detection Science*, 2019-Janua14, pp.1–20.

Lohinai, Z., Keremi, B., Szoko, E., Tabi, T., Szabo, C., Tulassay, Z. and Levine, M., (2012) Bacterial lysine decarboxylase influences human dental biofilm lysine content, biofilm accumulation, and subclinical gingival inflammation. *J Periodontol*, 838, pp.1048–1056.

Lowry, L.K., (1995) Role of biomarkers of exposure in the assessment of health risks. *Toxicol Lett*, 771–3, pp.31–38.

Luscinskas, F.W., Kansas, G.S., Ding, H., Pizcueta, P., Schleiffenbaum, B.E., Tedder, T.F. and Gimbrone, M.A., (1994) Monocyte rolling, arrest and spreading on IL-4-activated vascular endothelium under flow is mediated via sequential action of L-selectin, beta 1-integrins, and beta 2-integrins. *Journal of Cell Biology*, 1256, pp.1417–1427.

Lynge Pedersen, A.M. and Belstrøm, D., (2019) The role of natural salivary defences in maintaining a healthy oral microbiota. *J Dent*, 80 Suppl 1, pp.S3–S12.

M, S., H, L., NP, L., W, B., A, A. and H, B., (2004) The Clinical Course of Chronic Periodontitis. *Journal of clinical periodontology*, 3112, pp.1122–1127.

Macdougall, I.C., (2001) Role of uremic toxins in exacerbating anemia in renal failure. *Kidney Int Suppl*, 78, pp.S67-72.

Mandal, S., Mandal, A., Johansson, H.E., Orjalo, A. V and Park, M.H., (2013) Depletion of cellular polyamines, spermidine and spermine, causes a total arrest in translation and growth in mammalian cells. *Proc Natl Acad Sci U S A*, 1106, pp.2169–2174.

Mariggiò, M.A., Vinella, A., Pasquetto, N., Curci, E., Cassano, A. and Fumarulo, R., (2004) In vitro effects of polyamines on polymorphonuclear cell apoptosis and implications in the pathogenesis of periodontal disease. *Immunopharmacol Immunotoxicol*, 261, pp.93–101.

Marsh, P.D., (2009) Role of the Oral Microflora in Health. 123, pp.130–137.

Martín, O., Gutierrez, H.R., Maroto-Valiente, A., Terrones, M., Blanco, T. and Baselga, J., (2013) An efficient method for the carboxylation of few-wall carbon nanotubes with little damage to their sidewalls. *Materials Chemistry and Physics*, 1402–3, pp.499–507.

Martinez, F.O., Gordon, S., Locati, M. and Mantovani, A., (2006) Transcriptional Profiling of the Human Monocyte-to-Macrophage Differentiation and Polarization: New Molecules and Patterns of Gene Expression. *The Journal of Immunology*, 17710, pp.7303–7311.

Masyutin, A.G., Bagrov, D. V., Vlasova, I.I., Nikishin, I.I., Klinov, D. V., Sychevskaya, K.A., Onishchenko, G.E. and Erokhina, M. V., (2018) Wall Thickness of Industrial

Multi-Walled Carbon Nanotubes Is Not a Crucial Factor for Their Degradation by Sodium Hypochlorite. *Nanomaterials*, 89

Mayeux, R., (2004) Biomarkers: potential uses and limitations. *NeuroRx*, 12, pp.182–188.

Meng, C., Wang, B., Gao, Z., Liu, Z., Zhang, Q. and Zhai, J., (2017) Insight into the Role of Surface Wettability in Electrocatalytic Hydrogen Evolution Reactions Using Light-Sensitive Nanotubular TiO2 Supported Pt Electrodes. *Scientific Reports 2017 7:1*, 71, pp.1–8.

Mikysek, T., Stočes, M., Švancara, I. and Ludvík, J., (2012) The ohmic resistance effect for characterisation of carbon nanotube paste electrodes (CNTPEs). *RSC Advances*, 29, pp.3684–3690.

Migneault, I., Dartiguenave, M., Bertrand, M., Waldron, K., (2018) Glutaraldehyde: behavior in aqueous solution, reaction with proteins, and application to enzyme crosslinking. *Biotechniques,* 37.

Miller, C.S., Foley, J.D., Bailey, A.L., Campell, C.L., Humphries, R.L., Christodoulides, N., Floriano, P.N., Simmons, G., Bhagwandin, B., Jacobson, J.W., Redding, S.W., Ebersole, J.L. and McDevitt, J.T., (2010) Current developments in salivary diagnostics. *Biomark Med*, 41, pp.171–189.

Miller, D.R., Lamster, I.B. and Chasens, A.I., (1984) Role of the polymorphonuclear leukocyte in periodontal health and disease. *J Clin Periodontol,* 111, pp.1–15.

Mogensen, T.H., (2009) Pathogen Recognition and Inflammatory Signaling in Innate Immune Defenses. *Clinical Microbiology Reviews*, 222, p.240.

Mohamed Saheed, M.S., Mohamed, N.M. and Burhanudin, Z.A., (2013) Optimization of the Production of Aligned CNTs Array as the Gas Sensing Element. *Materials Science Forum*, 756, pp.156–163.

Mohanty, R., Asopa, S.J., Joseph, M.D., Singh, B., Rajguru, J.P., Saidath, K. and Sharma, U., (2019) Red complex: Polymicrobial conglomerate in oral flora: A review. *Journal of Family Medicine and Primary Care*, 811, p.3480.

Morioka, M., Hinode, D., Nagata, A., Hayashi, H., Ichimiya, S., Ueda, M., Kido, R. and Nakamura, R., (1993) Cytotoxicity of Porphyromonas gingivalis toward cultured human gingival fibroblasts. *Oral Microbiology and Immunology*, 84, pp.203–207.

Nakamya, M.F., Ayoola, M.B., Park, S., Shack, L.A., Swiatlo, E. and Nanduri, B., (2018) The Role of Cadaverine Synthesis on Pneumococcal Capsule and Protein Expression. *Med Sci (Basel)*, 61.

Nazir, M.A., (2017) Prevalence of periodontal disease, its association with systemic diseases and prevention. *Int J Health Sci (Qassim)*, 112, pp.72–80.

Nędzi-Góra, M., Kowalski, J. and Górska, R., (2017) The Immune Response in Periodontal Tissues. *Arch Immunol Ther Exp (Warsz)*, 655, pp.421–429.

Nicholson, R.S., (1965) Theory and Application of Cyclic Voltammetry for Measurement of Electrode Reaction Kinetics. *Analytical Chemistry*, 3711, pp.1351–1355.

Nickell, R.A., Zhu, W.H., Payne, R.U., Cahela, D.R. and Tatarchuk, B.J., (2006) Hg/HgO electrode and hydrogen evolution potentials in aqueous sodium hydroxide. *Journal of Power Sources*, 1612, pp.1217–1224.

Nikolaev, K.G., Ermolenko, Y.E., Offenhäusser, A., Ermakov, S.S. and Mourzina, Y.G., (2018) Multisensor systems by electrochemical nanowire assembly for the analysis of aqueous solutions. *Frontiers in Chemistry*.

Olsen, I. and Progulske-Fox, A., (2015) Invasion of *Porphyromonas gingivalis* strains into vascular cells and tissue. *Journal of Oral Microbiology*, 71, p.28788.

Ozeki, M., Nozaki, T., Aoki, J., Bamba, T., Jensen, K.R., Murakami, S. and Toyoda, M., (2016) Metabolomic Analysis of Gingival Crevicular Fluid Using Gas Chromatography/Mass Spectrometry. *Mass Spectrom (Tokyo)*, 51, p.A0047.

Parit, M. and Davis, V.A., (2021) Effects of Non-covalent Functionalization and Initial Mixing Methods on SWNT/PP and SWNT/EVOH Composites. *ACS Omega*, 616, pp.10618–10628.

Park, J.E., Park, I.S., Bae, T.S. and Lee, M.H., (2014) Electrophoretic deposition of carbon nanotubes over TiO2 nanotubes: Evaluation of surface properties and biocompatibility. *Bioinorganic Chemistry and Applications*, 2014.

Patil, P.B. and Patil, B.R., (2011) Saliva: A diagnostic biomarker of periodontal diseases. *J Indian Soc Periodontol*, 154, pp.310–317.

Patil, S., Rao, R.S., Sanketh, D.S. and Amrutha, N., (2013) Microbial flora in oral diseases. *J Contemp Dent Pract*, 146, pp.1202–1208.

Pegg, A.E., (2016) Functions of Polyamines in Mammals. *J Biol Chem*, 29129, pp.14904–14912.

Plombas, M., Gobert, B., De March, A.K., Sarda, M.N., Sixou, M., Béné, M.C., Miller, N. and Faure, G.C., (2002) Isotypic antibody response to plaque anaerobes in periodontal disease. *J Periodontol*, 7312, pp.1507–1511.

Preshaw, P.M., (2015) Detection and diagnosis of periodontal conditions amenable to prevention. *BMC Oral Health*, 15 Suppl 1, p.S5.

Rago, F., Saltzberg, D., Allen, K.N. and Tolan, D.R., (2015) Enzyme Substrate Specificity Conferred by Distinct Conformational Pathways. *Journal of the American Chemical Society*, 13743, pp.13876–13886.

Rahim, Z.A., Yusof, N.A., Haniff, M.A.S.M., Mohammad, F., Syono, M.I. and Daud, N., (2018) Electrochemical Measurements of Multiwalled Carbon Nanotubes under Different Plasma Treatments. *Materials*, 1110.

Ramenzoni, L.L., Lehner, M.P., Kaufmann, M.E., Wiedemeier, D., Attin, T. and Schmidlin, P.R., (2021) Oral Diagnostic Methods for the Detection of Periodontal Disease. *Diagnostics*, 113.

Randviir, E.P., (2018) A cross examination of electron transfer rate constants for carbon screen-printed electrodes using Electrochemical Impedance Spectroscopy and cyclic voltammetry. *Electrochimica Acta*, 286, pp.179–186.

Randviir, E.P., Brownson, D.A.C., Metters, J.P., Kadara, R.O. and Banks, C.E., (2014) The fabrication, characterisation and electrochemical investigation of screen-printed graphene electrodes. *Physical Chemistry Chemical Physics*, 1610, p.4598.

Rathee, M. and Jain, P., (2022) Gingivitis. *Australian Journal of Pharmacy*, 961141, pp.64–67.

Rebelo, S.L.H., Guedes, A., Szefczyk, M.E., Pereira, A.M., Araújo, J.P. and Freire, C., (2016) Progress in the Raman spectra analysis of covalently functionalized multiwalled carbon nanotubes: unraveling disorder in graphitic materials. *Physical Chemistry Chemical Physics*, 1818, pp.12784–12796.

Ritter, D.W., Newton, J.M., McShane, M.J., (2014) Modification of PEGylated enzyme with glutaraldehyde can enhance stability while avoiding intermolecular crosslinking. *RSC Adv.* 2014; 4(53), pp.28036-28040

Rocchitta, G., Spanu, A., Babudieri, S., Latte, G., Madeddu, G., Galleri, G., Nuvoli, S., Bagella, P., Demartis, M.I., Fiore, V., Manetti, R. and Serra, P.A., (2016) Enzyme Biosensors for Biomedical Applications: Strategies for Safeguarding Analytical Performances in Biological Fluids. *Sensors*, 30, 16(6).

Rock, K.L. and Kono, H., (2008) The inflammatory response to cell death. *Annual review of pathology*, 3, p.99.

Russell, D. and Snyder, S.H., (1968) Amine synthesis in rapidly growing tissues: ornithine decarboxylase activity in regenerating rat liver, chick embryo, and various tumors. *Proc Natl Acad Sci U S A*, 604, pp.1420–1427.

Rysz, J., Gluba-Brzózka, A., Franczyk, B., Jabłonowski, Z. and Ciałkowska-Rysz, A., (2017) Novel Biomarkers in the Diagnosis of Chronic Kidney Disease and the Prediction of Its Outcome. *Int J Mol Sci*, 188.

Saifuddin, N., Raziah, A.Z. and Junizah, A.R., (2013) Carbon nanotubes: A review on structure and their interaction with proteins. *Journal of Chemistry*.

Saini, R., Saini, S. and Sharma, S., (2011) Biofilm: A dental microbial infection. *Journal of Natural Science, Biology, and Medicine*, 21, p.71.

Saito, A., Takagi, T., Chung, T.G. and Ohta, K., (1983) Serum levels of polyamines in patients with chronic renal failure. *Kidney Int Suppl*, 16, pp.S234-7.

Sakanaka, A., Kuboniwa, M., Hashino, E., Bamba, T., Fukusaki, E. and Amano, A., (2017) Distinct signatures of dental plaque metabolic byproducts dictated by periodontal inflammatory status. *Sci Rep*, 7, p.42818.

Sakata, K., Kashiwagi, K., Sharmin, S., Ueda, S. and Igarashi, K., (2003) Acrolein produced from polyamines as one of the uraemic toxins. *Biochem Soc Trans*, 312, pp.371–37.

Sarapur, S. and Shilpashree, H.S., (2012) Salivary Pacemakers: A review. *Dent Res J (Isfahan)*, 9Suppl 1, pp.S20-5.

Šebek, J., Pele, L., Potma, E.O. and Benny Gerber, R., (2011) Raman spectra of long chain hydrocarbons: anharmonic calculations, experiment and implications for imaging of biomembranes. *undefined*, 1328, pp.12724–12733.

Selleck, M.J., Senthil, M. and Wall, N.R., (2017) Making Meaningful Clinical Use of Biomarkers. *Biomark Insights*, 12, p.1177271917715236.

Sessa, A. and Perin, A., (1994) Diamine oxidase in relation to diamine and polyamine metabolism. *Agents and Actions*, 431–2, pp.69–77.

Sezer, N. and Koç, M., (2019) Oxidative acid treatment of carbon nanotubes. *Surfaces and Interfaces*, 14, pp.1–8.Shah, P. and Swiatlo, E., (2008) A multifaceted role for polyamines in bacterial pathogens. *Mol Microbiol*, 681, pp.4–16.

Shaikh, H.F.M., Patil, S.H., Pangam, T.S. and Rathod, K. V, (2018) Polymicrobial synergy and dysbiosis: An overview. *J Indian Soc Periodontol*, 222, pp.101–106.

Sheets, S.M., Potempa, J., Travis, J., Casiano, C.A. and Fletcher, H.M., (2005) Gingipains from Porphyromonas gingivalis W83 induce cell adhesion molecule cleavage and apoptosis in endothelial cells. *Infect Immun*, 733, pp.1543–1552.

Shen, J., Liu, A., Tu, Y., Foo, G., Yeo, C., Chan-Park, M.B., Jiang, R. and Chen, Y., (2011) How carboxylic groups improve the performance of single-walled carbon nanotube electrochemical capacitors? *Energy & Environmental Science*, 410, p.4220.

Silva, N., Abusleme, L., Bravo, D., Dutzan, N., Garcia-Sesnich, J., Vernal, R., Hernández, M. and Gamonal, J., (2015) Host response mechanisms in periodontal diseases. *Journal of Applied Oral Science*, 233, pp.329–355.

Sindhu, K.K., (2016) Uremic toxins: some thoughts on acrolein and spermine. *Ren Fail*, 3810, pp.1755–1758.

Sireesha, M., Jagadeesh Babu, V., Kranthi Kiran, A.S. and Ramakrishna, S., (2018) A review on carbon nanotubes in biosensor devices and their applications in medicine. *Nanocomposites*, 42, pp.36–57.

Sochalska, M. and Potempa, J., (2017) Manipulation of Neutrophils by Porphyromonas gingivalis in the Development of Periodontitis. *Frontiers in Cellular and Infection Microbiology*, 7MAY, p.197.

Socransky, S.S., (1979) Criteria for the infectious agents in dental caries and periodontal disease. *J Clin Periodontol*, 67, pp.16–21.

Socransky, S.S., Haffajee, A.D., Cugini, M.A., Smith, C. and Kent, R.L., (1998) Microbial complexes in subgingival plaque. *J Clin Periodontol*, 252, pp.134–144.

Soldatkin, O.O., Kucherenko, I.S., Pyeshkova, V.M., Kukla, A.L., Jaffrezic-Renault, N., El'skaya, A.V., Dzyadevych, S.V. and Soldatkin, A.P., (2012) Novel conductometric biosensor based on three-enzyme system for selective determination of heavy metal ions. *Bioelectrochemistry*, 83, pp.25–30.

Song, B., Zhang, Y., Chen, L., Zhou, T., Huang, W., Zhou, X. and Shao, L., (2017) The role of Toll-like receptors in periodontitis. *Oral Diseases*, 232, pp.168–180.

Song, G., Wang, Y. and Tan, D.Q., (2022) A review of surface roughness impact on dielectric film properties. *IET Nanodielectrics*, 51, pp.1–23.

Spehar-Délèze, A.-M., Almadaghi, S. and O'Sullivan, C., (2015) Development of Solid-State Electrochemiluminescence (ECL) Sensor Based on Ru(bpy)32+-Encapsulated Silica Nanoparticles for the Detection of Biogenic Polyamines. *Chemosensors*, 32, pp.178–189.

Srivastava, N., Nayak, P.A. and Rana, S., (2017) Point of Care- A Novel Approach to Periodontal Diagnosis-A Review. *J Clin Diagn Res*, 118, pp.ZE01–ZE06.

Stathopoulou, P.G., Buduneli, N. and Kinane, D.F., (2015) Systemic Biomarkers for Periodontitis. *Current Oral Health Reports*, 24, pp.218–226

Stepien, K.M. and Guy, M., (2018) Caeruloplasmin oxidase activity: measurement in serum by use of o-dianisidine dihydrochloride on a microplate reader. *Annals of Clinical Biochemistry*, 551, pp.149–157.

Strimbu, K. and Tavel, J.A., (2010) What are biomarkers? *Curr Opin HIV AIDS*, 56, pp.463–466.

Stueckle, T.A., Davidson, D.C., Derk, R., Wang, P., Friend, S., Schwegler-Berry, D., Zheng, P., Wu, N., Castranova, V., Rojanasakul, Y. and Wang, L., (2017) Effect of surface functionalizations of multi-walled carbon nanotubes on neoplastic transformation potential in primary human lung epithelial cells. *Nanotoxicology*, 115, p.613.

Subbarao, K.C., Nattuthurai, G.S., Sundararajan, S.K., Sujith, I., Joseph, J. and Syedshah, Y.P., (2019) Gingival Crevicular Fluid: An Overview. *J Pharm Bioallied Sci*, 11Suppl 2, pp.S135–S139.

Sun, Y., He, K., Zhang, Z., Zhou, A. and Duan, H., (2015) Real-time electrochemical detection of hydrogen peroxide secretion in live cells by Pt nanoparticles decorated graphene–carbon nanotube hybrid paper electrode. *Biosensors and Bioelectronics*, 68, pp.358–364.

Suzuki, N., Yoneda, M. and Hirofuji, T., (2013) Mixed red-complex bacterial infection in periodontitis. *Int J Dent*, 2013, p.587279..

Syrgiannis, Z., Melchionna, M. and Prato, M., (2014) Covalent Carbon Nanotube Functionalization. *Encyclopedia of Polymeric Nanomaterials*, pp.1–8.

Szabó, S., Szabó, S. and Bakos, I., (2010) Reference Electrodes in Metal Corrosion. *International Journal of Corrosion*, 2010, p.20.

Taba, M., Kinney, J., Kim, A.S. and Giannobile, W. V, (2005) Diagnostic biomarkers for oral and periodontal diseases. *Dent Clin North Am*, 493, pp.551–71.

Takahashi, K., Mooney, J., Frandsen, E. V and Kinane, D.F., (1997) IgG and IgA subclass mRNA-bearing plasma cells in periodontitis gingival tissue and immunoglobulin levels in the gingival crevicular fluid. *Clin Exp Immunol*, 1071, pp.158–165.

Takahashi, T. and Kakehi, J., (2010) Polyamines: ubiquitous polycations with unique roles in growth and stress responses. *Ann Bot*, 1051, pp.1–6.

Tang, B.M., Shojaei, M., Parnell, G.P., Huang, S., Nalos, M., Teoh, S., O'Connor, K., Schibeci, S., Phu, A.L., Kumar, A., Ho, J., Meyers, A.F.A., Keynan, Y., Ball, T., Pisipati, A., Moore, E., Eisen, D., Lai, K., Gillett, M., Geffers, R., Luo, H., Gul, F., Schreiber, J., Riedel, S., Booth, D., McLean, A. and Schughart, K., (2017) A novel immune biomarker. *Eur Respir J*, 496.

Tariq, M., Iqbal, Z., Ali, J., Baboota, S., Talegaonkar, S., Ahmad, Z. and Sahni, J.K., (2012) Treatment modalities and evaluation models for periodontitis. *Int J Pharm Investig*, 23, pp.106–122.

Taylor, J.J. and Preshaw, P.M., (2016) Gingival crevicular fluid and saliva. *Periodontol 2000*, 701, pp.7–10.

Teles, R., Teles, F., Frias-Lopez, J., Paster, B. and Haffajee, A., (2013) Lessons learned and unlearned in periodontal microbiology. *Periodontol 2000*, 621, pp.95–162.

Thurnheer, T., Belibasakis, G.N. and Bostanci, N., (2014) Colonisation of gingival epithelia by subgingival biofilms in vitro: role of 'red complex' bacteria. *Arch Oral Biol*, 599, pp.977–986.

Thyagarajan, B., Howard, A.G., Durazo-Arvizu, R., Eckfeldt, J.H., Gellman, M.D., Kim, R.S., Liu, K., Mendez, A.J., Penedo, F.J., Talavera, G.A., Youngblood, M.E., Zhao, L. and Sotres-Alvarez, D., (2016) Analytical and biological variability in biomarker

measurement in the Hispanic Community Health Study/Study of Latinos. *Clin Chim Acta*, 463, pp.129–137.

Tîlmaciu, C.-M. and Morris, M.C., (2015) Carbon nanotube biosensors. *Frontiers in Chemistry*, 3.Tofalo, R., Cocchi, S. and Suzzi, G., (2019) Polyamines and Gut Microbiota. *Front Nutr*, 6, p.16.

Tonetti, M.S., Jepsen, S., Jin, L. and Otomo-Corgel, J., (2017) Impact of the global burden of periodontal diseases on health, nutrition and wellbeing of mankind: A call for global action. *J Clin Periodontol*, 445, pp.456–462.

Tonetti, M.S., Greenwell, H., Kornman, K.S. and Tonetti, M., (2018) Staging and grading of periodontitis: Framework and proposal of a new classification and case definition.Tribble, G.D. and Lamont, R.J., (2010) Bacterial invasion of epithelial cells and spreading in periodontal tissue. *Periodontology 2000*, 521, pp.68–83.

Tsuchida, S., Satoh, M., Takiwaki, M. and Nomura, F., (2017) Ubiquitination in Periodontal Disease: A Review. *Int J Mol Sci*, 187.

Urdea, M.S., Neuwald, P.D., Greenberg, B.L., Glick, M., Galloway, J., Williams, D. and Wong, D.T., (2011) Saliva, diagnostics, and dentistry. *Adv Dent Res*, 234, pp.353–359.

van Velzen, S.K., Abraham-Inpijn, L. and Moorer, W.R., (1984) Plaque and systemic disease: a reappraisal of the focal infection concept. *J Clin Periodontol*, 114, pp.209–220.

Vanegas, D.C., Patiño, L., Mendez, C., de Oliveira, D.A., Torres, A.M., Gomes, C.L. and McLamore, E.S., (2018) Laser scribed graphene biosensor for detection of biogenic amines in food samples using locally sourced materials. *Biosensors*, 82.

Verma, M.L., Naebe, M., Barrow, C.J. and Puri, M., (2013) Enzyme Immobilisation on Amino-Functionalised Multi-Walled Carbon Nanotubes: Structural and Biocatalytic Characterisation. *PLOS ONE*, 89, p.e73642.

Vinogradov, E. and Perry, M.B., (2000) Structural analysis of the core region of lipopolysaccharides from Proteus mirabilis serotypes O6, O48 and O57. *Eur J Biochem*, 2678, pp.2439–2446.

Waldbeser, L.S., Ajioka, R.S., Merz, A.J., Puaoi, D., Lin, L., Thomas, M. and So, M., (1994) The opaH locus of Neisseria gonorrhoeae MS11A is involved in epithelial cell invasion. *Molecular Microbiology*, 135, pp.919–928.

Wallis, R.S., Pai, M., Menzies, D., Doherty, T.M., Walzl, G., Perkins, M.D. and Zumla, A., (2010) Biomarkers and diagnostics for tuberculosis: progress, needs, and translation into practice. *Lancet*, 3759729, pp.1920–1937.

Wang, G.P., (2015) Defining functional signatures of dysbiosis in periodontitis progression. *Genome Med*, 71, p.40.

Wang, M., Shakhatreh, M.A., James, D., Liang, S., Nishiyama, S., Yoshimura, F., Demuth, D.R. and Hajishengallis, G., (2007) Fimbrial proteins of porphyromonas gingivalis mediate in vivo virulence and exploit TLR2 and complement receptor 3 to persist in macrophages. *J Immunol*, 1794, pp.2349–2358.

Wang, Q., Yu, Q., Lin, Q. and Duan, Y., (2015) Emerging salivary biomarkers by mass spectrometry. *Clin Chim Acta*, 438, pp.214–221.

Wang, T., Song, B., Qiao, K., Huang, Y. and Wang, L., (2018) Effect of Dimensions and Agglomerations of Carbon Nanotubes on Synchronous Enhancement of Mechanical and Damping Properties of Epoxy Nanocomposites. *Nanomaterials*, 812.

Wang, Y., Xu, H., Zhang, J. and Li, G., (2008) Electrochemical Sensors for Clinic Analysis. *Sensors (Basel, Switzerland)*, 84, p.2043.

Wilensky, A., Tzach-Nahman, R., Potempa, J., Shapira, L. and Nussbaum, G., (2015) Porphyromonas gingivalis & Gingipains Selectively Reduce CD14 Expression, Leading to Macrophage Hyporesponsiveness to Bacterial Infection. *Journal of Innate Immunity*, 72, pp.127–135.

Xu, W., Zhou, W., Wang, H. and Liang, S., (2020) Roles of Porphyromonas gingivalis and its virulence factors in periodontitis. pp.45–84.

Xu, X. and Veenstra, T.D., (2008) Analysis of biofluids for biomarker research. *Proteomics Clin Appl*, 210–11, pp.1403–1412.

Yamasaki, M., Nakata, K., Imaizumi, I., Iwama, A., Nakane, A. and Nakamura, H., (1998) Cytotoxic effect of endodontic bacteria on periapical fibroblasts. *Journal of Endodontics*, 248, pp.534–539.

Yazdanparast, S., Benvidi, A., Abbasi, S. and Rezaeinasab, M., (2019) Enzyme-based ultrasensitive electrochemical biosensor using poly(l-aspartic acid)/MWCNT bio-nanocomposite for xanthine detection: A meat freshness marker. *Microchemical Journal*, 149, p.104000.

Yoo, E.H. and Lee, S.Y., (2010) Glucose Biosensors: An Overview of Use in Clinical Practice. *Sensors (Basel, Switzerland)*, 105, p.4558.

Yu, Y., Wang, J., Shao, Q., Shi, J. and Zhu, W., (2016) The effects of organic solvents on the folding pathway and associated thermodynamics of proteins: a microscopic view. *Scientific Reports 2016 6:1*, 61, pp.1–12.

Yven, C., Bonnet, L., Cormier, D., Monier, S. and Mioche, L., (2006) Impaired mastication modifies the dynamics of bolus formation. *Eur J Oral Sci*, 1143, pp.184–190.

Zdrojek, M., Gebicki, W., Jastrzebski, C., Melin, T. and Huczko, A., (2004) Studies of Multiwall Carbon Nanotubes Using Raman Spectroscopy and Atomic Force Microscopy. *Solid State Phenomena*, 99–100, pp.265–268.

Zhang, Y., Kumar, A.K.S., Li, D., Yang, M. and Compton, R.G., (2020) Nanoparticle- and Nanotube-Modified Electrodes: Response of Drop-Cast Surfaces. *ChemElectroChem*, 722, pp.4614–4624.

Zhou, Q., Desta, T., Fenton, M., Graves, D.T. and Amar, S., (2005) Cytokine Profiling of Macrophages Exposed to *Porphyromonas gingivalis* , Its Lipopolysaccharide, or Its FimA Protein. *Infection and Immunity*, 732, pp.935–943.

Zhou, Y., Fang, Y. and Ramasamy, R.P., (2019) Non-Covalent Functionalization of Carbon Nanotubes for Electrochemical Biosensor Development. *Sensors (Basel, Switzerland)*, 192.

Ziyatdinova, G., Gainetdinova, A., Morozov, M., Budnikov, H., Grazhulene, S. and Red'kin, A., (2012) Voltammetric detection of synthetic water-soluble phenolic antioxidants using carbon nanotube based electrodes. *J Solid State Electrochem*, 16, pp.127–134.

Zolotukhin, S., (2013) Metabolic hormones in saliva: origins and functions. *Oral Dis*, 193, pp.219–229.